การแลกเปลี่ยนความร้อนจากชั้นดินกรุงเทพมหานครกับเครื่องปรับอากาศในอาคารที่อยู่อาศัย

นางสาวศศิมุกด์ โชคชัย

วิทยานิพนธ์นี้เป็นส่วนหนึ่งของการศึกษาตามหลักสูตรปริญญาวิทยาศาสตรมหาบัณฑิต
สาขาวิชาธรณีวิทยา ภาควิชาธรณีวิทยา
คณะวิทยาศาสตร์ จุฬาลงกรณ์มหาวิทยาลัย
ปีการศึกษา 2559

THERMAL EXCHANGE FROM BANGKOK SUBSOIL TO HOUSEHOLD AIR CONDITIONER

Miss Sasimook Chokchai

A Thesis Submitted in Partial Fulfillment of the Requirements
for the Degree of Master of Science Program in Geology
Department of Geology
Faculty of Science
Chulalongkorn University
Academic Year 2016

Thesis Title	THERMAL EXCHANGE FROM BANGKOK SUBSOIL TO HOUSEHOLD AIR CONDITIONER
By	Miss Sasimook Chokchai
Field of Study	Geology
Thesis Advisor	Associate Professor Srilert Chotpantarat, Ph.D.
Thesis Co-Advisor	Associate Professor Punya Charusiri, Ph.D.

Accepted by the Faculty of Science, Chulalongkorn University in Partial Fulfillment of the Requirements for the Master's Degree

.....Dean of the Faculty of Science
(Associate Professor Polkit Sangvanich, Ph.D.)

THESIS COMMITTEE

.....Chairman
(Professor Montri Choowong, Ph.D.)

.....Thesis Advisor
(Associate Professor Srilert Chotpantarat, Ph.D.)

.....Thesis Co-Advisor
(Associate Professor Punya Charusiri, Ph.D.)

.....Examiner
(Professor Isao Takashima, Ph.D.)

.....External Examiner
(Assistant Professor Krit Won-in, Ph.D.)

ศศิมุกด์ โชคชัย : การแลกเปลี่ยนความร้อนจากชั้นดินกรุงเทพมหานครกับเครื่องปรับอากาศในอาคารที่อยู่อาศัย (THERMAL EXCHANGE FROM BANGKOK SUBSOIL TO HOUSEHOLD AIR CONDITIONER) อ.ที่ปรึกษาวิทยานิพนธ์หลัก: รศ. ดร. ศรีเลิศ โชติพันธรัตน์, อ.ที่ปรึกษาวิทยานิพนธ์ร่วม: รศ. ดร. ปัญญา จารุศิริ, 107 หน้า.

ในปัจจุบันความต้องการด้านพลังงานมีแนวโน้มสูงขึ้น ดังนั้นแนวทางเลือกอีกทางหนึ่งของการจัดการพลังงานคือการลดการใช้พลังงาน เครื่องปรับอากาศระบบ Geothermal heat pump (GHP) ถูกใช้งานอย่างแพร่หลายในต่างประเทศตั้งแต่สงครามโลกครั้งที่ 2 เพื่อเป็นการลดการใช้กระแสไฟฟ้า สำหรับในประเทศไทยการติดตั้งระบบ GHP อย่างเป็นระบบได้ดำเนินการครั้งแรกที่กรุงเทพมหานคร โดยมีวัตถุประสงค์ในการศึกษาครั้งนี้เพื่อวิเคราะห์อุณหภูมิใต้ดินในบริเวณพื้นที่วิจัย เปรียบเทียบลำดับชั้นดินกรุงเทพมหานครกับลำดับชั้นดินบริเวณพื้นที่วิจัย และเปรียบเทียบการประหยัดพลังงานของเครื่องปรับอากาศที่ใช้ระบบ GHP กับเครื่องปรับอากาศปกติ โดยขั้นตอนการศึกษาเริ่มจากการขุดบ่อเจาะสองหลุม ลึกหลุมละ 100 เมตร โดยให้มีความยาวรวม 170 เมตร และใช้ท่อ PVC คุณภาพดีมากเชื่อมต่อกันโดยไม่ให้มีรอยรั่ว โดยปล่อยให้น้ำหมุนเวียนในท่อเพื่อระบายน้ำเข้าสู่ระบบ GHP ที่ถูกจัดตั้งขึ้นที่ห้องทำงานขนาดเล็กภายในเรือนภะรตราชา ผลการศึกษาแสดงให้เห็นว่าอุณหภูมิใต้ดินที่ได้จากการวัดระยะสั้นที่ความลึก 0 - 50 มีค่า 29 - 30 องศาเซสเซียส ผลการวัดอุณหภูมิน้ำที่ไหลเข้าระบบ GHP จากใต้ดินมีค่าต่ำกว่าอุณหภูมิน้ำที่ไหลออกจากระบบ GHP ลงสู่ใต้ดินประมาณ 1.5 องศาเซสเซียส ส่วนผลการวัดในระยะยาว แสดงให้เห็นว่าอุณหภูมิใต้ดินที่ความลึกประมาณ 1.5 - 8 เมตร มีความคงที่ คือประมาณ 29 - 30 องศาเซสเซียส จากค่าอุณหภูมิใต้ดินเฉลี่ยซึ่งต่ำกว่าอุณหภูมิอากาศภายนอกห้อง ตลอดในช่วง 2 ปี โดยสภาพอุณหภูมิใต้ดินที่คงที่นี้มีประโยชน์มาก เนื่องจากทำให้การใช้กระแสไฟฟ้าลดต่ำลงมา ผลการศึกษานี้ทำให้ทราบว่ากระแสไฟฟ้าที่ใช้กับเครื่องปรับอากาศระบบ GHP เมื่อเทียบกับเครื่องปรับอากาศระบบปกติลดลงอย่างน้อยร้อยละ 30 นอกจากนี้ผลการศึกษายังพบว่าความชื้นมีส่วนทำให้การใช้ไฟฟ้าของระบบ GHP สูงขึ้นด้วย และผลการศึกษาธรณีวิทยาใต้ดินของกรุงเทพฯ พบว่าสภาพใต้ดินประกอบด้วยชั้นตะกอนหนาที่ไม่แข็งตัวและกึ่งแข็งตัว ซึ่งเป็นตัวบ่งชี้ว่าสภาพใต้ดินมีผลต่อการใช้ระบบ GHP อย่างประสบความสำเร็จ

ภาควิชา ธรณีวิทยา ลายมือชื่อนิสิต .....

สาขาวิชา ธรณีวิทยา ลายมือชื่อ อ.ที่ปรึกษาหลัก .....

ปีการศึกษา 2559 ลายมือชื่อ อ.ที่ปรึกษาร่วม .....

5772162923 : MAJOR GEOLOGY
KEYWORDS: GHP, UNDERGROUND TEMPERATURE, OUTSIDE AIR TEMPERATURE, ELECTRICITY SAVING, BANGKOK

SASIMOOK CHOKCHAI: THERMAL EXCHANGE FROM BANGKOK SUBSOIL TO HOUSEHOLD AIR CONDITIONER. ADVISOR: ASSOC. PROF. SRILERT CHOTPANTARAT, Ph.D., CO-ADVISOR: ASSOC. PROF. PUNYA CHARUSIRI, Ph.D., 107 pp.

The demand of energy is increasing at present, so the alternative way of energy management is to reduce energy consumption. Geothermal Heat Pump (GHP) has been widely used in many countries since the World War II to reduce electricity consumption. In Thailand, a systematic installation of GHP was first established in Bangkok. The objectives are to investigate analyze subsurface temperature in study area; to compare soil profiles of Bangkok with the study area and to compare energy saving between normal air-conditioner and GHP. The research work commences with drilling 2 boreholes with the length of about 50 meters. The high-quality PVC pipes were inserted into these holes. The pipes were connected and drilled with 100 meters length without any leakage. The Japanese – made GHP system was established at a small room in Parot Racha Building, Chulalongkorn University. The result displays that subsurface temperatures in a short – term measurement at the depths of 0 to 50 meters fall within the average range of about 29 to 30 °C. The result also shows that the inlet temperature flowing to the GHP is lower than the outlet temperature about at 1.5 °C. The result of the long – term measurement indicates that subsurface temperatures at depth of 1.5 to 8 meters are more constant (29 to 30°C) and lower than the outside air temperatures throughout the whole 2 years. The constant underground temperature condition is useful because the electricity consumption is greatly reduced. When GHP was adopted in the room along with the normal air-condition, it is found that electricity consumption can be reduced a little more than 30 %. Additionally, it is recognized that high humidity greatly decrease efficiency of GHP and increase electricity consumption. The study on subsurface geology of Bangkok reveals that the underground condition of thick sequences of un- to semi- consolidated sediments can be one of the parameters which affects the successful application of GHP.

Department:	Geology	Student's Signature	.....
Field of Study:	Geology	Advisor's Signature	.....
Academic Year:	2016	Co-Advisor's Signature	.....

ACKNOWLEDGEMENTS

First of all, the author would like to express my gratitude to the thesis advisor, Associate Professor Srilert Chotpantarat and the thesis co-advisor, Associate Professor Dr. Punya Charusiri for providing great support, invaluable knowledge, enthusiastic suggestion and good encouragement throughout this study to achieve the goal efficiently.

Secondly, the author sincerely thanks to Professor Dr. Isao Takashima (Professor emeritus, Akita University, Akita, Japan) for the great assistance such as GHP installation, data recording, system repairing and invaluable knowledge regarding GHP system.

The special acknowledgement goes to the Food and Water Cluster, Ratchadaphisek Somphot Endowment Fund, Chulalongkorn University for granting project support during research working, Prof. Dr. Somsak Panha (the leader of the Food and Water Cluster) for his crucial comment and support and Associate Professor Dr. Chakapan Sutthirat for searching a good laboratory room on the GHP instalment.

Then, the author gives special thanks to the National Institute of Advanced Industrial Science and Technology (AIST), Dr. Youhei Uchida and Dr. Kasumi Yasukawa for great experience in Ground Source Heat Pump training course at Japan as well as good opportunity in workshop. Besides, the author would like to thank to Geological Survey of Japan (GSJ) for providing GSHP instrument, Data logger and flow meter in this study. The special thank also goes to Dr. Arif Widiatmojo for enthusiastic help in terms of data analysis.

The author thanks to Department of Groundwater Resources (DGP) for providing all the subsurface data and the Bureau of Groundwater Resources Region 8 (Ratchaburi) for GHP drilling.

Finally, the author thanks to Mr. Narong Sodsaard, Mr. Pojana Ngenjam, Mr. Suracaht Wachirapokjaroen and Mr. Suriya Chokmoh for GHP installation, Mr. Stapana Kongsen, Mr. Monawat Kamolsilp, Miss Chadaporn Busarakum and Miss Kulamas Krueworramunee for grammatically checking as well as Sai Punya and Geology Master Degree Student for good advice and cheering up. Housekeeper and gardener are also acknowledged for keeping taking care of the study area.

Most importantly, the author thanks to my Family for financial support and the best understanding without any conditional pressure.

CONTENTS

Page

Page

LIST OF TABLES

LIST OF FIGURES

CHAPTER 1
INTRODUCTION

1.1 Rationale

Nowadays, Thailand face a problem on insufficient energy, especially due to the price of the energy is continually increasing. Therefore, renewable and alternative energy for energy saving are necessary (Yamtraipat et al., 2006). In this study, the existing cooling in the underground was utilized by the device called Geothermal Heat Pump (GHP) or Ground Source Heat Pump (GHP) (Figure 1.1). This cooling was applied in the closed system of controlled temperatures room. GHP or GHP are the new technology that can compensate heat in the winter and traditional air conditioner in the summer (Hepbasli and Akdemir, 2004). This is another way to reduce the energy problem at present because the underground temperature is more stable than the atmospheric temperature (Omer, 2008). Atmospheric temperature varies by many factors, especially radiation of the sun and humidity.

Geothermal Heat Pump (GHP) has been widely used in many countries since the World War II (Spitler, 2005). As mentioned, GHP, one of the alternative energy system, replaces a heater in winter and a normal air conditioner in summer (Blum et al., 2010). Thus, it can help to significantly decrease the current energy shortage because the underground temperature is stable more than the air temperature. This condition depends on many factors. The GHP has been commonly used in many countries particularly in the cold regions (Rybach et al., 2000); (Fridleifsson, 2001); (Sanner et al., 2003). However, the GHP cannot be applied in every area (Yasukawa et al., 2009a) because it depends on the underground temperature and geological background of the individual areas. In Thailand, GHP can only be used for space cooling because the country is located near equator (Takashima, 2011). This made subsurface temperatures to be similar to atmospheric temperatures (Tenma et al., 2009). Based on this assumption, the subsurface temperatures need to be investigated in order to specify the suitability of GHP installation in Thailand. According to the preliminary worked by Yasukawa et al. (2009a), many areas in central Thailand, including Bangkok, have a relatively stable underground temperature; so it is possible to use the GHP in this area.

The objective of this study was to find out whether the GHP system installed at Chulalongkorn University can be efficiently used or not.

Geothermal Heat Pump (GHP) or Ground Source Heat Pump (GHP) can be classified in many types by installation and using. For the installation, there are 2 type as followed; 1) Closed loop heat pumps system, exchanging temperature from underground to household building by using special liquid within water circulation pipes (Figure 1.2A) and 2) Open loop heat pumps system, exchanging temperature from underground water or surface water to household building (Figure 1.2B) (Lund et al., 2004). Moreover, there are 2 type of using as follows: 1) Dual system, which can be heated in winter time and cooled in summer time, and 2) Single system, which can use only cooling system in summer time. As mentioned above, GHP is also classified into 2 types by characteristics of pipelines as follows: 1) Vertical loop, which is suitable for a small area and 2) Horizontal loop, which is appropriate for a big area. The closed loop heat pumps system is selected in Parot Racha building in Chulalongkorn University because there is no suitable surface water or underground water. Besides, we installed the system in a vertical loop due to the limited area.

1.2 Literature Review

1.2.1 Definition of Geothermal Heat pump (GHP)

Ground Source Heat Pump (GHP), also known as Geothermal Heat Pump (GHP), GeoExchange, earth-coupled or ground-source, that has been used in worldwide. Furthermore, GSHP/GHP is one of the fastest growing renewable energy in the world (Curtis et al., 2005). The Ground Source Heat Pump (GHP) or geothermal heat pump (GHP) system is the heating and/or cooling system, transferring heat to or from the ground (Hepbasli et al., 2003). Therefore, it uses the earth as a heat source in the winter and a heat sink in the summer. Ground source heat pumps (GHP) use energy within the earth for electrically powered system. This system uses the constant temperature in underground as the heat exchange instead of the atmospheric (outside-air) temperature to provide heating and cooling for buildings as shown in Figure 1.1.

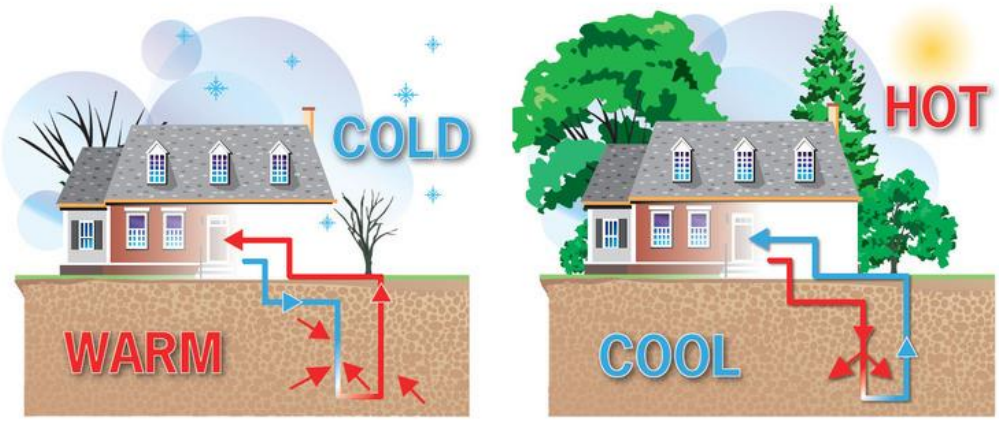

Figure 1.1 Ground Source Heat Pumps (GHP) are heating and/or cooling system that transfers heat to or from the ground. It uses the earth as a heat source in the winter and a heat sink in the summer (Orbis Geothermal).

1.2.2 Types of GHP

Geothermal Heat pump (GHP) can be classified on the basis of system installation into closed loop and open loop systems (Lund et al., 2004). The closed loop systems are operated by the circulation of water or water/antifreeze fluid through a sealed water-circulating pipe network (İnallı and Esen, 2004). Therefore, the GHP can exchange temperatures from underground to household building by collecting or discharging heat, when the circulating fluid flows in a continuous loop. The only interaction with the environment is the transfer of heat through pipe walls (Figure 1.2A). The open loop systems operated by extracting fluid directly from the environment, either as surface water or groundwater. The water is passed through a heat exchanger before being discharged. Theoretically, the water is not consumed, contaminated or modified in any way, except for a slight change in temperature (Figure 1.2B).

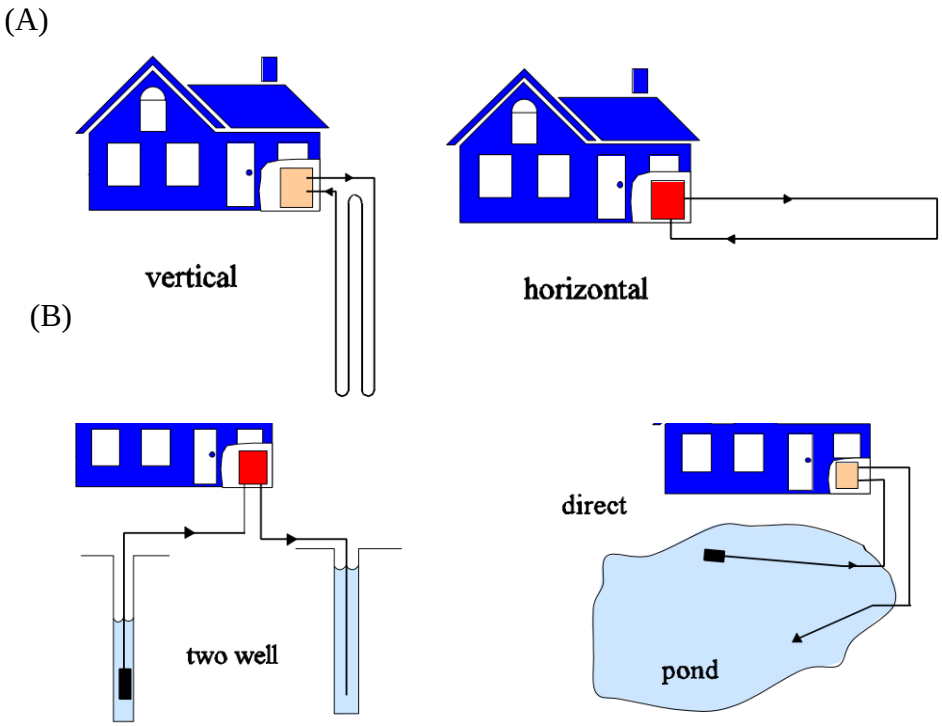

Figure 1.2 Closed loop (A) and open loop (B) geothermal heat pump systems (Lund et al., 2004).

1.2.3 Underground temperature

The possibility of geothermal heat-pump application in tropical Asia from groundwater temperature data was carried out by Yasukawa et al. (2009b). The results suggested that average atmospheric temperature in tropical zones was normally lower than subsurface temperature, causing an improper condition for installation the geothermal heat-pump system. However, some locations where underground water was suitable may be used as a cold heat-source (Yasukawa et al., 2009b).

Consequently, in order to prove the assumption, groundwater temperature surveys were performed along Chao-Phraya plain in the Central of Thailand. The comparison between groundwater and atmospheric temperature data was also carried out (Figure 1.3). Notably, the subsurface temperature in Bangkok was lower than average monthly maximum temperature throughout a year. In brief, the underground in Bangkok may be used as cold heat-source and in other parts of the tropical region, the underground can be used as well.

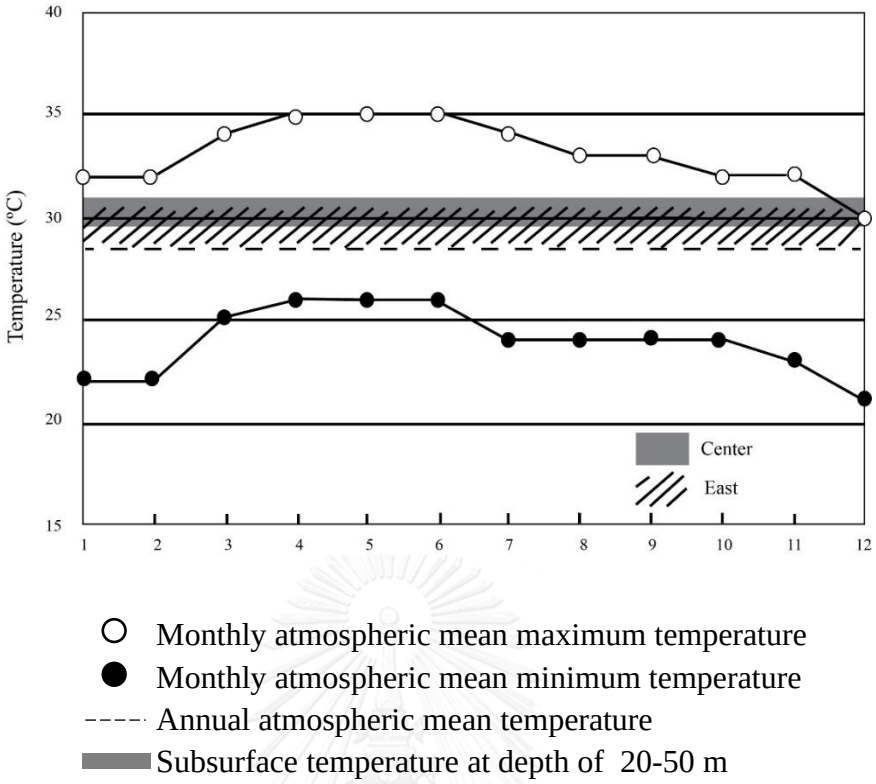

Figure 1.3 Comparison of atmospheric and subsurface temperature at Bangkok and Bangkok each (Yasukawa, K. et al., 2009b).

1.2.4 GHP in Thailand

According to the study of Takashima et al. (2011), GHP system in Bangkok was conducted. In 2006, the first attempt to use GHP application on the tropical land was performed in Kamphangpet province, the Central of Thailand and then operated in Bangkok in 2010. The underground temperature of Thailand is lower than the atmospheric temperature around 5-10 °C. GHP system in Bangkok was, therefore, designed for space cooling by means of using horizontal piping line at 1 metre depth. Additionally, the COP - coefficient of performance - was around 3 to 4 and the underground temperature here was also recovered rapidly (Figure 1.4). Finally, the shallow horizontal system is best suited to use in the tropical countries owing to the lowest temperature as well as low cost construction (Takashima et al., 2011).

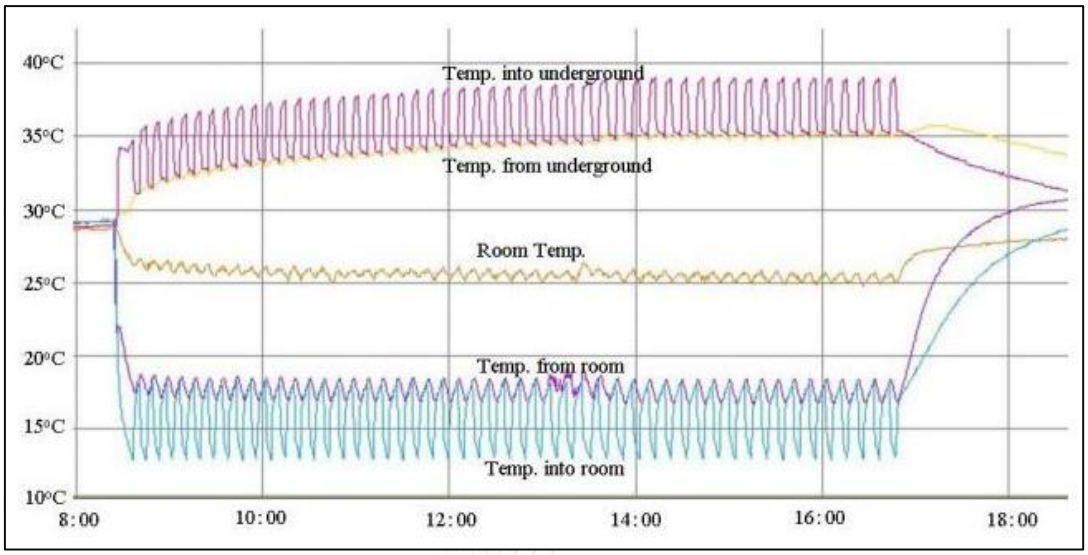

Figure 1.4 One day operation of GHP on 3 May 2011 of the Kasetsart University system (Takashima et al., 2011).

1.2.5 Lithology of Bangkok

Back-analysisinterpretred the driven and bored pile tests data in Bangkok sub-soils were studied by Balasubramaniam et al. (2009). At the lower part of the upper soft clay layer, stiff clay was generally observed. Moreover, at the down deeper part of stiff clay, the alternating layers between dense sand and stiff clay were present. Weathered clayinthe uppermost layer with a wide range of thickness from approximately1 to 4 m isoverlaid by high-natural-water-content soft clay layer with an aprroximately10 to 15 m thick. Below this layer, the medium stiff-to-stiff clay with a vary thickness from 10 to 20 m were found. The first sand layer at the depth of 20 to 30 m was under the stiff clay, intercalating between sandy clay and/or clayey sand and stiff clay layers. Silty sand (SM) was considered as the first sand layer. Below this first sand layer, hard clay or second stiff clay which is likely to be consolidated was found. Furthermore, the second sand layer lowered second stiff clay was found at depth more than 50 m as shown in Figure 1.5.

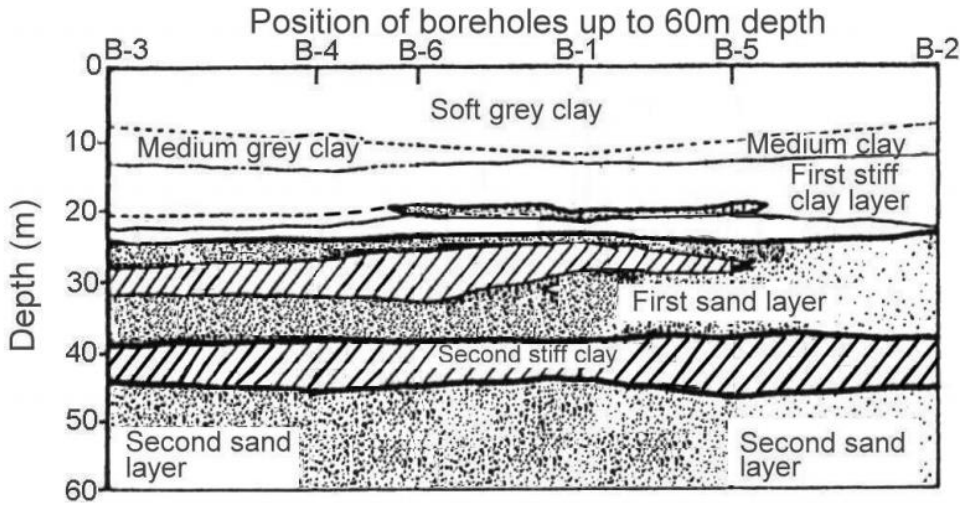

Figure 1.5 The typical deep soil profiles described by Sambhandaraksa and Pitupakorn in 1985 (Balasubramaniam et al., 2009).

1.2.6 Soil thermal properties

The thermal conductivity of soil and rock, as the essential value, affect the ground loop circulating design of the Ground Source Heat Pump (GHP) or the Geothermal Heat Pump (GHP), leading to effects on the installation cost and energy requirements. The thermal conductivity indicates the rate of heat transferred between the circulation loop and surroundings. As shown in Table 1.1, the different soil types represent different thermal conductivity values, increasing in water-saturated saturated (Build-It-Solar). Loam texture has an intermediate thermal conductivity between sand and clay because there are more porous texture to hold more water content. For this reason, groundwater level is significant factor for the GSHP/GHP installation.

Table 1.1 The thermal conductivity of different soil types.

Texture Class	Thermal Conductivity
	Btu/ft hr °F
Sand	0.44
Clay	0.64
Loam	0.52
Saturated sand	1.44
Saturated silt or clay	0.96

1.2.7 Coefficient of Performance **(**COP) of air-conditioner

The coefficient of performance (COP) is the performance of data, measured as the heat output (kWh) and divided by the electrical input (kWh) (Energy Saving Trust, 2007). In other word, COP is ratio between energy transferred for heating or cooling to the input of the electric energy into the system as shown in Figure 1.6 (National Rural Electric Cooperative, A., & Oklahoma State University. Division of Engineering, T., 1988; Widiatmojo, 2017).

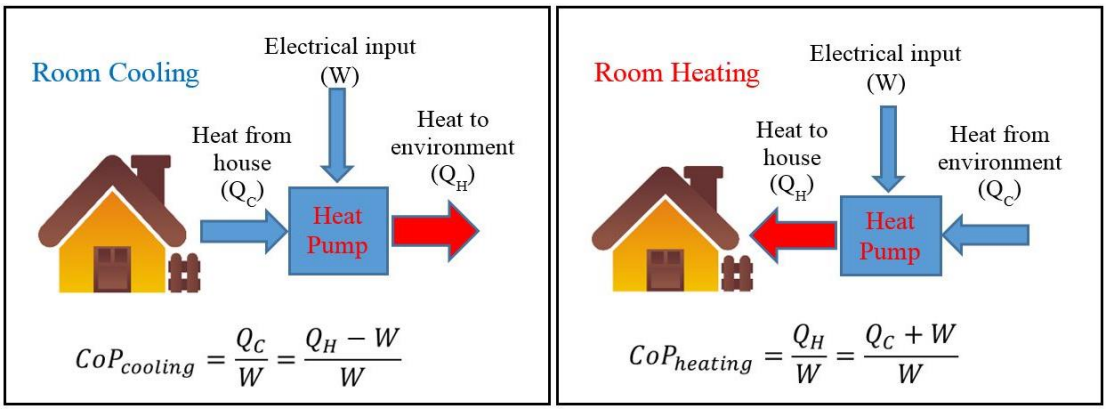

Figure 1.6 COP is ratio between energy transferred for heating or energy removed for cooling to the input of the electric energy into the system (Widiatmojo, 2017).

As shown in Figure 1.7, the brine or water heat pumps was tested under the standard conditions (i.e. inlet brine temperature of 0°C and outlet brine temperature of 50°C, etc.). In the standard, brine is applied to indicate any water or antifreeze solution. However, the higher of COP is the higher of the efficient in the GHP system. As shown

in Figure 1.6, coefficients of performance (COP) was measured under the test conditions as a representative of the GHP. Moreover, the efficiency for the GHP's installation depends on the power from the circulation of the underground pump, which should be low in order to obtain a good efficiency.

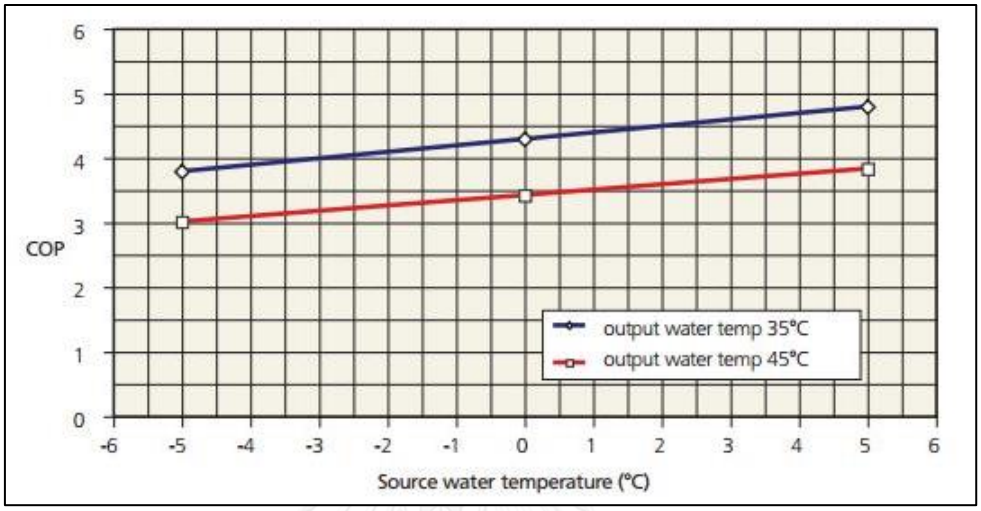

Figure 1.7 The coefficients of performance (COP) of the typical small GHPs (Energy saving trust, Online).

1.3 Objectives

There are 3 main objectives in this study as follows:

1. to investigate subsurface temperature in the study area;

2. to compare between the soil profile of Bangkok and the soil profile of study area

3. to compare energy saving between the normal air-conditioner and GHP

1.4 Scope of work

This thesis used the Geothermal (Ground Source) Heat Pump system in the closed-loop systems, drilling two wells in a vertical loop at depth 50 m with a total length of 200 m and will operate the GHP system for 1 year.

1.5 Expectation of the research

Installation of the Geothermal Heat Pump (GHP) in Thailand can reduce the total electric consumption efficiently.

CHAPTER 2
METHODOLOGY

2.1 Site selection

In this study, we installed Geothermal (Ground Source) Heat Pump system (GHP) in Bangkok which is located in the Central plain of Thailand as shown in Figure 2.1A.

In addition, the experimental room is in Parot Racha building, Chulalongkorn University as shown in Figure 2.1B.

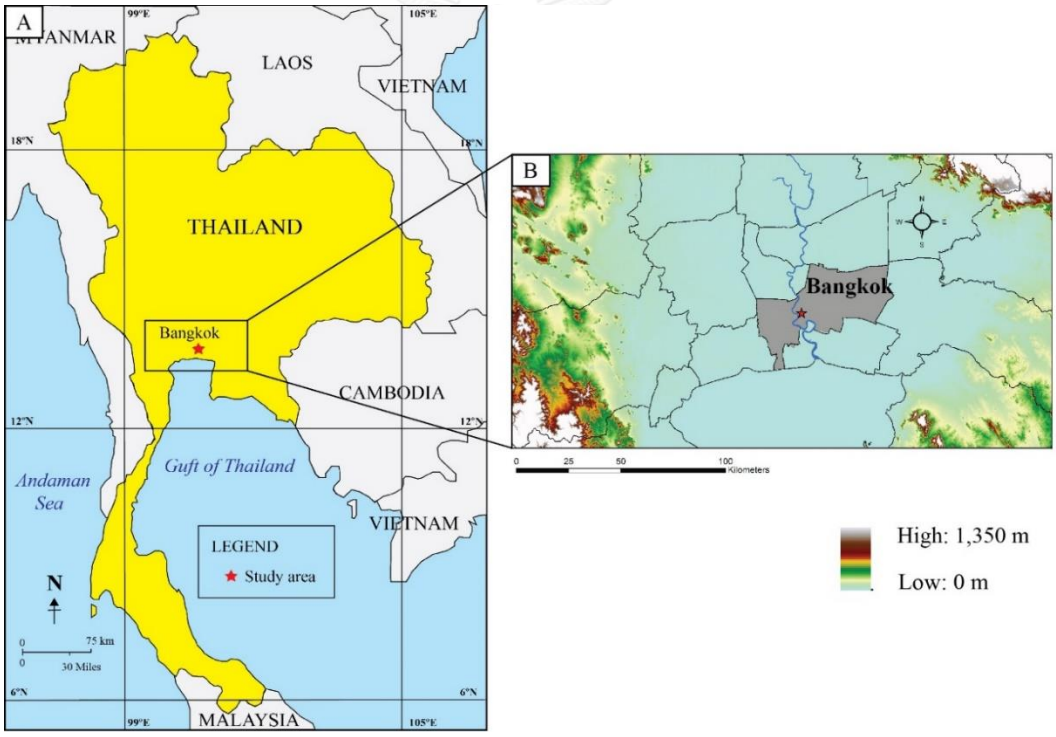

Figure 2.1 The location of installed GHP system**:** Index map of Thailand **(**A**)** and Chulalongkorn University **(**star**)** in Bangkok **(**B**).**

In the study area, we have installed Geothermal Heat Pump system (GHP) on the second floor of Parot Racha building (red star). Two wells were drilled for water circulation of GHP on the surface below Parot Racha building as shown in Figure 2.2.

Moreover, there is the nearest observation well of Department of Groundwater Resources (DGR) that located in Chulalongkorn University Dharma Centre (Figure 2.2).DGR well was used for groundwater level and lithology observation.

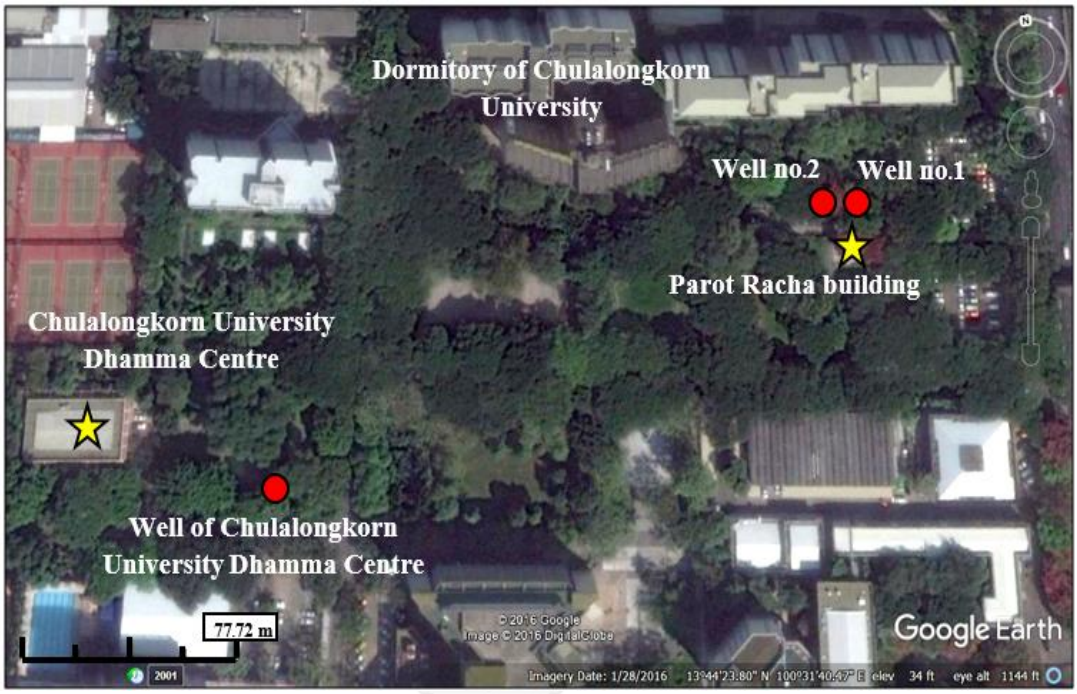

Figure 2.2 Google Earth Map showing the location of Paraot Racha, well nos. 1 & 2 in Chulalongkorn University and the nearest artesian well (Chulalongkorn University Dharma Centre).

2.2 Selection of the GHP type

According to Lund et al., 2004, GHP can be also divided into two type; horizontal and vertical loop which depend on size of area. Horizontal loop is used for large area and vertical loop is used for limited area. For this reason, we selected vertical loop for Chulalongkorn University where is limited and expensive land. Firstly, we installed Geothermal Heat Pump (GHP) in vertical loop system because the study area is limited in space. Secondly, we utilized two wells for water circulation of GHP system by installing 50 meters-long pipes in each well. Unfortunately, the pipe in well no.1 was broke so we need to insert more pipes in that well. One is 10 meters-long and another is 15 meters-long.

Furthermore, thermistors for subsurface temperatures measurement was attached with these pipes as shown in Figure 2.23. Output thermistors have been connected to the pipes of both wells at several depths (Figure 2.23). The thermistors for measuring subsurface temperatures in well no. 1 were set - up into the 10 meters-long in PVC pipe at depths of 1.5, 3, 8 and 10 meters. In well no. 2, the thermistors were set-up at depth of 25 and 50 meters without any PVC casing pipe (see more detail in Figure 2.23).

2.3 Equipment preparation

The equipment used in this study can be divided into 5 important parts; Equipment for water circulation system, Geothermal (Ground Source) Heat Pump air-conditioner (GHP) and Normal air-conditioner (AC), Thermistors, Flow meter Data logger and Electricity meter.

2.3.1 Installation of water circulation

This part consist of polyethylene pipes (Figure 2.3) and submersible pump (Figure 2.4).

- Polyethylene pipe (PE): We used High Density Polyethylene (HDPE) type because this type is lightweight, flexible, long lifetime and non-brittle. In this study, there are 4 pipe lines with the size of32 mm diameter, 50 meters length. They were connected into U-shape (100 meters-long) as shown in Figure 2.3.

Figure 2.3 High-density polyethylene (HDPE) in U -shape.

- Submersible pump: The size is 1 inch x 100 Watt, 7 meters-force maximum and 80 l/min-maximum flow rate for pumping test as shown in 2.4.

Figure 2.4 Submersible Pump for pumping test.

2.3.2 GHP and "normal" air-conditioners

In this study, we selected two air- conditioner system for energy saving comparison including Geothermal Heat Pump air-conditioner (GHP) (Figure 2.5) and Normal air-conditioner (Figure 2.6).

- Geothermal (Ground Source) Heat Pump air-conditioner (GHP): We used CORONA brand, CSH-C4000G model with 13,652 BTU. GHP indoor unit was set up in experimental room (second floor of Parot Racha building) and GHP outdoor unit was set up on the first floor of Parot Racha building as shown in Figure 2.5.

Figure 2.5 Geothermal Heat Pump air-conditioner (GHP) consists of GHP indoor unit and GHP outdoor unit.

- Normal air-conditioner: We have used Panasonic CS-PC12QKT model because the specification is similar to GHP air-conditioner. One 12,319 BTU air-conditioner with fan coil unit (indoor unit) was set up in experimental room (second floor of Parot Racha building) and condensing unit (outdoor unit) was set up on the first floor of Parot Racha building as shown in Figure 2.6.

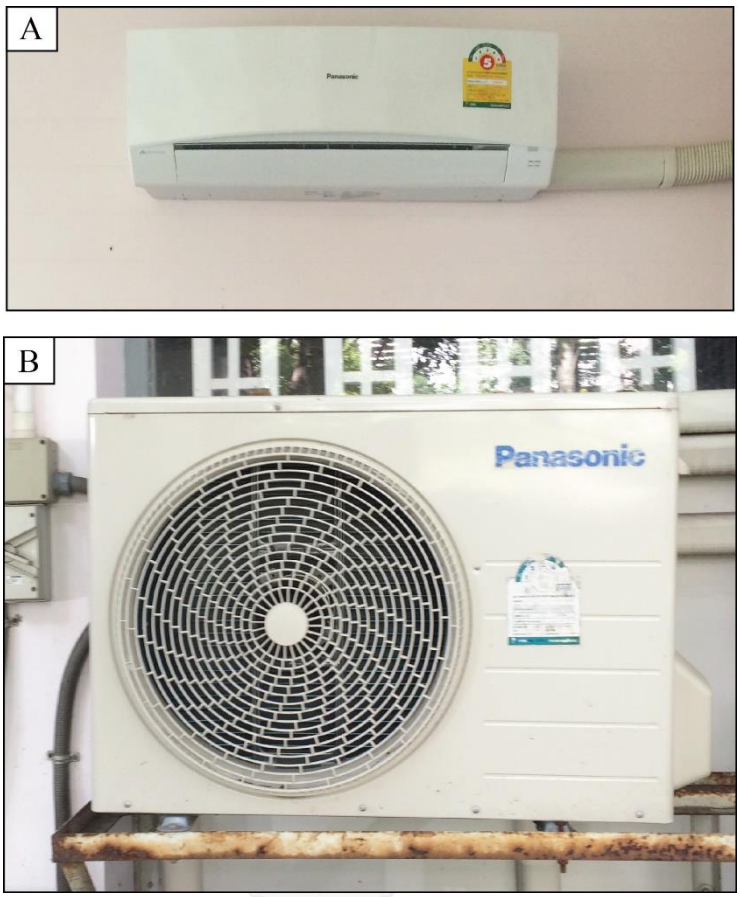

Figure 2.6 Normal air-conditioner (AC) consists of (A) fan coil unit (indoor unit) and (B) condensing unit (outdoor unit).

Table 2.1 Specification of Normal air-conditioner (AC) and GHP air-conditioner (GHP).

Detail	**AC[1]**	**GHP[2]**
Brand	PANASONIC	CORONA
Model	CS-PC12QKT	CSH-C4000G
BTU (BTU/hr.)	12,319 BTU/hr.	13,652 BTU/hr.
EER (BTU/hr./W)	11.88 BTU/hr./W	13.652 BTU/hr./W
Power (W)	1,037 W	1,000 W

Detail	AC[1]	GHP[2]
Electricity (A)	4.8 A	5 A
Voltage (V)	220 V	200 V

[1] (Hatyaiair)

[2] (Corona, 2012)

2.3.3 Thermistors

Thermistors were installed for measuring room temperature, outside air temperature, inlet liquid temperature, outlet liquid temperature and subsurface temperature at depths of 1.5, 3, 8, 10, 25 and 50 meters as shown in Figure 2.7.

Figure 2.7 Thermistors for subsurface temperature measurement at depths of 1.5, 3, 8, 10, 25 and 50 meters.

2.3.4 Flow meter

Flow rate of water circulation was measured by using flow meter Keyence brand, FD-M series model with rate of 50 l/min as shown in Figure 2.8.

Figure 2.8 Flow meter for flow rate.

2.3.5 Data logging

All data from thermistors and flow meter were recorded every 20 minutes in 24 hours by using data logger as shown in Figure 2.9). Graphtec brand, midi Logger GL220 model in volt unit was used for recording room temperature, atmospheric (outside air) temperature, inlet liquid temperature, outlet liquid temperature, subsurface temperature at depths of 1.5, 3, 8, 25 and 50 meters from thermistors and flow rate from flow meter. The data logger was installed in experimental room as shown in Figure 2.26.

Figure 2.9 Data Logger for recording.

2.3.6 Electricity measurement

Electricity consumption was measured by using Sankomec brand of electricity meter in kilowatt per hour (kWh) unit. It was installed in experimental room as shown in Figure 2.10.

Figure 2.10 Electricity meter for measuring electricity consumption.

2.4 Steps of installation and data recording

In this study, methodology can be divided into parts 9 as shown in Figure 2.11

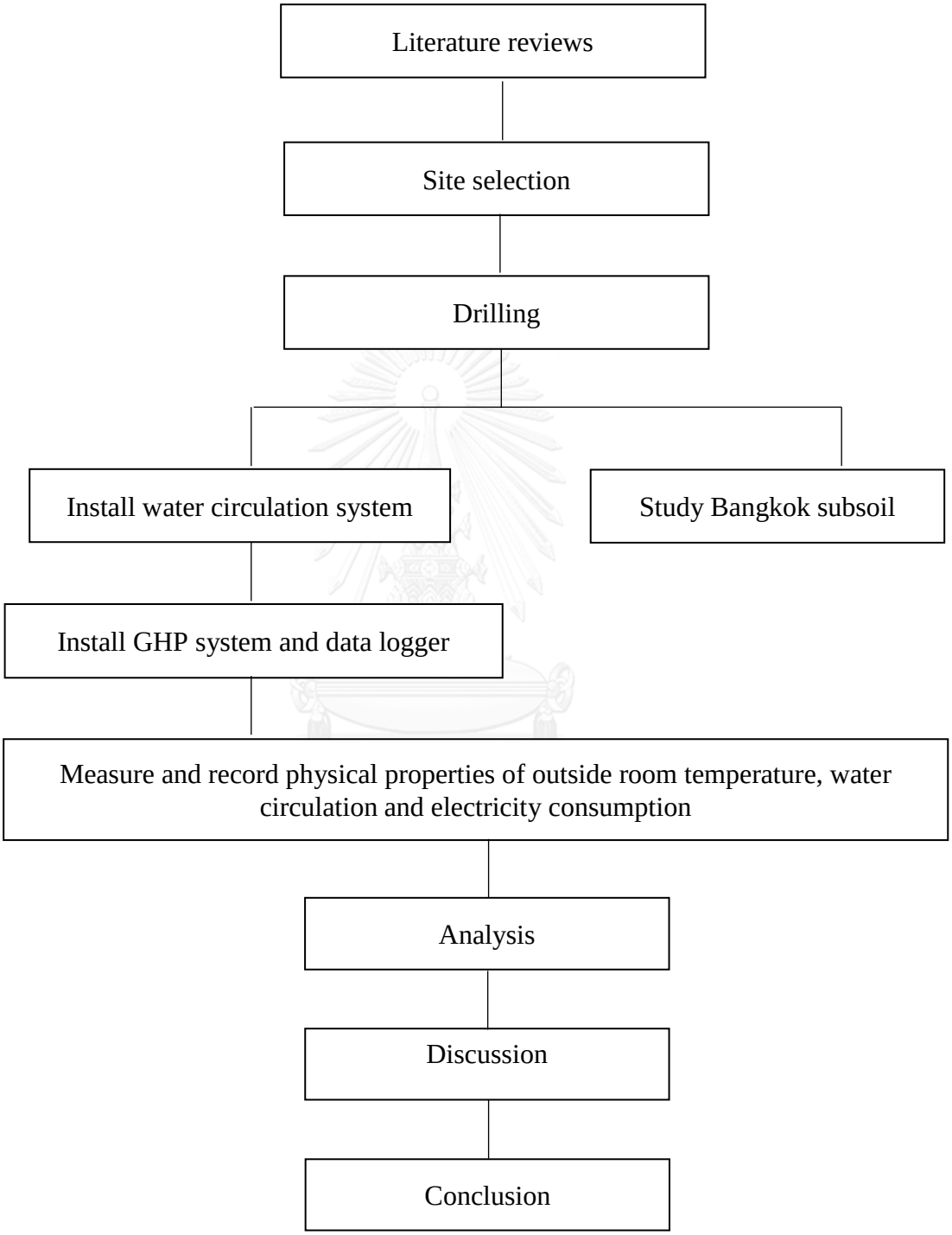

Figure 2.11 Flow chart of work.

2.4.1 Installation of water circulation system

The study area is Parot Racha. It is located in Southern dormitory of Chulalongkorn University that is 20 meters from Phayathai Road (Main Street) about (Figure 2.12 and 2.13). The experimental room is old secretary room that is located on the second floor of building. Its size is 2.84 meters-wide, 4.74 meters-long and 3.50 meters-high as shown in Figure 2.14.

After we selected study area, well nos. 1&2 was drilled into 50 meters-depths at back of the building without any wire lines or another barrier underground and not far from the experimental room.

The first hole (well no.1) is located 4 meters from the building and the second hole is located in about 6 meters west of well no.1 as shown in Figure 2.12.

Figure 2.12 Position of well nos.1&2 where is located in back of Parot Racha building.

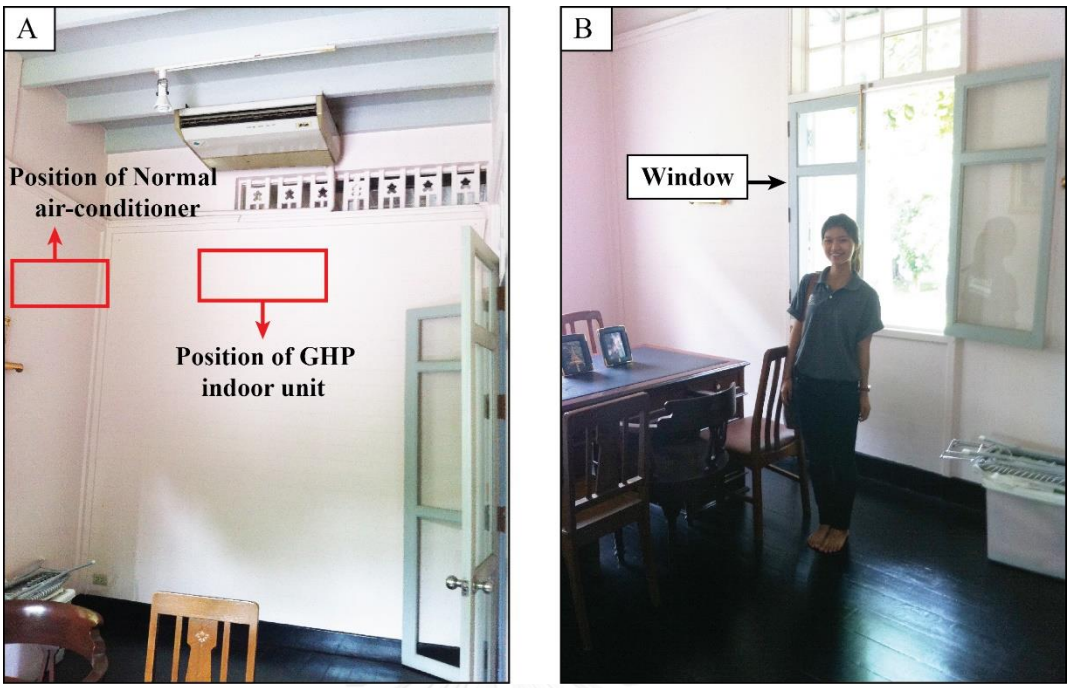

Figure 2.13 Experimental room at the second floor of Parot Racha building with 2.84 meters-wide, 4.74 meters-long and 3.50 meters-high. (A) Position for installing GHP indoor unit and Normal air-conditioner (AC) indoor unit (B) Window of back side of the building (Miss Sasimook Chokchai, tall 160 meters).

The process of water circulation system installation conducted by drilling 2 borehole in the vertical into 50 meters-depth, 12 inches-diameter and 6 meters-space at the back side of Parot Racha building (Figure 2.14 and Figure 2.15). Next, put PVC casing with 12-inch-diameter and 1.5 meters-long into well no.1 for preventing the borehole as shown in Figure 2.15. After that, collect sample of sediment and debris (cutting) in every 1 meter from 2 boreholes (Figure 2.16) for identifying characteristics of sediment. Then, install thermistors for measuring subsurface temperature of well no.1 in PVC pipe at depths of 1.5, 8 and 10 meters and outside of HDPE pipe of well no.2 at depths of 25 and 50 meters. Finally, put HDPE pipes into the holes (Figure 2.17 and 2.18).

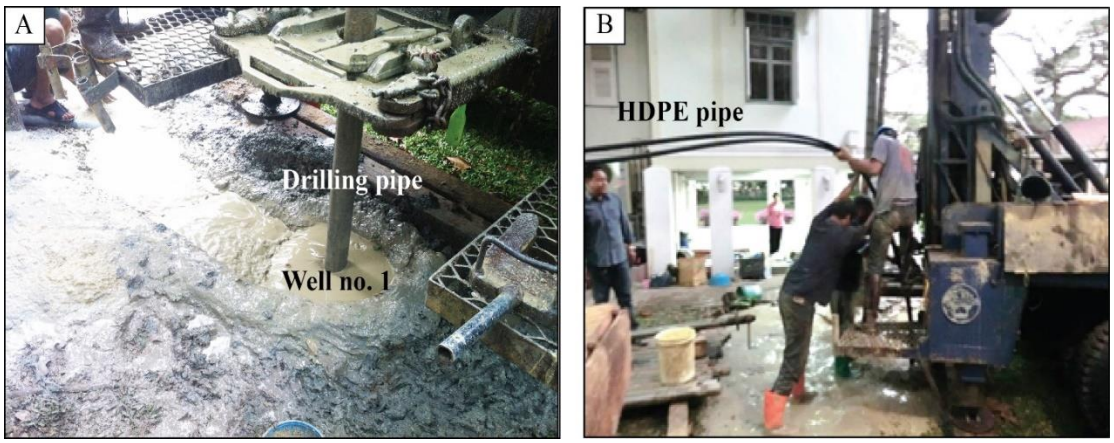

Figure 2.14 (A) Sample of drilling 2 wells range from 0 - 50 meters (well no.1). Note: There is no picture of well no.2 (B) Putting HDPE (high - density polyethylene) pipe with U shape in continuous lengths up to 50 meters- long for fluid circulation into 2 wells. Note: There is no picture of well no.2.

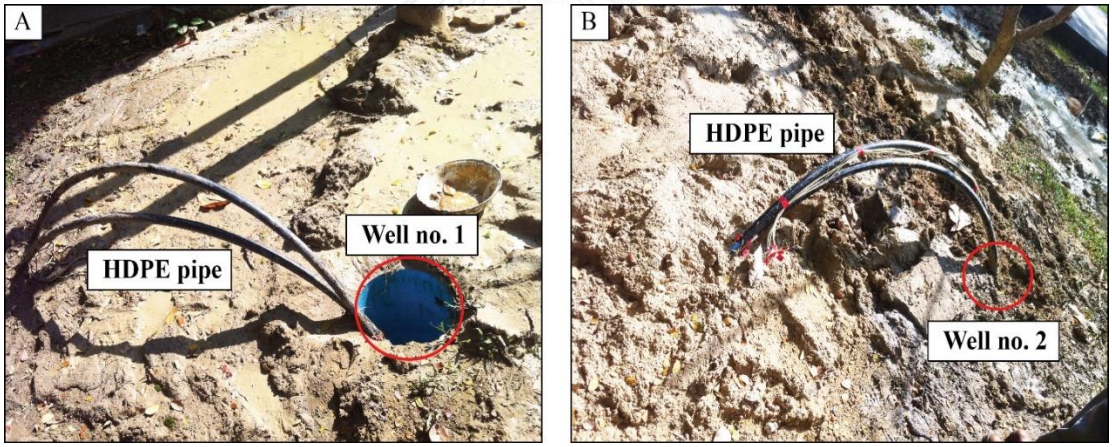

Figure 2.15 (A) HDPE (high - density polyethylene) pipe in well no.1 (B) HDPE (high density polyethylene) pipe in well no.2.

Figure 2.16 Samples of from well no.1 that's collected every 1 meter-depth.

After putting HDPE pipes into 2 wells and connecting them together (Figure 2.17A), trench with 6 inches-depth and 6 meters-long was dug from well .2 to well no. 1. The trench extending from well no. 1 to the first floor the building where GHP outdoor unit was installed (Figure 2.17B). Then, put two HDPE pipes with 6 meters-long into the trench between well nos. 1&2 and connect it to HDPE pipes in well nos.1&2.

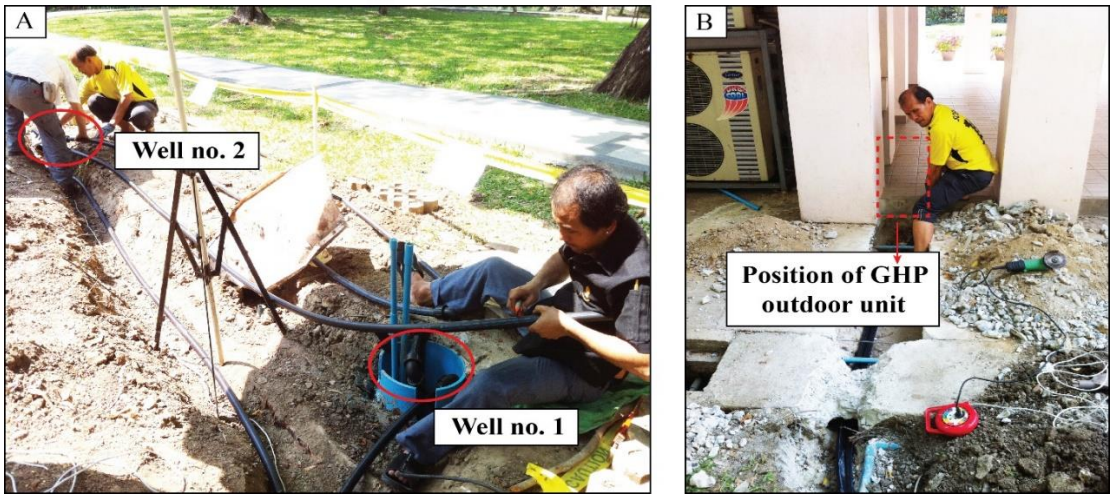

Figure 2.17 (A) Connecting HDPE pipe of well no.1 to HDPE pipe of well no.2 (Mr. Surachat Wachipokcharoen, tall 169 centimeters) (B) Preparing HDPE of well nos.1&2 for connect to GHP outdoor unit.

Then, connect same HDPE pipe type with 4 meters-long (32 mm-diameter, 10 meter-long) with the HDPE pipes of well nos. 1&2 before connect to a GHP outdoor unit. Lastly, bury everything into trench with local soil (Figure 2.18).

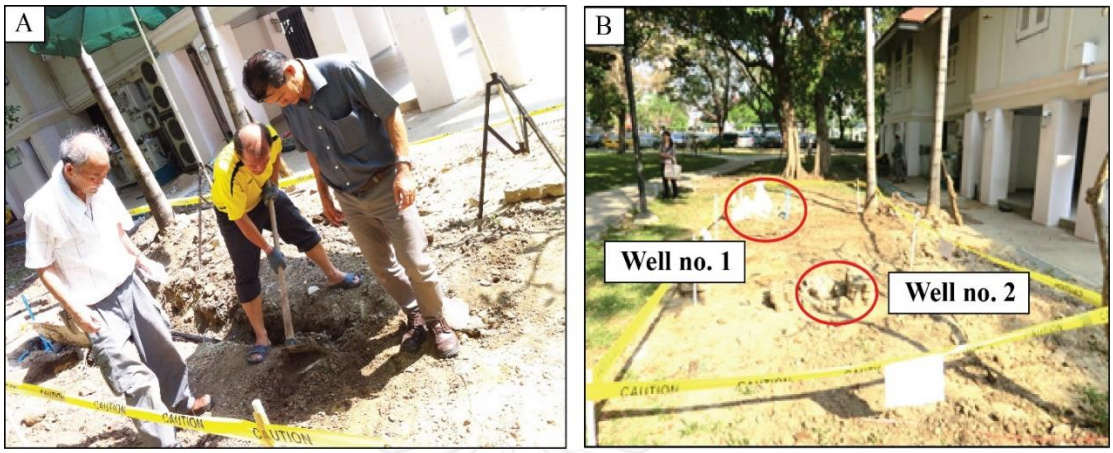

Figure 2.18 (A) Burring all HDPE pipes to underground for preserving temperature and safety (B) after bury all into the subsurface.

2.4.2 Installation of GHP air-conditioner

Geothermal Heat Pump (GHP) machine consists of GHP indoor unit for installing in the experimental room and GHP outdoor unit and GHP outdoor unit for installing in the first floor of the building that was connected with HDPE pipes from well nos. 1&2.

Firstly, connect thermistors for recording subsurface temperature (Figure 2.19A) with Data logger that was installed in the experimental room (Figure 2.19B). Secondly, install GHP indoor unit in the experimental room (Figure 2.19A) and installed GHP outdoor unit on the first floor of building (under the experimental room). After that, connect GHP outdoor unit to HDPE pipes of well nos. 1&2 (Figure 2.20A). Next step, add the anti- corrosion and water for water circulation. Note: The anticorrosion is special liquid for preventing corrosion of engine (Figure 2.20B).

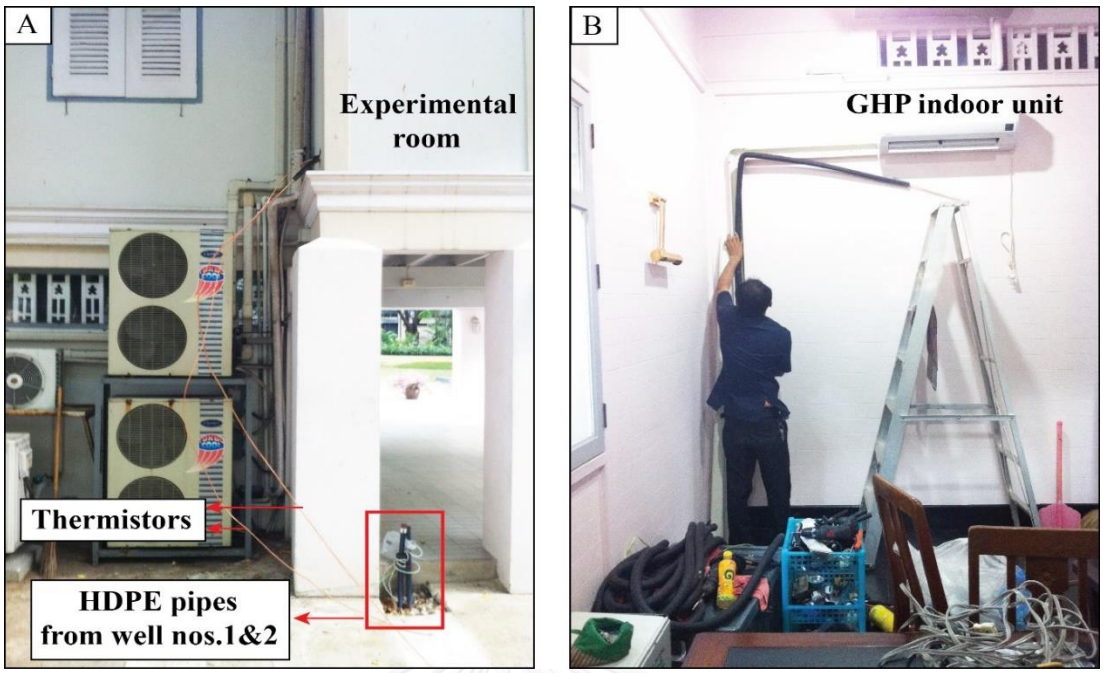

Figure 2.19 (A) Connecting thermistors to Data logger in the experimental room (B) Installing GHP indoor unit in the experimental room.

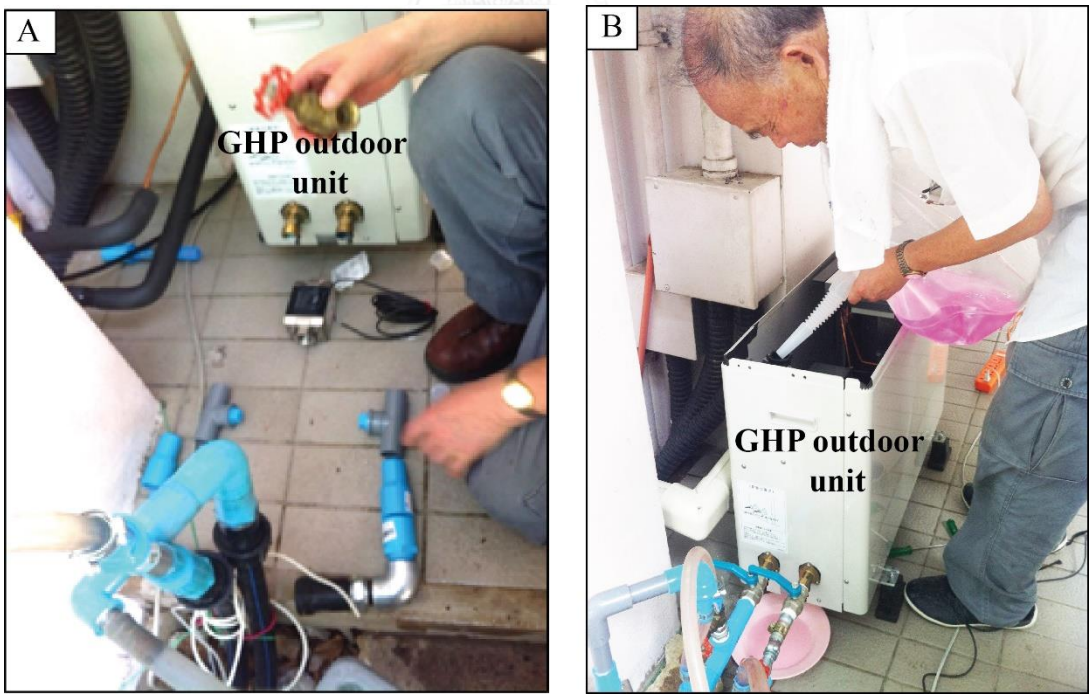

Figure 2.20 (A) Connecting inlet and outlet HDPE pipes (HDPE pipes of well nos. 1&2) to GHP outdoor unit without any leakage (B) Filling anticorrosion into GHP outdoor unit.

. Then, connect HDPE pipe to GHP outdoor unit from well no. 1 for inlet liquid to machine or experimental room and connect HDPE pipe from well no. 2 with GHP outdoor unit for outlet liquid from machine (Figure 2.21). Finally, renovate the garden (Figure 2. 22). See Schematic installation of geothermal heat pump system in Figure 2.23.

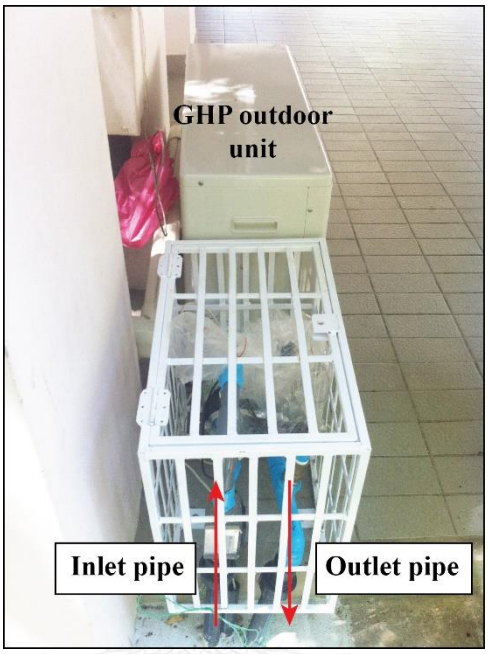

Figure 2.21 Connecting HDPE pipe from well nos. 1&2 to GHP outdoor unit.

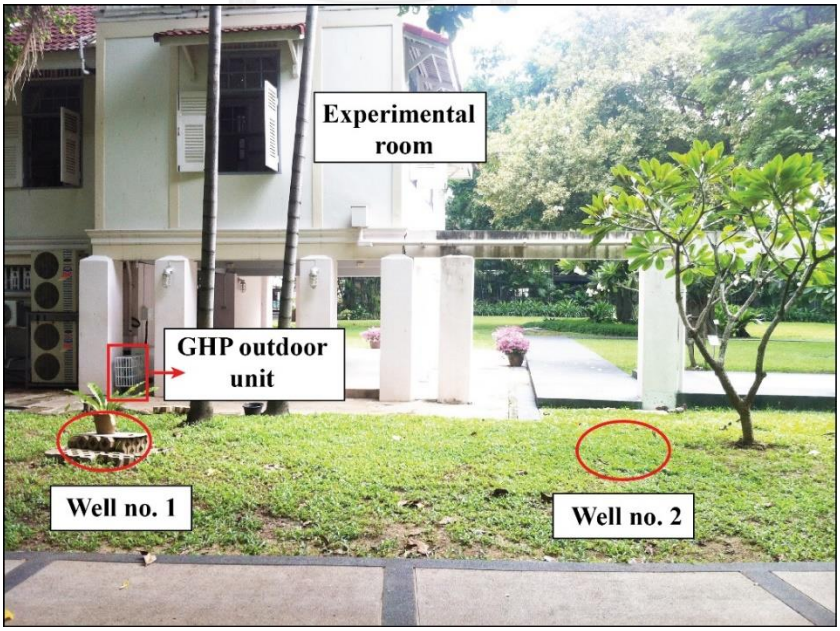

Figure 2.22 Renovating the garden after all finish GHP installation.

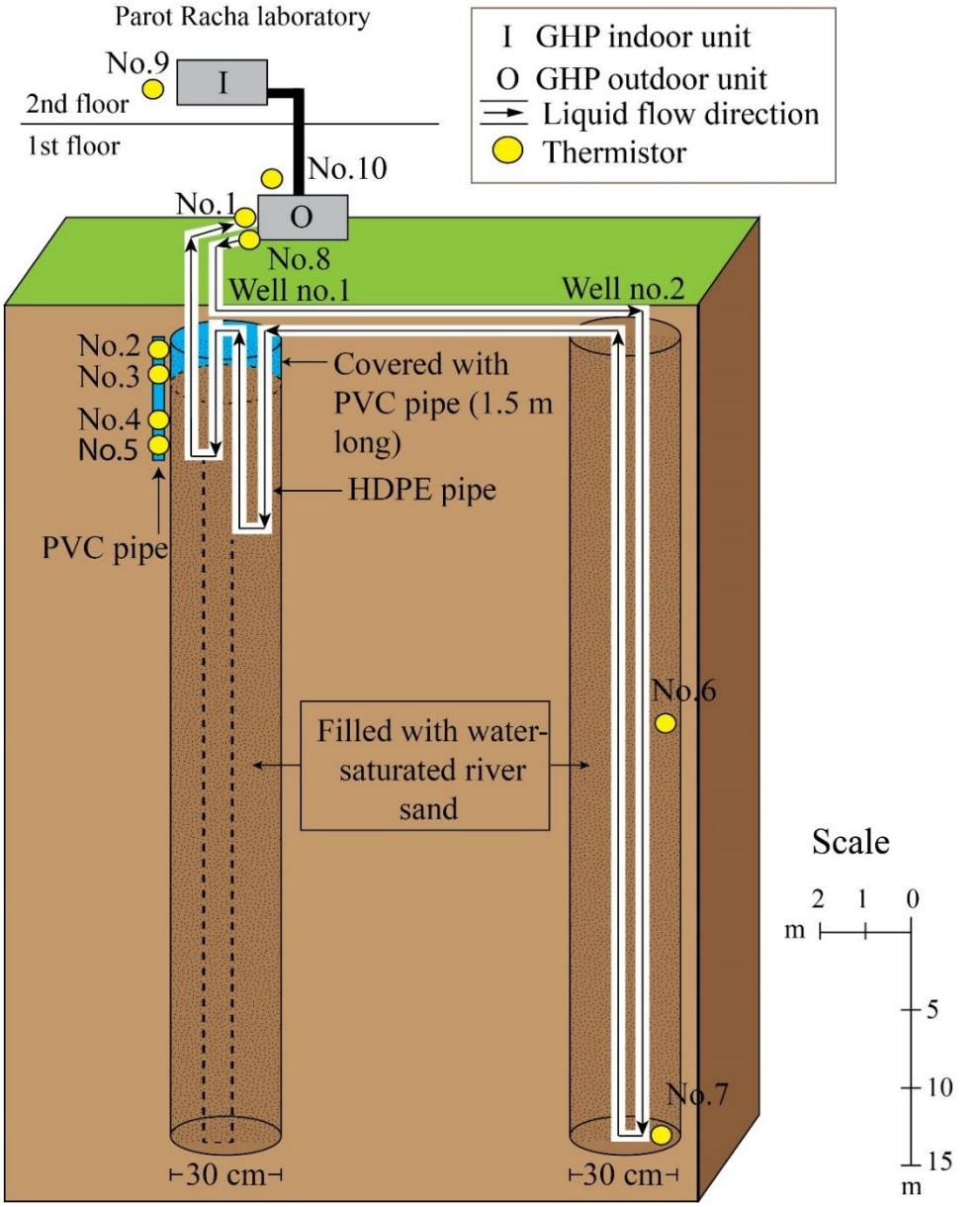

Figure 2.23 Schematic installation of geothermal heat pump system at Parot Racha laboratory room. Note: HDPE pipe in well no.1 was broken. Therefore two new HDPE pipes with the lengths of 10 and 15 meters were inserted and connected to the well no. 2.

2.4.3 Data logger recording

Data Logger was installed in the experimental room (Figure 2.26) for recording room temperature, atmospheric temperature, inlet- , outlet liquid temperature, subsurface temperature at depths of 1.5, 3, 8 and 10 meters- depth, humidity and flow rate every 20 minutes in 24 hours (Figure 2.24).

Description of Data logger recording

Channel no.1: Showing room temperature in degrees Celsius (°C).

Channel no.2: Showing outside temperature or atmospheric (outside air) temperature degrees Celsius (°C).

Channel no.3: Showing inlet liquid temperature in degrees Celsius (°C).

Channel no.4: Showing outlet liquid temperature in degrees Celsius (°C).

Channel no.5: Showing flow rate of water circulation in volt unit (v).

Channel no.6: Showing subsurface temperature at depth of 8 meters in volt unit (v) in well no. 1.

Channel no.7: Showing subsurface temperature at depth of 10 meters in volt unit (v) in well no. 1.

Channel no.8: Showing subsurface temperature at depth of 3 meters in volt unit (v) in well no. 1.

Channel no.9: Showing subsurface temperature at depth of 1.5 meters in volt unit (v) in well no. 1.

Figure 2.24 Recording temperature, humidity and flow rate by Data Logger.

2.4.4 Electricity measurement

There are two electricity meters for measuring electricity of GHP air-conditioner (GHP) and Normal air-conditioner (AC) which were installed in the experimental room (Figure 2.26) in kilowatt (kWh) unit as shown in Figure 2.25.

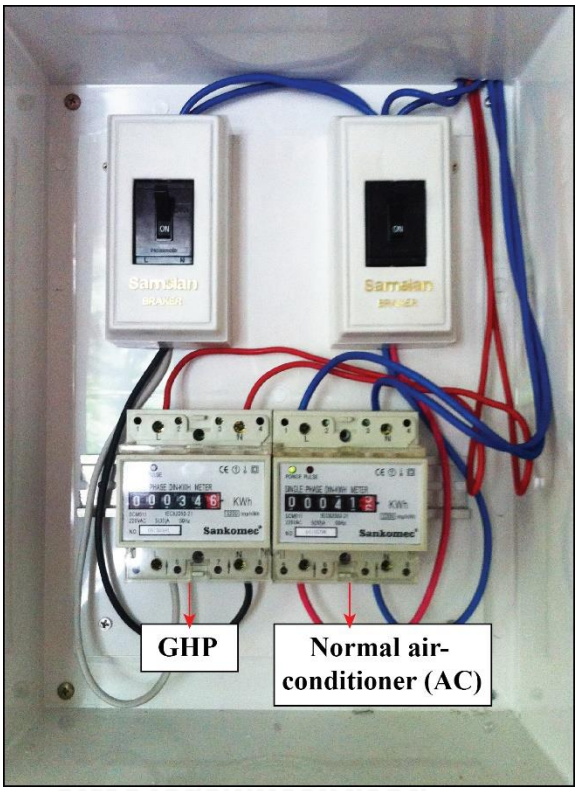

Figure 2.25 Electricity meter in the experimental room for measuring electricity consumption of GHP air-conditioner (GHP) (left side) and Normal air-conditioner (AC) (right side).

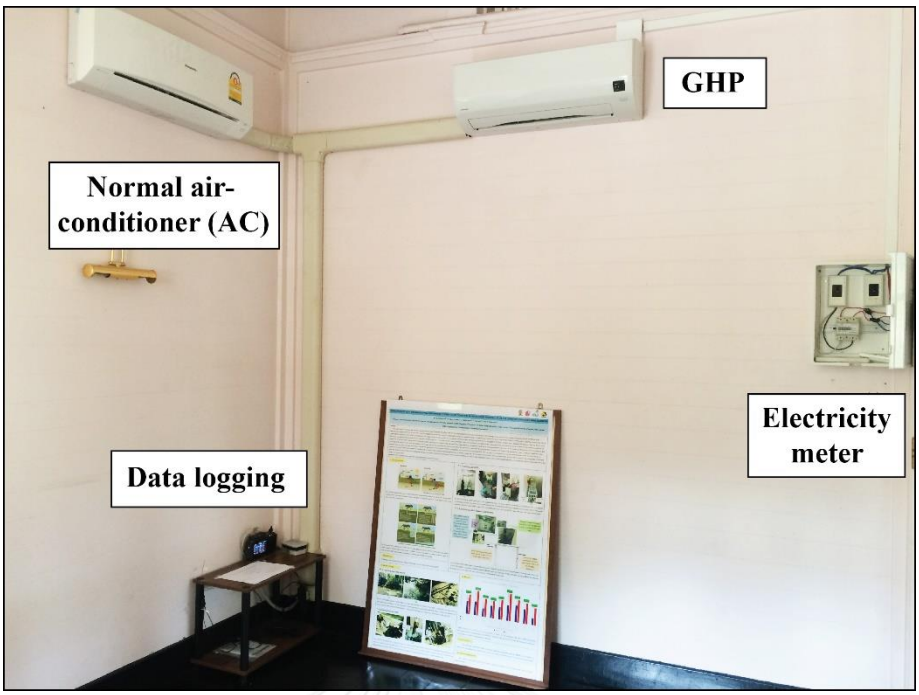

Figure 2.26 GHP indoor unit with the data logger and electricity meter in the experimental room.

CHAPTER 3
RESULTS

This Chapter was divided into 5 parts as following items: Cenozoic stratigraphy, Temperature measurement, Humidity measurement, Flow rate, and Electricity consumption.

3.1 Cenozoic stratigraphy

Well nos. 1&2 were drilled into 50 meters-depth and 6-meters spacing between wells. They were collected cuttings in every 1 meter to investigate characteristics of sediments, as shown Lithologic logs in Figures 3.1 & 3.2.

3.1.1 Lithologic logs of the study areas

The cutting samples collected from well no.1 can be classified into 5 layers as shown in Figure 3.1.

- Layer A is dark gray clay with highly plastic and homogeneous texture, which was collected from 0 to 17 meters depth (17 meters thickness) as shown in Figure 3.3A.

- Layer B consists of pale brown to yellowish brown clay that is highly plastic and homogeneous, which was collected from 18 to 20 (3 meters thickness) meters depth as shown in Figure 3.3B.

- Layer C comprises pale brown to yellowish brown sandy clay, which was collected from 21 to 26 meters depth (6 meters thickness). It is composed of 60 % of clay that is moderate plastic, heterogeneous and 40 % of sand that is fine- to medium-grained, poorly sorted and sub-angular. Moreover, it is composed of quartz, feldspar and rock fragments as shown in Figure 3.3C.

- Layer D consists of pale brown to yellowish brown sand that is fine- to medium-grained, good sorted and sub-angular, which was collected from 27 to 41 meters depth (15 meters thickness). Furthermore, it is composed of quartz, feldspar, rock fragments and some parts of coarse sand as shown in Figure 3.3D.

- Layer E consists of yellowish brown clay that is moderate plastic, heterogeneous and comprises some parts of medium sand. This layer was collected from 42 to 50 meters depth (9 meters thickness) as shown in Figure 3.3E.

Additionally, the real thickness may be disturbed from collecting sediments.

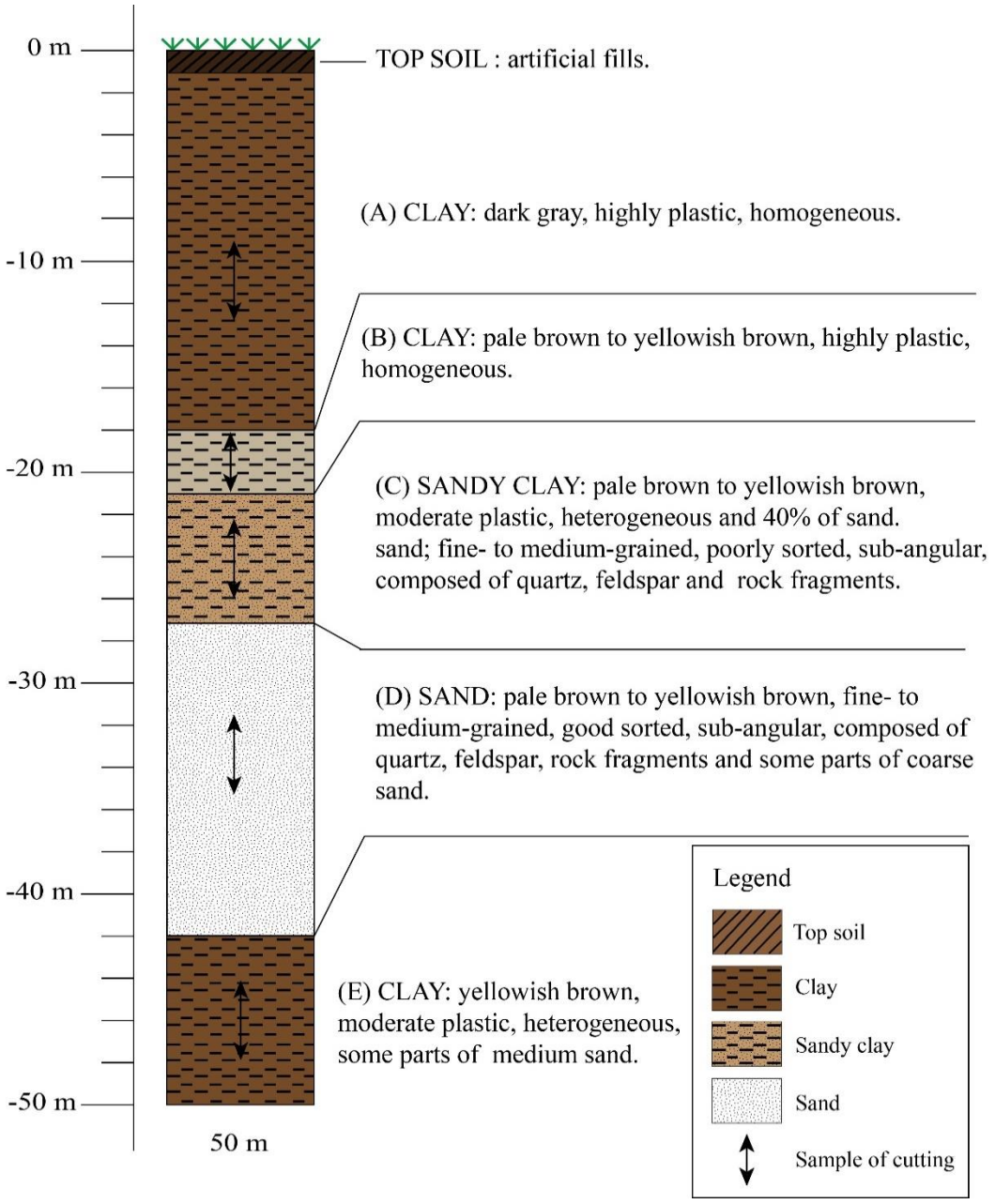

Figure 3.1 The lithologic log showing lithostratigraphy of Quaternary deposits, well no. 1 at Parot Racha building, Chulalongkorn University (see the location in Figure 2.2).

The cutting samples of well no.2 can be classified into 6 layers as shown in Figure 3.2.

- Layer A consists of dark gray clay that is highly plastic and homogeneous, which was collected from 0 to 14 meters depth (14 meters thickness) as shown in Figure 3.4A.

- Layer B consists of pale brown to yellowish brown clay that is highly plastic and homogeneous, which was collected from 15 to 20 meters depth (6 meters thickness) as shown in Figure 3.4B.

- Layer C is composed of pale brown to yellowish brown sandy clay. It comprises 60 % of clay that is moderate plastic, heterogeneous and 40 % of sand that is fine- to medium-grained, poorly sorted and sub-angular. Furthermore, it is composed of quartz, feldspar and rock fragments. The layer was collected from 21 to 23 meters-depth (3 meters-thickness) as shown in Figure 3.4C.

- Layer D consists of pale brown to yellowish brown sand that is fine- to medium-grained, good sorted and sub-angular. Moreover, it is composed of quartz, feldspar, rock fragments and some parts of coarse sand. The layer was collected from 24 to 38 meters depth (14 meters thickness) as shown in Figure 3.4D.

- Layer E consists of yellowish brown sandy to silty clay. It comprises of 55 % of clay that is moderate plastic, heterogeneous and 45 % of sand that is fine- to medium-grained, poorly sorted and sub-angular. In addition, it is composed of quartz, feldspar and rock fragments. The layer was collected from 39 to 39 meters depth (1 meters thickness) as shown in Figure 3.4E.

- Layer F consisting of pale brown clayey sand. It is composed of 20 % of clay and 80 % of sand that is medium-grained, good sorted, sub-angular. In terms of composition, this part of sand comprises quartz, feldspar and rock fragments. The layer was collected from 40 to 48 meters depth (9 meters thickness) as shown in Figure 3.4F.

Additionally, the real thickness may be disturbed from collecting sediments.

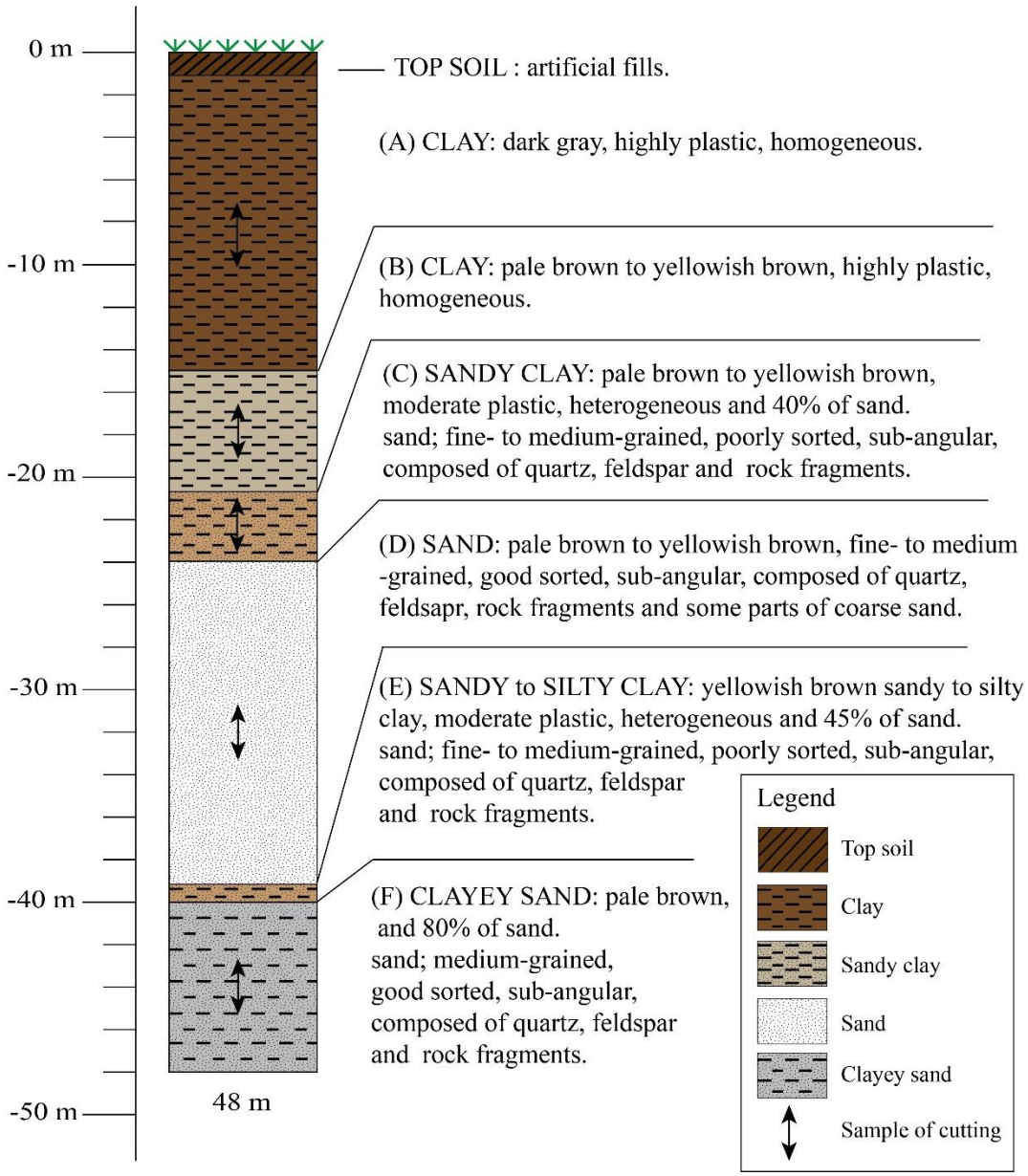

Figure 3.2 The lithologic log showing lithostratigraphy of Quaternary deposits, well no. 2 at Parot Racha building, Chulalongkorn University (see the location in Figure 2.2).

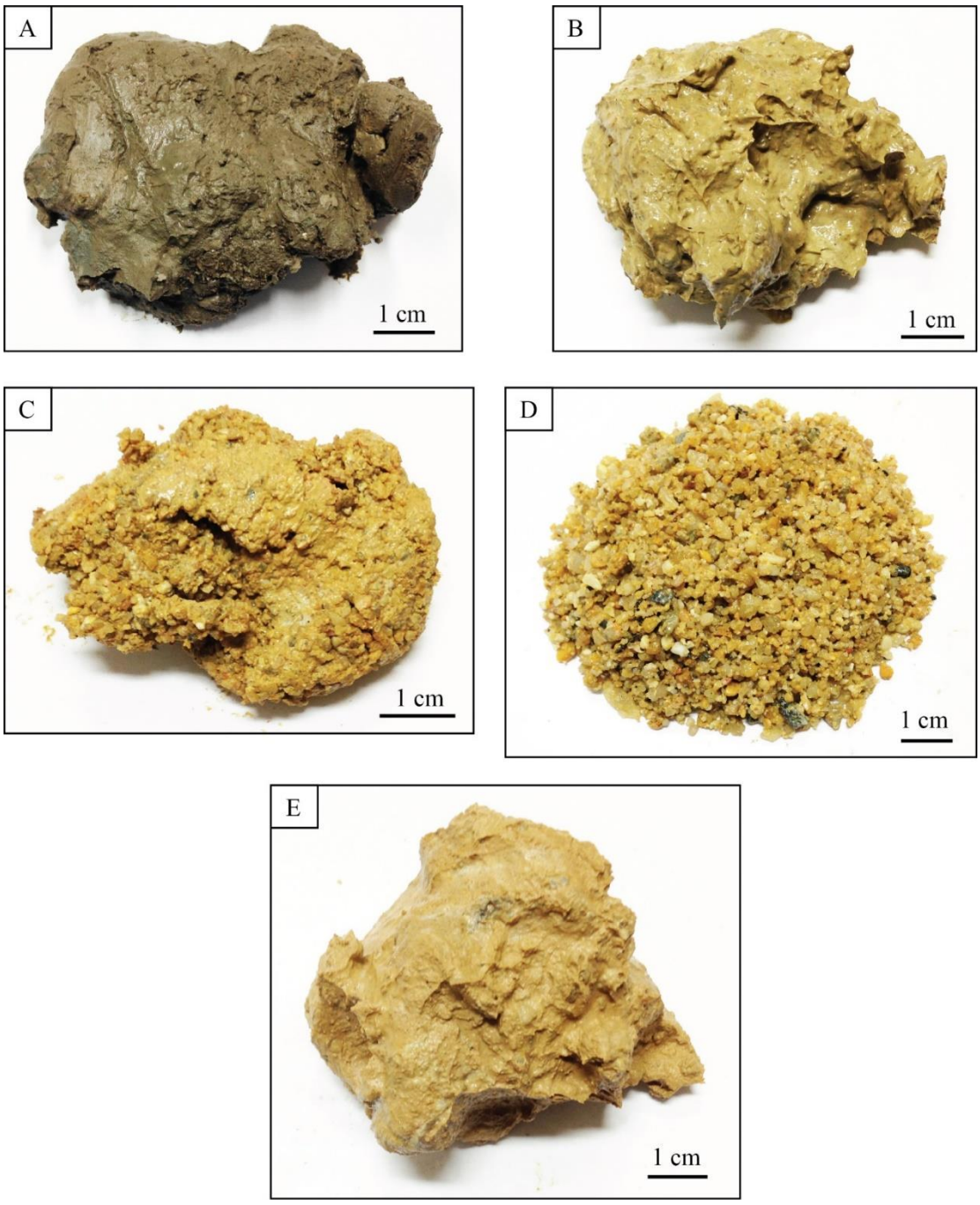

Figure 3.3 Samples of cuttings were collected from the well no.1 at Parot Racha Building, Chulalongkorn University.

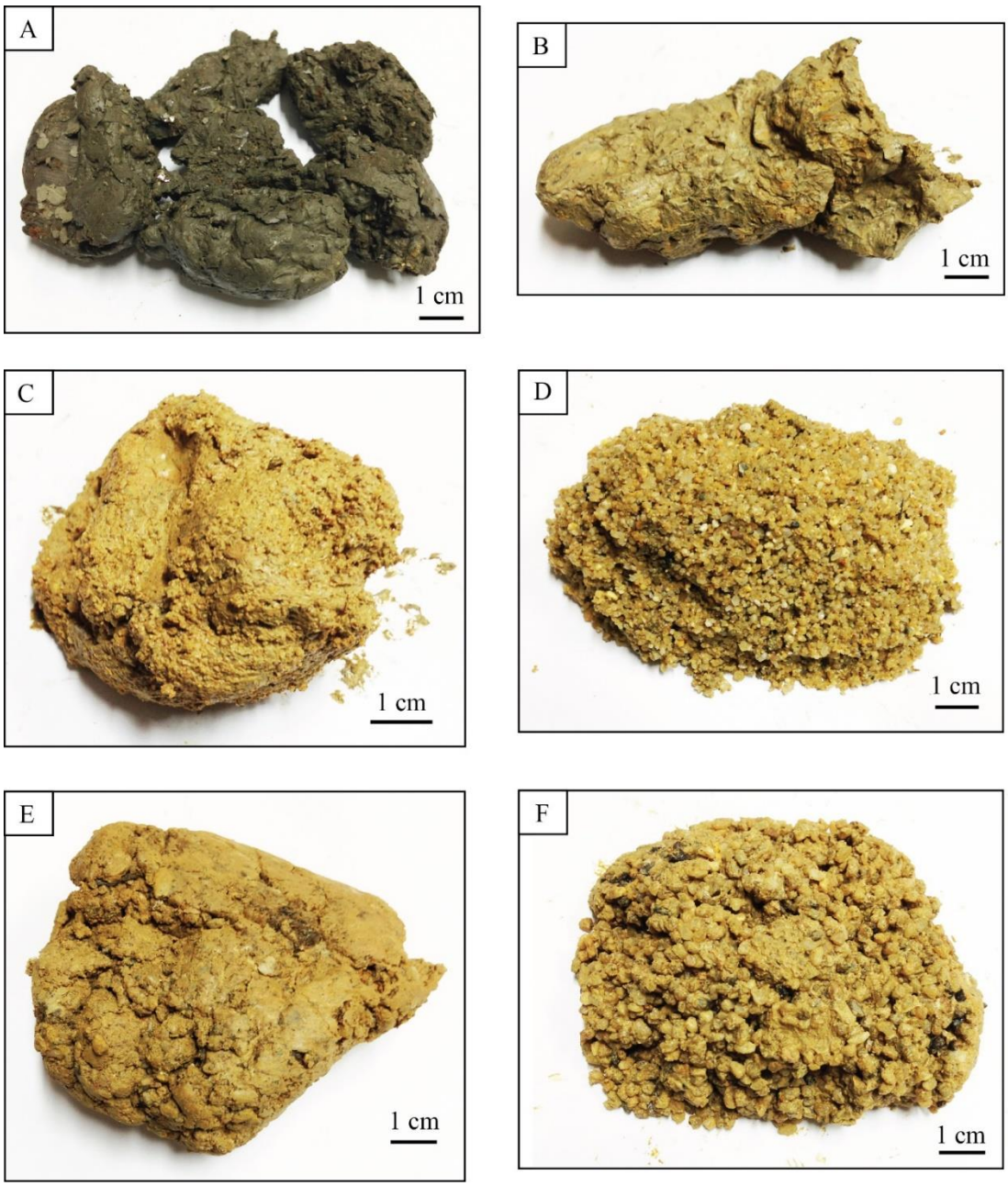

Figure 3.4 Samples of cuttings are collected from well no.2 at Parot Racha Building, Chulalongkorn University.

According to sediment characteristics of each lithologic log, they can be correlated into 5 layers as shown in Figure 3.5.

- Layer A ranges from 0 to 17 meters depth (17 meters thickness), consisting of dark gray clay that is highly plastic and homogeneous.

- Layer B ranges from 18 to 20 meters depth (3 meters thickness), comprising of pale brown to yellowish brown clay that is highly plastic and homogeneous.

- Layer C ranges from 21 to 26 meters depth (6 meters thickness), with pale brown to yellowish brown sandy clay. It consists of 60 % of clay that is moderate plastic, heterogeneous and 40 % of sand that is fine- to medium-grained, poorly sorted and sub-angular. In terms of composition, sand is composed of quartz, feldspar and rock fragments.

- Layer D ranges from 27 to 41 meters depth (15 meters thickness) with pale brown to yellowish brown sand, which is fine- to medium-grained, good sorted and sub-angular. In terms of composition, it is composed of quartz, feldspar, rock fragments and some parts of coarse sand.

- Layer E ranges from 42 to 50 meters depth (9 meters thickness) with yellowish brown sandy to silty clay, which is moderate plastic, heterogeneous and comprises some parts of medium sand.

Additionally, the real thickness may be disturbed from collecting sediments.

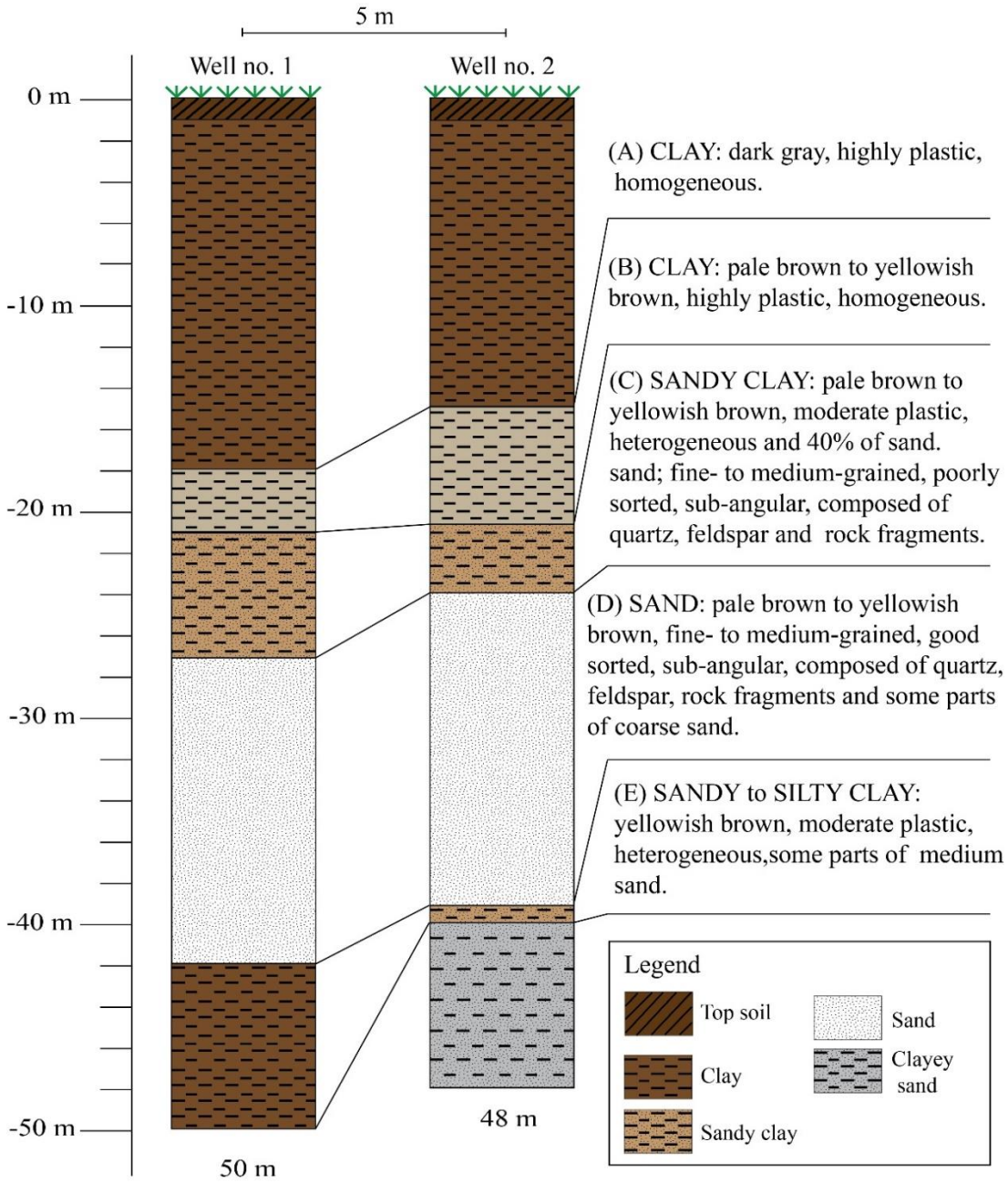

Figure 3.5 The correlation of 2 lithologic logs in this study (see the location in Figure 2.2).

3.1.2 The lithologic log of the adjacent area

The sediment characteristics of the artesian well of Department of Groundwater Resources (DGR), which is located at Chulalongkorn University Dhamma Centre, can be classified into 5 layers as shown in Figure 3.6. These layers conform to lithologic logs of those wells in this study.

- The 1st layer, situated from 0 to 17 meters depth (17 meters thickness), is dark gray clay that is highly plastic and homogeneous.

- The 2nd layer, situated from 18 to 29 meters depth (12 meters thickness), consists of pale brown to yellowish brown sandy clay. It composed 70 of % clay that is moderate plastic, heterogeneous and 30 % of sand that is very fine- to medium-grained, poorly sorted and sub-angular. Moreover, it mostly composes of quartz with subordinated feldspar and rock fragments.

- The 3rd layer, situated from 30 to 41 meters depth (12 meters thickness), mostly comprises clay.

- The 4th layer, situated from 42 to 49 meters depth (8 meters thickness), consists of pale brown sand that is fine- to coarse-grained, poorly sorted, sub-angular. It is mostly composed of quartz with subordinated feldspar, rock fragments and clay minerals.

- The 5th layer, situated from 50 to 58 meters depth (9 meters thickness), comprises yellowish brown clay that is moderate plastic, heterogeneous and some part of silt.

- The 6th layer, situated from 59 to 62 meters depth (3 meters thickness), comprises sand.

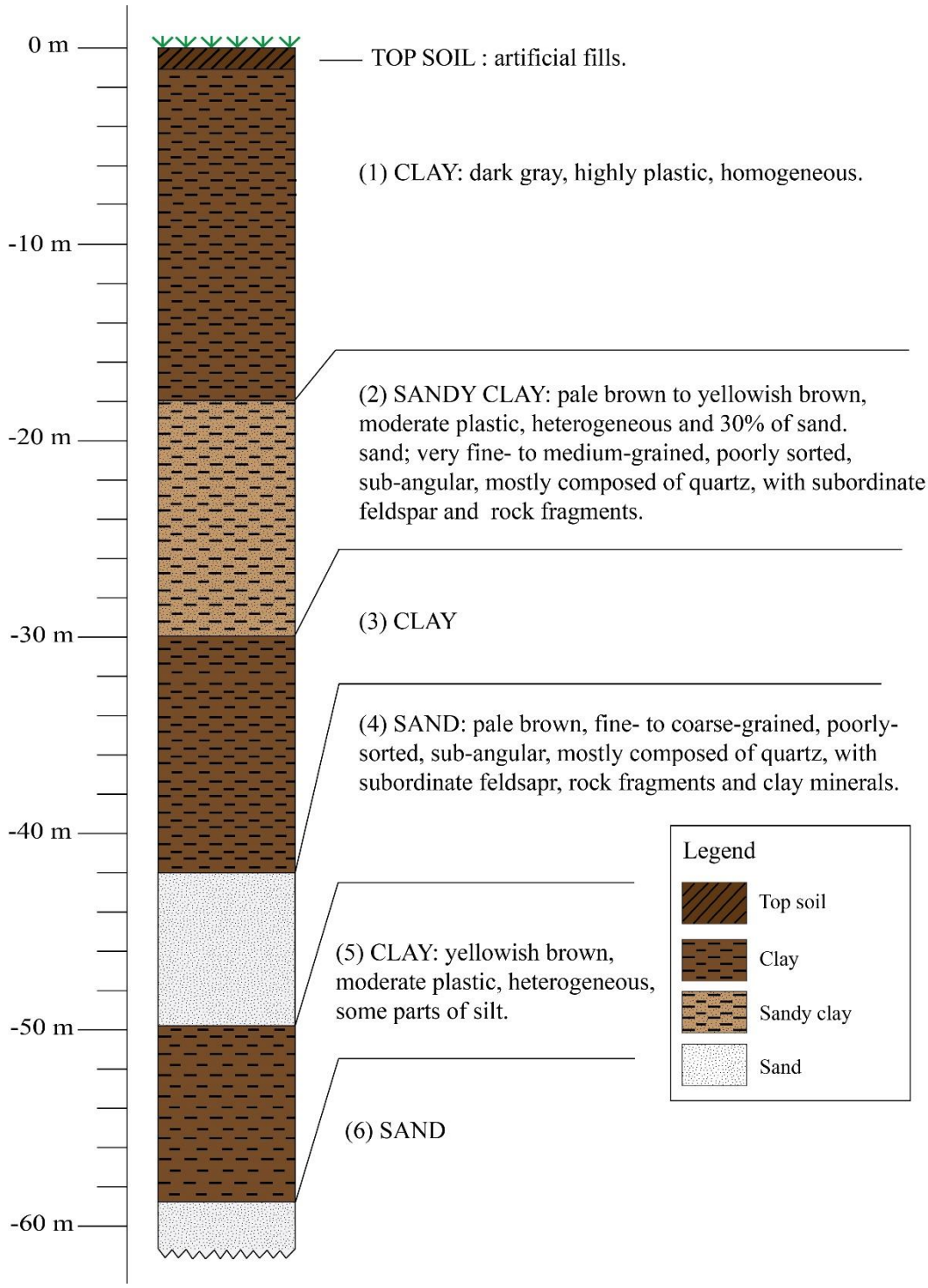

Figure 3.6 The lithologic log of Chulalongkorn University Dhamma Centre showing lithostratigraphy of Quaternary deposits between 0 to 62 m depth (see the location in Figure 2.2) (modified after Department of Groundwater Resources (DGR) (2011)).

3.1.3 The correlation of lithologic log

In this study, we have selected 7 groundwater wells from DGR in order to compare lithostratigraphy in Bangkok area (see locations in Figure 3.7). These 7 wells consist of TLC-1, TLC-2 (western part), HK, PKN, BKP (central part), as well as LKB-1 and LKB-2, located in the eastern part.

(1) Lithologic log of TLC-1

TLC-1 is the groundwater well of DGR, which can be divided into 4 layers as shown in Figure 3.8.

- Layer A, situated from 0 to 28 meters depth (28 meters thickness), consists of clay.
- Layer B, situated from 28 to 62 meters depth (34 meters thickness), consists of clayey gravel.
- Layer C, situated from 62 to 73 meters depth (11 meters thickness), consists of clay.
- Layer D, situated from 73 to 92 meters depth (19 meters-thickness), consists of clayey gravel.
- Layer E, situated from 92 to 125 meters depth (33 meters-thickness), consists of sandy gravel and some parts of clay.

(2) Lithologic log of TLC-2

TLC-2 is the groundwater well belonged to DGR, which can be divided into 8 layers as shown in Figure 3.8.

- Layer A, situated from 0 to 16 meters depth (16 meters thickness), consists of clay and some parts of gravel.
- Layer B, situated from 16 to 29 meters depth (13 meters thickness) consists of gravel.
- Layer C, situated from 29 to 34 meters depth (5 meters thickness) consisting of sandy gravel.
- Layer D, situated from 34 to 38 meters depth (4 meters thickness) consists of sand.

- Layer E, situated from 38 to 42 meters depth (4 meters thickness) consists of clay and some parts of gravel.

- Layer F, situated from 42 to 70 meters depth (28 meters thickness) consists of sandy gravel.

- Layer G, situated from 70 to 78 meters depth (8 meters thickness) consists of sandy clay.

- Layer H, situated from 78 to 102 meters depth (24 meters thickness) consists of clayey sand.

(3) Lithologic log of HK

HK is the groundwater well from DGR, which can be divided in to 7 layers as shown Figure 3.8.

- Layer A, situated from 0 to 27.5 meters depth (27.5 meters thickness) consists of clay.

- Layer B, situated from 27.5 to 35.5 meters depth (8 meters thickness) consists of sand.

- Layer C, situated from 35.5 to 45.5 meters depth (10 meters thickness) consists of clay.

- Layer D, situated from 45.5 to 61.0 meters depth (15.5 meters thickness) consists of sand.

- Layer E, situated from 61.0 to 80.0 meters depth (19 meters thickness) consists of gravel.

- Layer F, situated from 80.0 to 89.0 meters depth (9 meters thickness) consists of clay.

- Layer G, situated from 89.0 to 105.0 meters depth (16 meters thickness) consists of sand.

(4) Lithologic log of PKN

PKN is the artesian well from DGR, which can be divided in to 9 layers as shown in Figure 3.8.

- Layer A, situated from 0 to 10 meters depth (10 meters thickness) consists of clay.

- Layer B, situated from 10 to 20 meters depth (10 meters thickness) consists of sandy clay.

- Layer C, situated from 20 to 30 meters depth (10 meters thickness) consists of clayey sand.

- Layer D, situated from 30 to 35 meters depth (5 meters thickness) consists of clay.

- Layer E, situated from 35 to 52 meters depth (17 meters thickness) consists of sandy clay.

- Layer F, situated from 52 to 65 meters depth (13 meters thickness) consists of clay and some parts of gravel.

- Layer G, situated from 65 to 86 meters depth (21 meters thickness) consists of clayey sand.

- Layer H, situated from 86 to 92 meters depth (6 meters thickness) consists of clay and some parts of gravel.

- Layer I, situated from 92 to 109 meters depth (17 meters thickness) consists of clayey sand.

(5) Lithologic log of BKP

BKP is the artesian well from DGR, which can be divided in to 7 layers as shown in Figure 3.8.

- Layer A, situated from 0 to 20 meters depth (20 meters thickness) consists of clay.

- Layer B, situated from 20 to 31 meters depth (11 meters thickness) consists of sand.

- Layer C, situated from 31 to 48 meters depth (17 meters thickness) consists of clay.

- Layer D, situated from 48 to 72 meters depth (24 meters thickness) consists of sand.

- Layer E, situated from 72 to 79 meters depth (7 meters thickness) consists of gravel.

- Layer F, situated from 79 to 82 meters depth (3 meters thickness) consists of clay.

- Layer G, situated from 82 to 100 meters depth (18 meters thickness) consists of sand.

(6) Lithologic log of LKB-1

LKB-1is the artesian well from DGR, which can be divided in to 7 layers as shown in Figure 3.8.

- Layer A, situated from 0 to 23.5 meters depth (23.5 meters thickness) consists of clay.

- Layer B, situated from 23.5 to 31.5 meters depth (8 meters thickness) consists of sand.

- Layer C, situated from 31.5 to 40.9 meters depth (9.4 meters thickness) consists of clay.

- Layer D, situated from 40.9 to 54.8 meters depth (13.9 meters thickness) consists of sand.

- Layer E, situated from 54.8 to 62.8 meters depth (8 meters thickness) consists of clay.

- Layer F, situated from 62.8 to 73.8 meters depth (11 meters thickness) consists of sand.

- Layer G, situated from 73.8 to 102.7 meters depth (28.9 meters thickness) consists of clay.

(7) Lithologic log of LKB-2

LKB-2 is the artesian well from DGR, which can be divided in to 7 layers as shown in Figure 3.8.

- Layer A, situated from 0 to 21 meters depth (21 meters thickness) consists of clay.

- Layer B, situated from 21 to 51 meters depth (30 meters thickness) consists of sand.

- Layer C, situated from 51 to 69 meters depth (18 meters thickness) consists of clay.

- Layer D, situated from 69 to 89 meters depth (20 meters thickness) consists of sandy clay.

- Layer E, situated from 89 to 92 meters depth (3 meters thickness) consists of sand.

- Layer F, situated from 92 to 98 meters depth (6 meters thickness) consists of clay.

- Layer G, situated from 98 to 110 meters depth (12 meters thickness) consists of sand.

As a result, lithostratigraphy of Central part-, Eastern part- and Western part of Bangkok can be divided into 4 major layers such as clay (Bangkok clay), sand (Bangkok aquifer), clay and sand (Phra Pradaeng aquifer) respectively as shown in Figure 3.8.

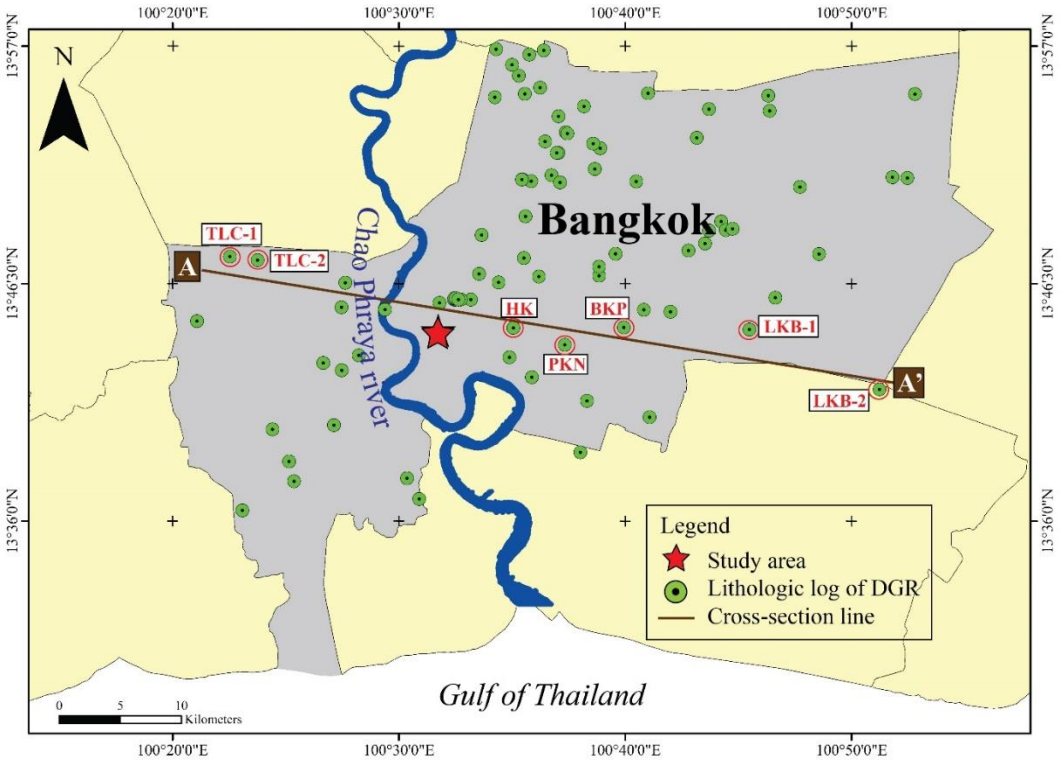

Figure 3.7 Index map of the Lower Chao Phraya Plain showing the locations of the study area (★) and nearest temperature observation wells (circle). Western part including; TLC-1 and TLC-2. Central part including; HK, PKN and BKP. Eastern part including; LKB-1 and LKB-2.

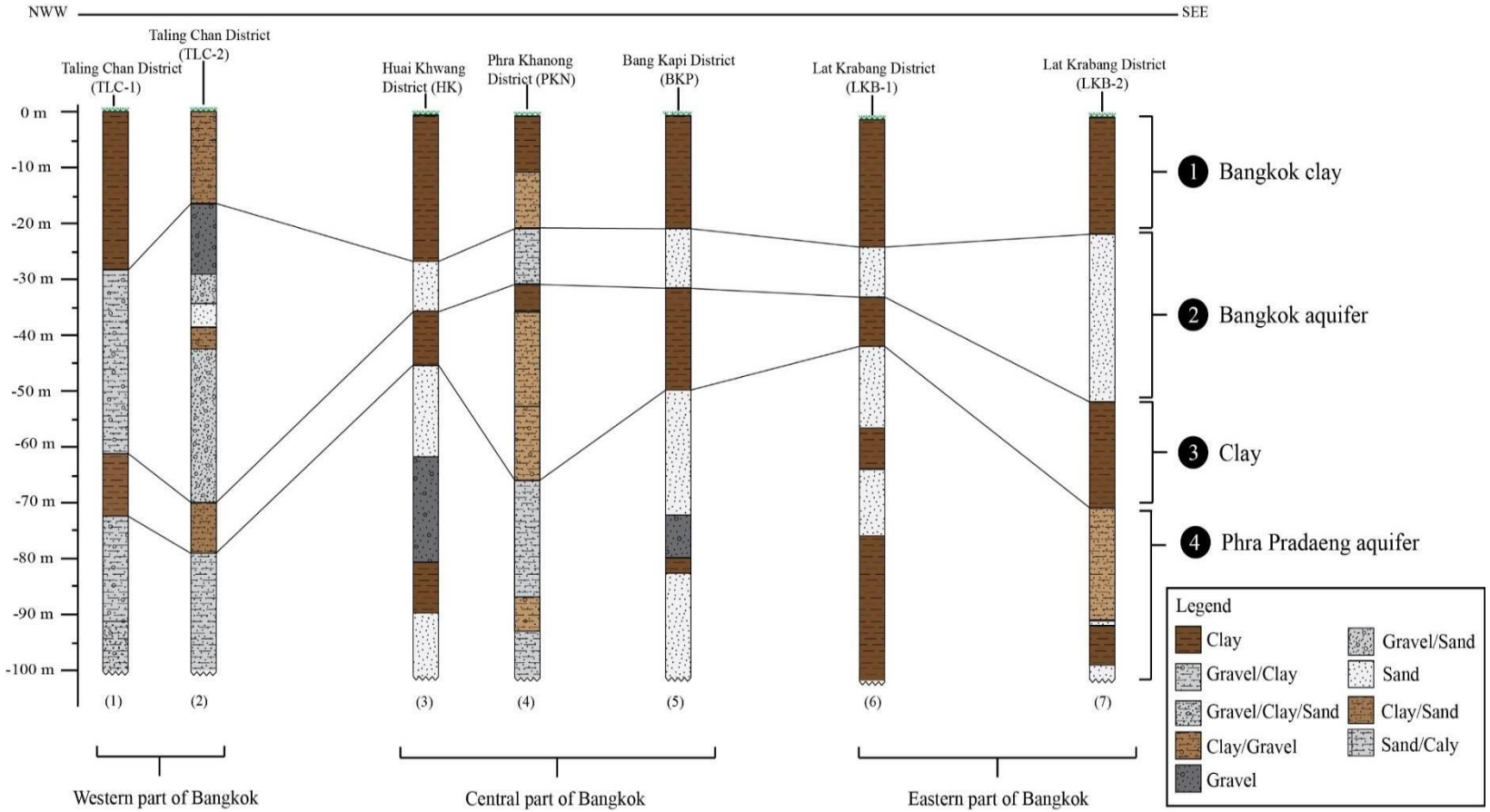

Figure 3.8 The correlation of lithologic log showing lithostratigraphy of Quaternary deposits of TLC-1, TLC-2, HK, PKN, BKP, LKB-1 and LKB-2 (data from DGR, Digital file) (see locations in Figure 3.7).

3.2 Temperature measurements

In this study, there were 4 parts of temperature measurement as follows: subsurface and outside-air temperatures, outside-air temperature, cooling room temperature, and inlet liquid temperature and outlet liquid temperature of GHP system.

3.2.1 Subsurface and outside-air temperatures

As depicted in Figure 3.9, subsurface temperature data have been recorded at depth of 8 m (thermistor no. 4), 10 m (thermistor no. 5), 25 m (thermistor no. 6), and 50 m (thermistor no. 7). An example of data output for underground temperature measurement was illustrated in Figure 3.7. The data was recorded on 15th May, 27th June, 4th, 10th, 19th and 24th June 2014. The results shows that the ranges of subsurface temperatures were 29.6 - 29.8 °C, 29.6 - 29.8 °C, 29.8 - 30 °C and 30.5- 30.7 °C at depths of 8, 10, 25 and 50 m, respectively (see Table 3.1). The graph also indicated that the temperatures were almost constant at the same depth for 45 days as shown in Figure 3.9.The graph showed that the subsurface temperature gradually increase at deeper depth.

Table 3.1 Subsurface temperature measurement at depths of 8, 10, 25 and 50 m in 6 days measurement (for a short –time).

Date	Time	Subsurface temperature (°C)			
		8 m	10 m	25 m	50 m
15/5/2014	10.00 AM	29.6	29.6	30.0	30.5
27/5/2014	10.00 AM	29.7	29.8	29.9	30.7
4/6/2014	10.36 AM	29.7	29.7	29.8	30.7
10/6/2014	10.05 AM	29.8	29.7	29.9	30.7
19/6/2014	10.00 AM	29.7	29.8	30.0	30.7
24/6/2014	10.00 AM	29.8	29.8	30.0	30.7

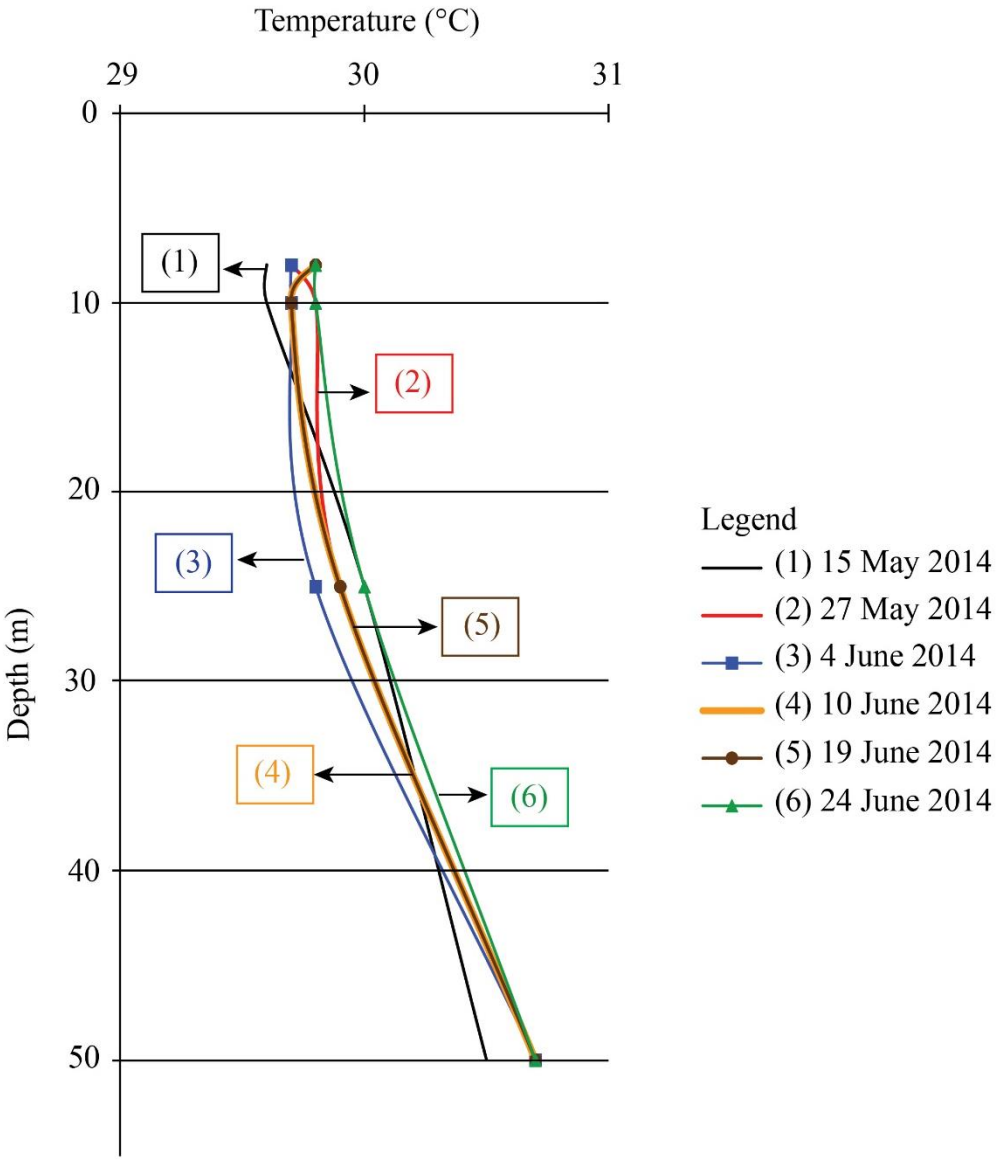

Figure 3.9 Temperature profiles of the observation well nos.1 and 2 at depths of 8, 10, 25 and 50 m at Parot Racha Building, Chulalongkorn University. Noted that the data logger was installed in August 2014 together with thermistor at depth of 1.5 m (thermistor no. 2) and 3 m (thermistor no. 3). However thermistors at depths of 10, 25 and 50 m were broken so they were not able to use after that.

The data logger was installed in August 2014 together with thermistor at depth of 1.5 m (thermistor no. 2) and 3 m (thermistor no. 3), so there were long-term recorded data of subsurface temperature as shown in Table 3.2.

Table 3.2 Monthly average subsurface temperature measurement at depths of 1.5, 3, 8, 10, 25 and 50 m (for a long – time) from May 2014 to September 2016.

Month/Year	**Subsurface temperature (°C)**					
	1.5 m	**3 m**	**8 m**	**10 m**	**25 m**	**50 m**
May 2014	-	-	29.7	29.7	30.0	30.6
June 2014	-	-	29.8	29.8	29.9	30.7
July 2014	-	-	29.9	-	-	-
August 2014	29.3	29.2	29.9	-	-	-
September 2014	29.3	29.1	29.9	-	-	-
October 2014	29.0	28.9	29.8	-	-	-
November 2014	29.0	28.9	29.8	-	-	-
December 2014	28.8	28.5	29.8	-	-	-
January 2015	28.6	28.4	29.7	-	-	-
February 2015	29.0	28.9	30.0	-	-	-
March 2015	29.5	29.2	30.0	-	-	-
April 2015	29.5	29.1	30.0	-	-	-
May 2015	29.7	29.3	30.1	-	-	-
June 2015	29.0	29.0	29.7	-	-	-
July 2015	29.1	29.0	29.8	-	-	-
August 2015	29.0	-	29.8	-	-	-
September 2015	28.9	-	29.7	-	-	-
October 2015	28.9	-	30.0	-	-	-
November 2015	29.2	-	30.0	-	-	-
December 2015	28.9	-	29.8	-	-	-

Month/Year	Subsurface temperature (°C)					
	1.5 m	**3 m**	**8 m**	**10 m**	**25 m**	**50 m**
January 2016	28.7	-	29.6	-	-	-
February 2016	28.6	-	29.6	-	-	-
March 2016	29.1	-	30.0	-	-	-
April 2016	29.7	-	30.0	-	-	-
May 2016	30.4	-	30.1	-	-	-
June 2016	29.3	-	30.3	-	-	-
July 2016	29.4	-	30.2	-	-	-
August 2016	29.2	-	30.2	-	-	-
September 2016	29.1	-	30.4	-	-	-
Average	**29.2**	**29.0**	**29.9**	**29.7**	**29.9**	**30.7**

An average subsurface temperature of 1.5, 3, 8, 10, 25 and 50 meter-depth were 29.2°C, 29.0°C, 29.9°C, 29.7°C, 29.9°C and 30.7°C, respectively, and constant for a long-time from May 2014 to September 2016, but at depth of 1.5 meters gave a highest fluctuation of caused by atmospheric temperature as shown in Figure 3.10.

Note: Thermistors at depths of 10, 25 and 50 m were broken before data logger was installed in August, 2014.

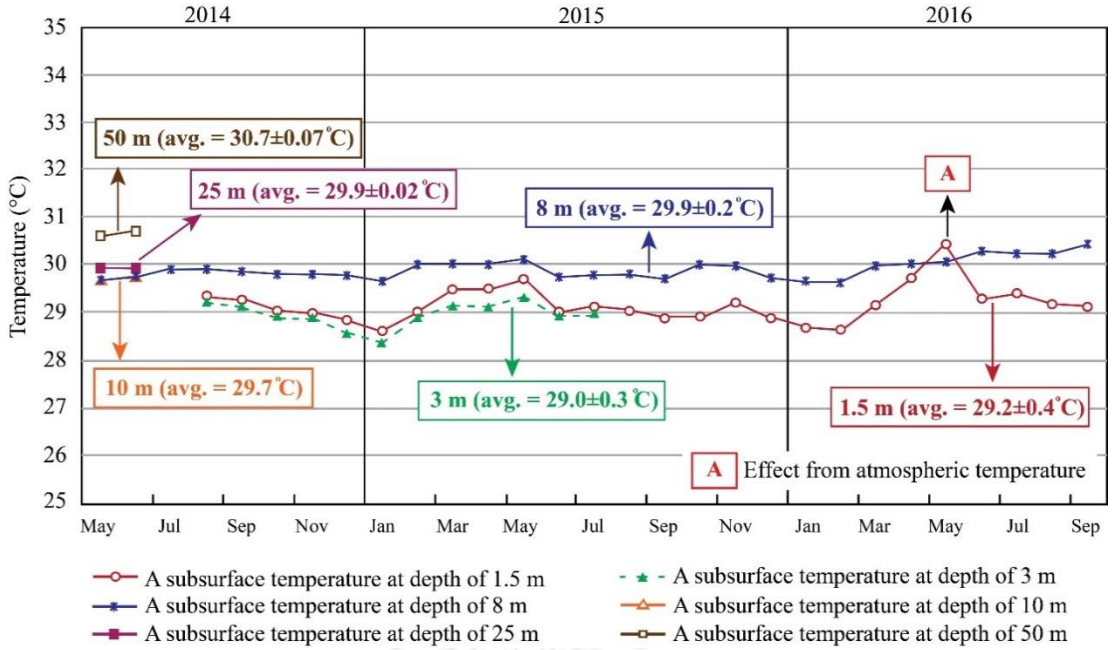

Figure 3.10 Temperature (°C)-time (month) plots showing a fairly constant subsurface temperature in a long-term measurement at depths 1.5, 3, 8, 10, 25 and 50 m, Parot Racha Building, Chulalongkorn University, from May 2014 to September 2016. Noted that point A (at 1.5 m) gave a highest fluctuation of temperature than the adjoining points because of the effect of high air-temperature moisture and atmospheric temperature.

3.2.2 Outside-air temperature

The atmospheric temperature (outside-air temperature) data have been recorded at surroundings of Parot Racha building. In a long-term, outside-air temperatures were recorded during 9.00 to 16.00 in each month as shown in Table 3.3.

Table 3.3 Monthly average atmospheric maximum and minimum temperature measurement during 9.00 AM to 4.00 PM from July 2014 to September 2016.

Month/Year	**Average atmospheric maximum temperature (ºC)**	**Average atmospheric minimum temperature (ºC)**
July 2014	32.0	28.8
August 2014	31.4	28.1
September 2014	31.7	27.6
October 2014	30.2	26.7
November 2014	29.2	27.6
December 2014	28.6*[2]	25.8
January 2015	28.8	24.9*[2]
February 2015	31.2	27.0
March 2015	31.5	28.4
April 2015	32.9	28.8
May 2015	33.5	30.9*[1]
June 2015	32.3	29.1
July 2015	32.1	29.4
August 2015	32.2	29.0
September 2015	31.2	27.8
October 2015	30.6	27.1
November 2015	32.0	27.9
December 2015	32.0	27.6

Month/Year	Average atmospheric maximum temperature (ºC)	Average atmospheric minimum temperature (ºC)
January 2016	30.2	25.6
February 2016	31.1	26.5
March 2016	32.8	28.7
April 2016	34.6*[1]	30.7
May 2016	34.4	30.7
June 2016	31.6	28.2
July 2016	31.6	28.1
August 2016	31.8	28.2
September 2016	30.8	27.4

*[1] highest temperature (S)
*[2] lowest temperature (W)

A highest monthly average atmospheric maximum was 34.6 °C in April, 2016 and a lowest monthly average atmospheric maximum was 28.6 °C in December, 2014. Moreover, a highest monthly average atmospheric minimum was 30.9 °C in May, 2015 and a lowest monthly average atmospheric minimum was 24.9 °C in January, 2015 as shown in Figure 3.11.

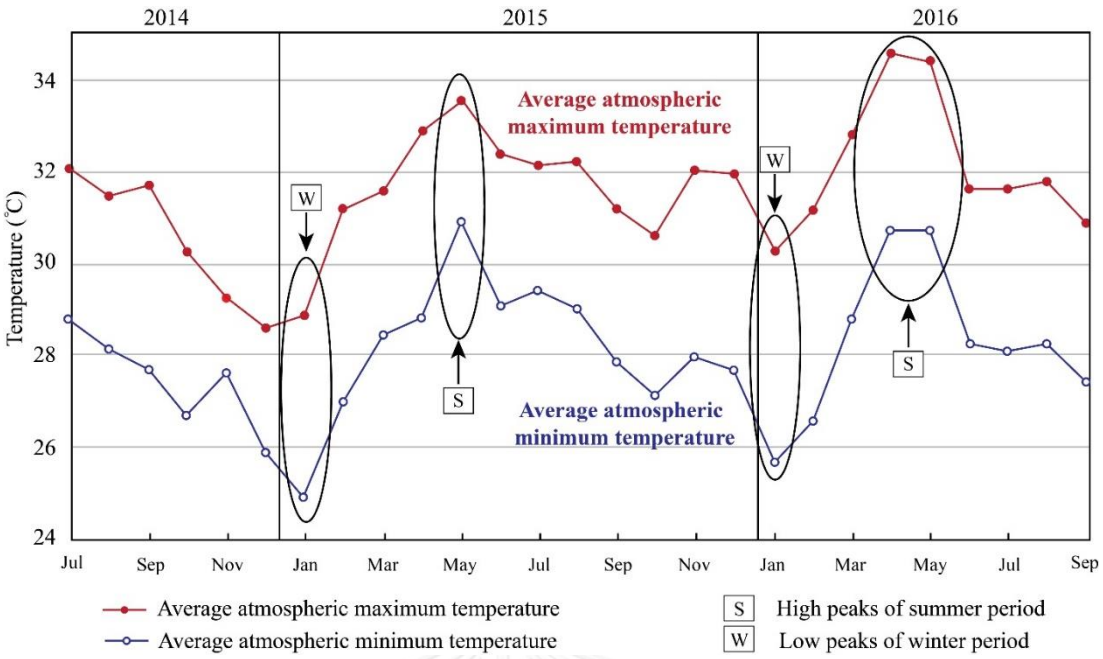

Figure 3.11 Temperature (°C)-time (month) plots showing fluctuation of monthly atmospheric (outside-air) temperatures in a long-term measurement (from July 2014 to September 2016), Parot Racha Building, Chulalongkorn University. Noted that point S gave high temperature because of summer period.

In a long-term comparison, outside-air and subsurface temperatures were reported. The outside-air temperatures were recorded during 9.00 to 16.00, whereas the subsurface temperatures were measured at depths of 1.5 to 8 meters in each month. The subsurface temperatures were more stable within the approximate range of 29 to 30 °C. Moreover, the subsurface temperatures were lower than monthly mean maximum outside air temperatures almost throughout the year as shown in Figure 3.12.

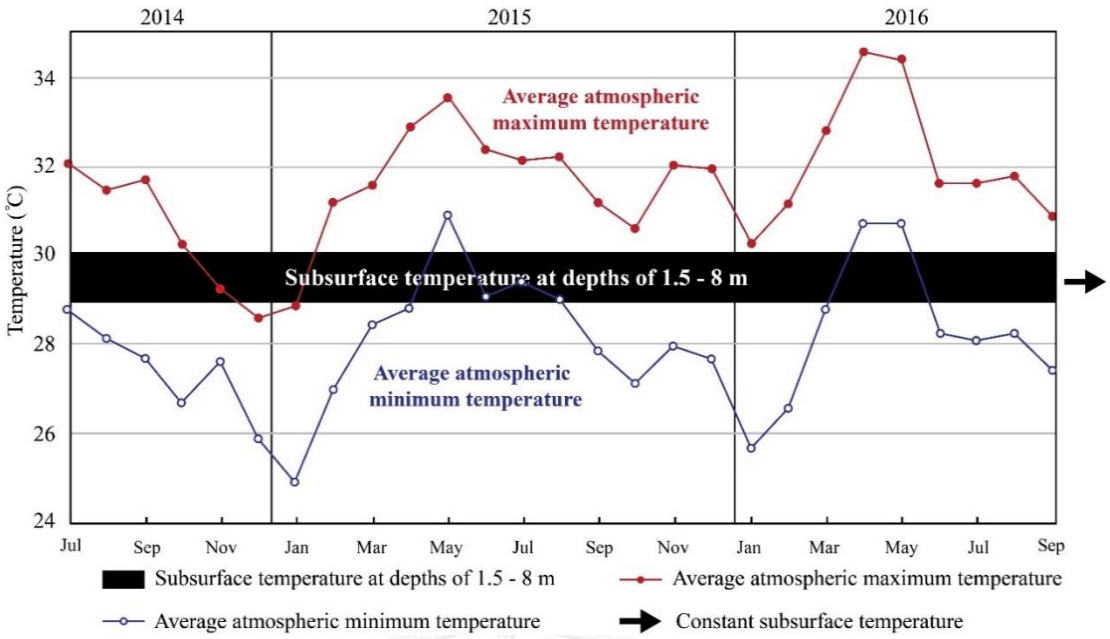

Figure 3.12 Comparison of atmospheric (outside-air) temperatures and subsurface temperatures in a long-term measurement (from July 2014 to September 2016), Parot Racha Building, Chulalongkorn University.

3.2.3 Cooling room temperature

In this study, room temperature of GHP air-conditioner (GHP) and normal air-conditioner (AC) were controlled at 25 °C and data have been recorded at the experimental room. In the long-term recorder from June, 2015 to Sep., 2016, both room temperatures were recorded during operation in each month as shown in Table 3.4

Table 3.4 Average room temperature during operation at 25 °C by remote control from June 2015 to September 2016.

Month/Year	**Average room temperature during operation (°C)**	
	GHP	**AC**
June 2015	-	25.0
July 2015	25.6	24.3
August 2015	25.6	25.0
September 2015	25.7	24.6
October 2015	25.6	24.6
November 2015	24.7	-
December 2015	24.7	24.6
January 2016	24.8	24.4
February 2016	24.6	-
March 2016	24.8	24.7
April 2016	24.7	24.6
May 2016	24.2	24.1
June 2016	24.5	24.3
July 2016	24.5	24.4
August 2016	24.2	24.4
September 2016	24.6	24.0
Average	**24.9**	**24.5**

In a long-term operation, cooling room temperature of GHP air-conditioner (GHP) and normal air-conditioner (AC) were controlled at 25 °C, showing average temperature 24.9 °C and 24.5 °C respectively. This results showed that GHP air-conditioner (GHP) and normal air-conditioner (AC) were stable and almost the same cooling efficiency as shown in Figure 3.13.

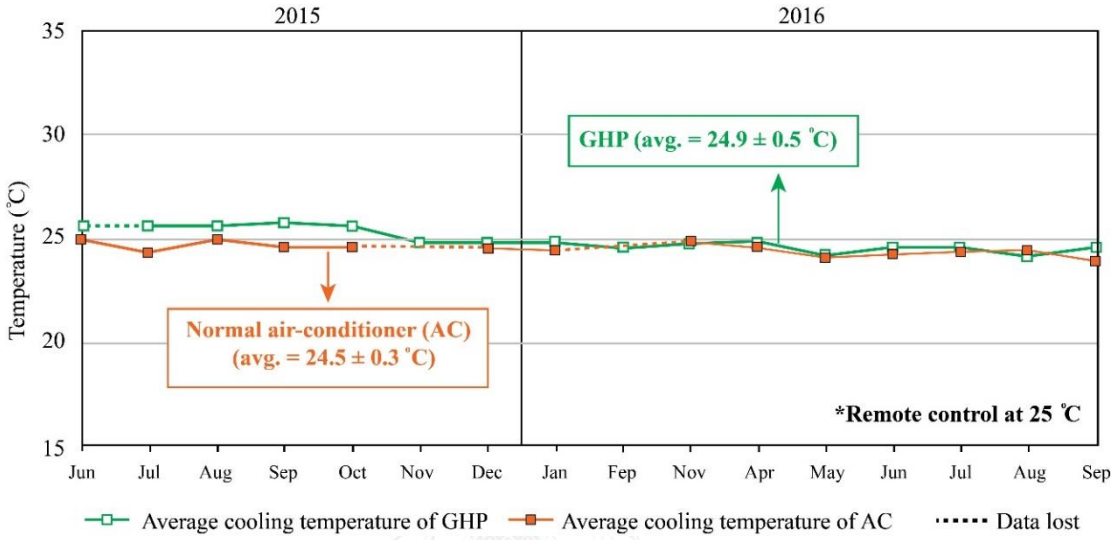

Figure 3.13 Comparison of cooling room temperatures of GHP air-conditioner (GHP) and normal air-conditioner (AC) in a long-term measurement (from June 2015 to September 2016) at experimental room, Parot Racha Building, Chulalongkorn University.

3.2.4 Inlet liquid temperature and outlet liquid temperature of GHP system

As depicted in Figure 2.23, inlet liquid temperature and outlet liquid temperature data of GHP air-conditioner (GHP) have been recorded at thermistor nos. 1 & 8 respectively. In the long-term, there were inlet liquid temperature and outlet liquid temperature during operation as shown in Table 3.5.

Table 3.5 Average inlet liquid temperature and outlet liquid temperature of GHP in each month during operation from July 2015 to September 2016.

Month/Year	**Average inlet liquid temperature (°C)**	**Average outlet liquid temperature (°C)**
July 2015	32.1	33.4
August 2015	32.0	33.4
September 2015	31.5	32.9
October 2015	30.2	31.6*[2]
November 2015	31.7	33.2
December 2015	30.1*[2]	31.6*[2]
January 2016	31.2	32.6
February 2016	31.3	32.8
March 2016	32.1	33.6
April 2016	34.2*[1]	36.0*[1]
May 2016	32.9	34.3
June 2016	31.6	33.2
July 2016	31.0	32.5
August 2016	31.4	32.9
September 2016	31.0	32.6
Average	**31.6**	**33.1**

*[1] highest temperature
*[2] lowest temperature

The highest average inlet liquid temperature was 34.2 °C in April, 2016 and a lowest average inlet liquid temperature was 30.1 °C in December, 2015. Besides, the highest average outlet liquid temperature is 36.0 °C in April, 2016 and the lowest average outlet liquid temperature is 31.6 °C in October and December, 2015 as shown in Figure 3.14.

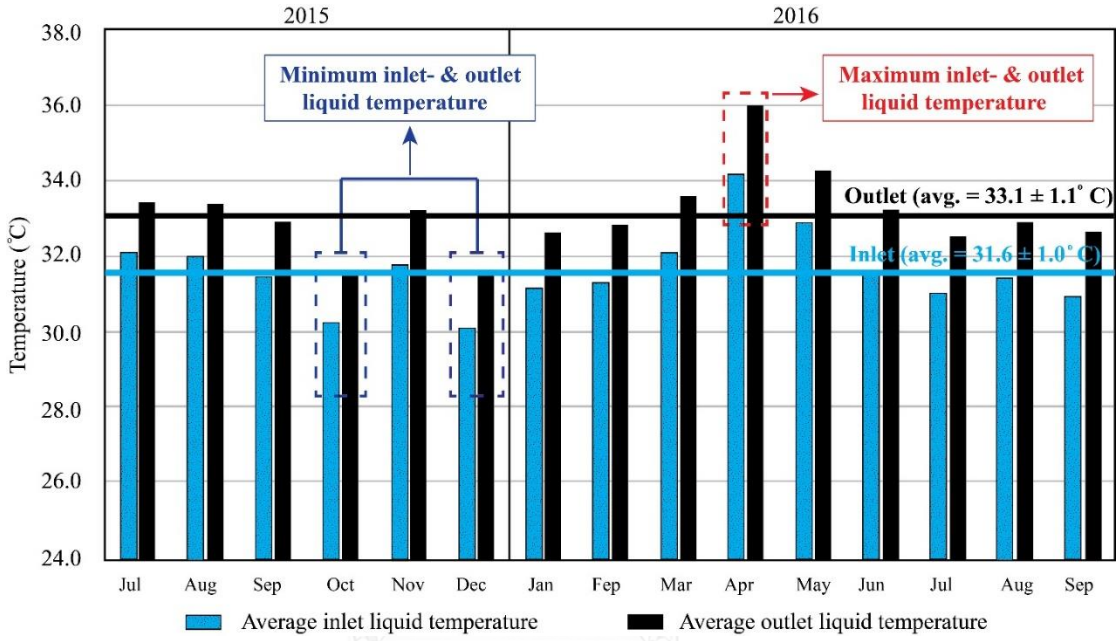

Figure 3.14 Average inlet- and outlet liquid temperatures (°C) of the GHP air-conditioner in a long-term measurement (from July 2015 to September 2016).

3.3 Flow rate

In this study, flow rates of GHP air-conditioner were recorded during operation in each month as shown in Table 3.6.

Table 3.6 Average flow rate of GHP during operation from July 2015 to September 2016.

Month/Year	**Average flow rate (l/min)**
July 2015	20.4
August 2015	19.7
September 2015	15.6
October 2015	10.1
November 2015	20.9
December 2015	9.5*[2]
January 2016	17.2
February 2016	19.2
March 2016	19.4
April 2016	24.0*[1]
May 2016	21.1
June 2016	17.8
July 2016	17.1
August 2016	19.8
September 2016	17.1
Average	**17.9**

*[1] highest flow rate
*[2] lowest flow rate

A highest average flow rate was 24.0 l/min in April, 2016 and a lowest average flow rate was 9.5 % in December, 2015 as shown in Figure 3.15.

The average flow rate of inlet- and outlet liquid temperature were reported. For long-term comparison, all data were recorded during operations in each month. The results showed that higher average flow rate gave higher inlet- and outlet liquid temperature. In the same way, lower average flow rate gave lower inlet- and outlet liquid temperature so that flow rate affects on inlet- and outlet liquid temperature as shown in Figure 3.16.

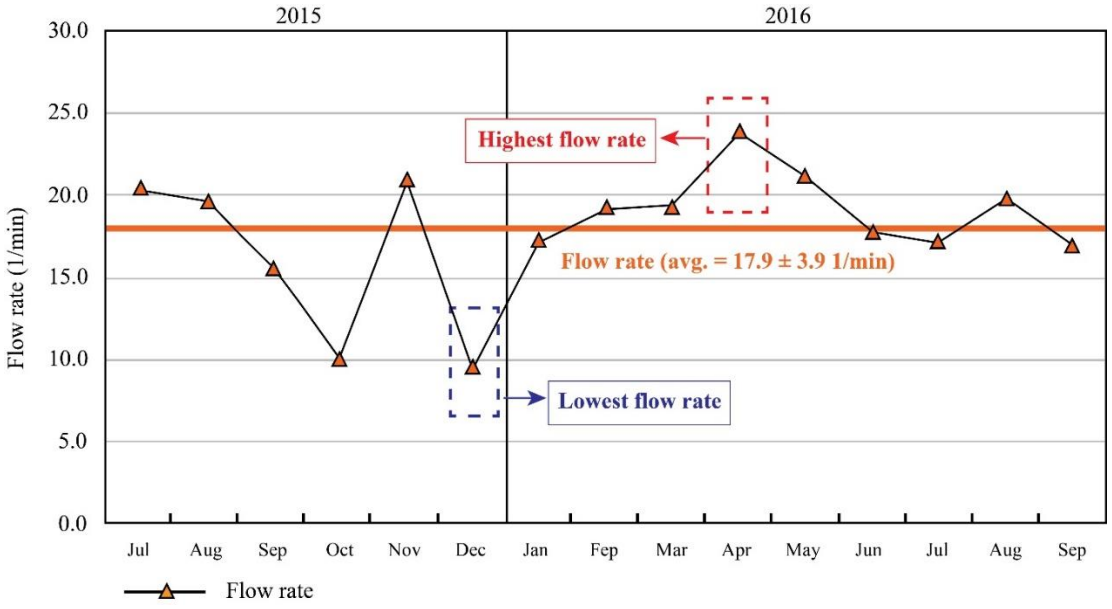

Figure 3.15 Fluctuation of flow rates (l/min) in a long-term measurement (from July 2015 to September 2016) of the GHP air-conditioner.

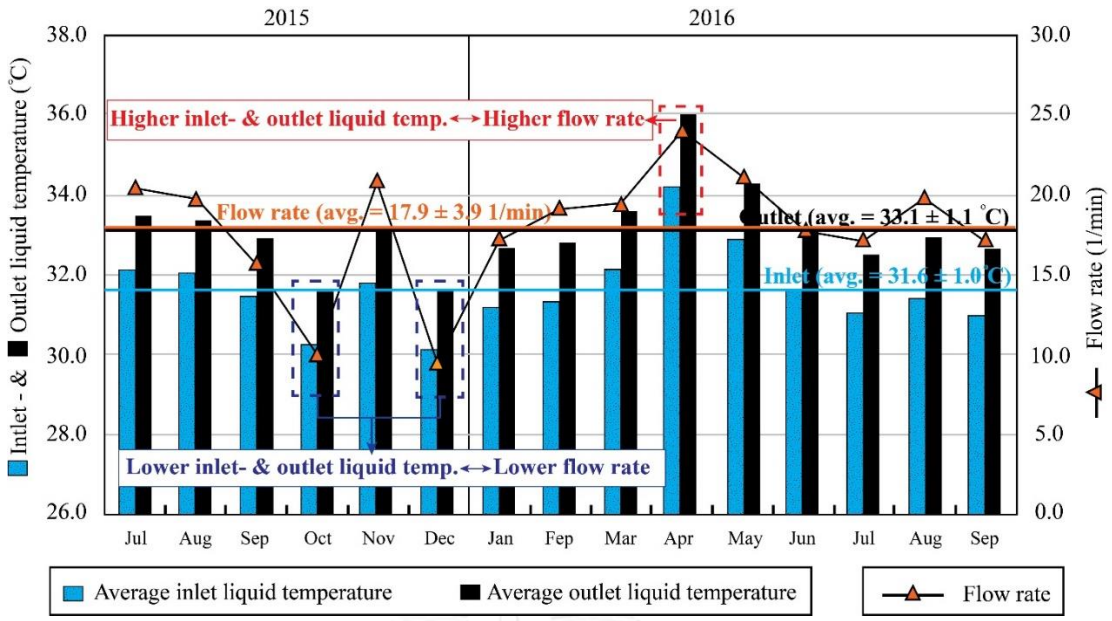

Figure 3.16 Comparison of flow rates and atmospheric (outside-air) temperatures in a long-term measurement (from July 2015 to September 2016) of the GHP air-conditioner during operation.

3.4 Humidity measurement

In this study, humidity data were recorded at the experimental room during operation in each month as shown in Table 3.7.

Table 3.7 Average humidity during operation from October 2015 to September 2016.

Month/Year	Average humidity (%)
October 2015	72.2*[1]
November 2015	61.7
December 2015	64.1
January 2016	64.1
February 2016	55.1
March 2016	52.1
April 2016	45.9*[2]
May 2016	50.9
June 2016	56.5
July 2016	57.5
August 2016	52.1
September 2016	58.5
Average	**57.6**

*[1] highest humidity

*[2] lowest humidity

The highest average humidity is 72.2 % in October, 2015 and the lowest average humidity is 45.9 % in April 2016 as shown in Figure 3.18. Humidity depends on seasonal variations.

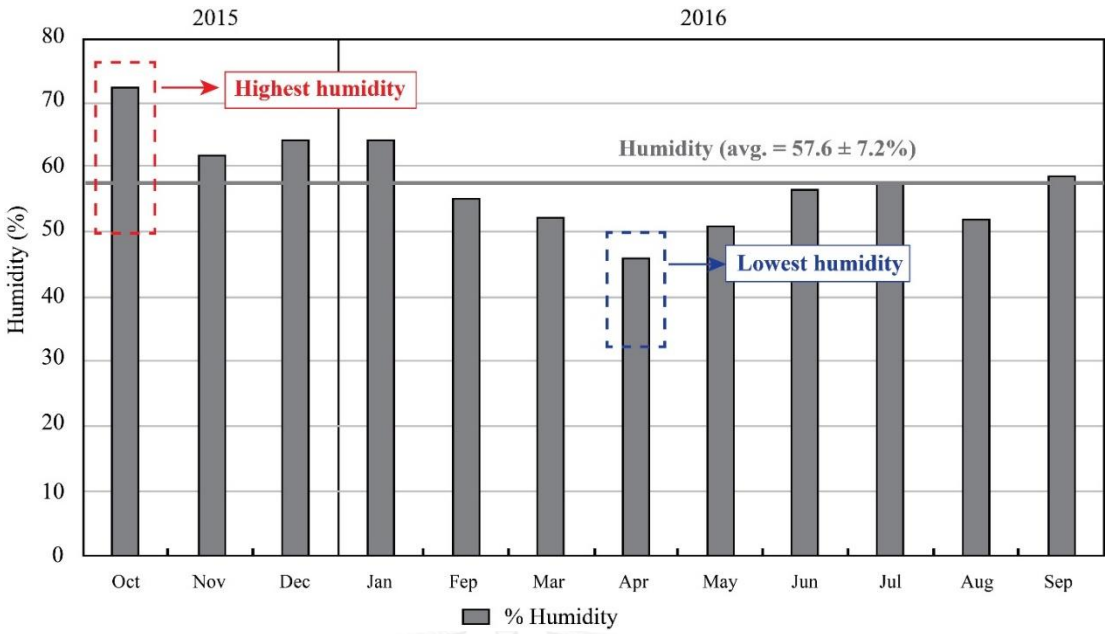

Figure 3.17 Percentages of humidity in a long-term measurement (from October 2015 to September 2016) at the experimental room, Parot Racha Building, Chulalongkorn University.

3.5 Electricity consumption

3.5.1 Statistical tests

The average of 2 population groups can be statistically compared by the t-Test method. The condition of statistical t-Test is that the quantity of sample must be less than 30 samples in each sample set. In general, the statistical t-Test can be divided into 2 methods: independent t-Test and paired t-Test (Wanichbuncha, 2009). In this study, the samples in each set were randomized independently and not controlled by other factors that possibly affected the dependent variable. Therefore, these conditions were appropriate with the independent t-Test method.

There are 2 steps to compare the average of outside-air (atmospheric) temperatures, including humidity when GHP and AC were operated.

Step 1 **F-Test Two-Sample for Variance**s: to verify whether the variance of 2 populations are equal or not

Uses the hypothesis below:

H_0: Variance for a population 1 = Variance for a population 2

H_1: Variance for a population 1 ≠ Variance for a population 2

Order | Data ➡ Data Analysis ➡ F-Test Two-Sample for Variances |

By Program **Microsoft Excel 2013**

Summary of **F-Test Two-Sample for Variances**

There are 2 cases to summarize **F-Test Two-Sample for Variances**

1. If F is more than 1

H_0 will be refused, if F > F Critical one-tail

or P(F ≤ f) one-tail < $\frac{\alpha}{2}$

2. If F is less than1

H_0 will be refused, if F < F Critical one-tail

or P(F ≤ f) one-tail < $\frac{\alpha}{2}$

Step 2 **t-Test** to compare the averages of 2 populations

Uses the hypothesis below:

H_0: The average of population 1 = The average of population 2

H_1: The average of population 1 ≠ The average of population 2

This can be divided into 2 cases based on the variance of population from step 1 (F-Test Two-Sample for Variances) and each cases use the different orders in the Microsoft Excel.

Case1: The variances are equal

Order | Data ➡ Data Analysis ➡ t-Test: Two-Sample Assuming Equal Variance |

Case2: The variances are not equal

Order | Data ➡ Data Analysis ➡ t-Test: Two-Sample Assuming Unequal Variance |

Summary of **t-Test** to compare the averages of 2 populations using Excel

H_0 will be refused: if |t Stat| > t Critical two-tail or P(T ≤ t) two-tail < α

By Program **Microsoft Excel 2013**

In this study, the averages of atmospheric temperature and humidity of the day, that GHC and AC were operated, were verified whether these 2 populations were significantly different or not. Temperature and humidity in July, 2016 were selected to be test since the highest amount of these parameters was investigated. This statistical test focused only the results of atmospheric temperature and humidity in July, 2016. The statistical tests was divided into 2 parts: the test for atmospheric (outside-air) temperature and humidity.

Atmospheric (outside-air) temperature

Table 3.8 The average of atmospheric (outside-air) temperature (°C) in each day when the GHP are operated and when the normal air-conditioner (AC) are operated in June, 2016.

Date of June, 2016	**Atmospheric (outside-air) temperature (°C)**	
	GHP	**AC**
3^1 , 9^2	31.4	33.4
13^1 ,14^2	32.2	32.3
15^1 ,16^2	31.6	28.7
17^1 ,21^2	26.8	28.2
22^1 ,23^2	29.6	30.0
27^1 ,28^2	28.9	29.3
29^1 ,30^2	30.3	30.3
Average	**30.1**	**30.3**

Note ^{1} = the day that GHP are operated

^{2} = the day that AC are operated

Step 1 **F-Test Two-Sample for Variance**s: to verify whether the variance of 2 populations were equal or not

Uses the hypothesis below

H_0: the variance of outside-air temperature for GHP = the variance of outside-air temperature for AC

H_1: the variance of outside-air temperature for GHP ≠ the variance of outside-air temperature for AC

Table 3.9 F-Test Two-Sample for Variances of atmospheric (outside-air) temperature between GHP and normal air-conditioner (AC) in June, 2016.

	GHP	**AC**
Mean	30.11	30.29
Variance	3.58	3.57
Observations	7	7
df	6	6
F	1.002	
P(F<=f) one-tail	0.499	
F Critical one-tail	4.284	

According to Table 3.9, F is more than 1. Therefore, the result of **F-Test Two-Sample for Variances** can be summarized by the case 1.

So F = 1.002

F Critical one-tail = 4.284

Then F Critical one-tail > F

Therefore accept H_0

To summarize, the variance of atmospheric (outside-air) temperature between the day that GHP and normal air-conditioner (AC) were operated are not significantly different.

Step 2 **t-Test** to compare the averages of 2 populations

Uses the hypothesis below:

H_0: The average of outside-air temperature for GHP = The average of outside-air temperature for AC

H_1: The average of outside-air temperature for GHP ≠ The average of outside-air temperature for AC

According to F-Test Two-Sample for Variances in step 1, H_0 is accepted. In other words, the variance of atmospheric (outside-air) temperature between the day, that GHP and normal air-conditioner (AC) were operated, are not significantly different. Therefore, the case 1 of step 2 was selected to verify with t-Test.

Table 3.10 t-Test: Two-Sample Assuming Equal Variances of atmospheric (outside-air) temperature between GHP and normal air-conditioner (AC) in June, 2016.

	GHP	**AC**
Mean	30.11	30.29
Variance	3.58	3.57
Observations	7	7
Pooled Variance	3.58	
Hypothesized Mean Difference	0	
df	12	
t Stat	-0.174	
P(T<=t) one-tail	0.432	
t Critical one-tail	1.782	
P(T<=t) two-tail	0.865	
t Critical two-tail	2.179	

Based on the Table 3.9, |t Stat| = 0.174

t Critical two-tail = 2.179

Then |t Stat| < t Critical two-tail

Therefore **Accept H_0**

In conclusion, the averages of atmospheric (outside-air) temperature between the day that, GHP and normal air-conditioner (AC) were operated, were not significantly different.

Humidity

Table 3.11 The average of Humidity in each day when the GHP and normal air-conditioner (AC) were operated in June, 2016.

Date of June, 2016	Humidity (%)	
	GHP	AC
3^1 , 9^2	49.5	38.0
13^1 ,14^2	46.7	43.2
15^1 ,16^2	48.0	57.3
17^1 ,21^2	71.7	63.3
22^1 ,23^2	62.3	55.7
27^1 ,28^2	62.6	55.4
29^1 ,30^2	54.8	52.3
Average	56.5	52.2

Note ^{1} = the day that GHP are operated

^{2} = the day that AC are operated

Step 1 **F-Test Two-Sample for Variance**s: to verify whether the variance of 2 populations are equal or not.

Uses the hypothesis below:

H_0: the variance of humidity for GHP = the variance of humidity for AC

H_1: the variance of humidity for GHP ≠ the variance of humidity for AC

Table 3.12 F-Test Two-Sample for Variances of percentage of humidity between GHP and normal air-conditioner (AC) in June, 2016.

	GHP	AC
Mean	56.5086414	52.17644143
Variance	87.28751638	75.97876063
Observations	7	7
df	6	6
F	1.148841014	
P(F<=f) one-tail	0.435270791	
F Critical one-tail	4.283865714	

According to the table 3.12, F is more than 1. Therefore, the result of **F-Test Two-Sample for Variances** can be summarized by the case 1.

So F = 1.148841014

F Critical one-tail = 4.283865714

Then F Critical one-tail > F

Therefore accept H_0

To summarize, the variance of humidity between the day, that GHP and normal air-conditioner (AC) were operated, were not significantly different.

Table 3.13 t-Test: Two-Sample Assuming Equal Variances of humidity between GHP and normal air-conditioner (AC) in June, 2016.

	GHP	**AC**
Mean	56.51	52.18
Variance	87.29	75.98
Observations	7	7
Pooled Variance	81.63	
Hypothesized Mean Difference	0	
df	12	
t Stat	0.897	
P(T<=t) one-tail	0.194	
t Critical one-tail	1.782	
P(T<=t) two-tail	0.387	
t Critical two-tail	2.179	

Based on the Table 3.13 |t Stat| = 0.897

t Critical two-tail = 2.179

Then |t Stat| < t Critical two-tail

Therefore **accept H_0**

In conclusion, the averages of Humidity between the day that GHP and normal air-conditioner (AC) were operated, were not significantly different.

3.5.2 GHP and normal air-conditioner (AC)

In this study, electricity consumption can be divided into 2 parts: electricity consumption of GHP air-conditioner (GHP) and of Normal air-conditioner (AC).

Electricity consumption of GHP air-conditioner (GHP) for 1-hour operation at 25 °C have been recorded in each month as shown in Table 3.14.

Table 3.14 Electricity consumption of GHP for 1-hour operation at 25°C from July 2015 to September 2016.

Month/Year	**Electricity consumption of GHP (kWh)**
July 2015	0.37
August 2015	0.35
September 2015	0.31
October 2015	0.23
November 2015	0.34
December 2015	0.22*[2]
January 2016	0.32
February 2016	0.32
March 2016	0.39
April 2016	0.61*[1]
May 2016	0.42
June 2016	0.39
July 2016	0.31
August 2016	0.37
September 2016	0.34
Average	**0.35**

*[1] highest electricity consumption
*[2] lowest electricity consumption

The highest electricity consumption of GHP air-conditioner (GHP) was 0.61 kWh in April, 2016 and the lowest electricity consumption was 0.22 kWh in December, 2015 as shown in Figure 3.18. An average electricity consumption of GHP air-conditioner (GHP) was 0.35 kWh.

In a long-term analysis, electricity consumption of GHP air-conditioner (GHP) and average flow rate was reported. All data were compared for 1-hour operation at 25 °C in each month. The results showed that the higher average flow rate yielded the higher electricity consumption. In contrast, the lower average flow rate yielded lower electricity consumption as shown in Figure 3.19.

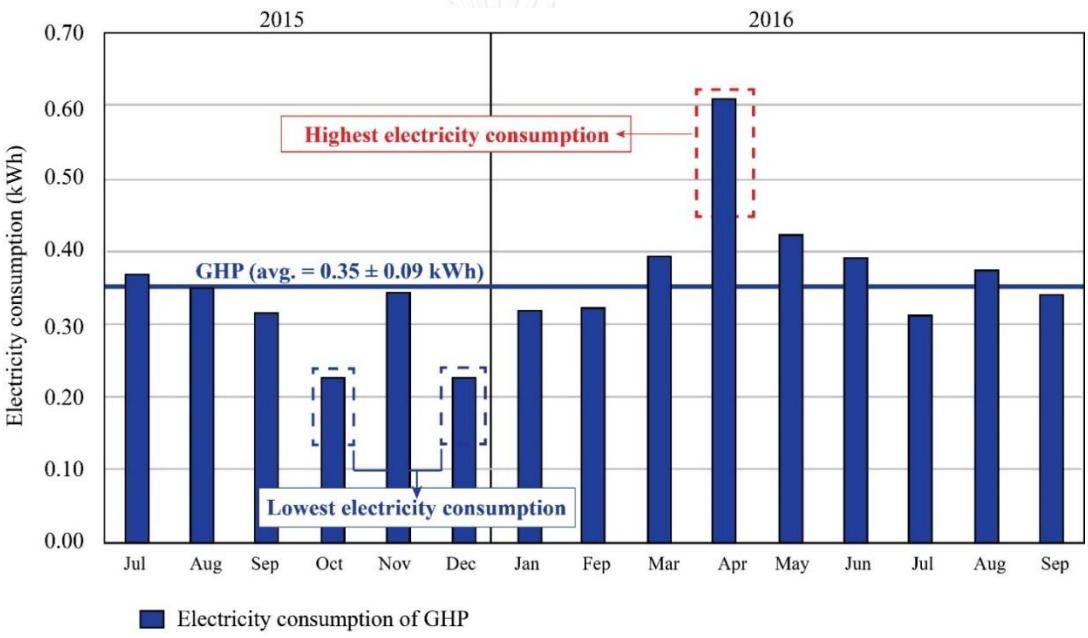

Figure 3.18 Electricity consumption of the GHP air-conditioner when operating at 25°C in long-term measurement (from July, 2015 to September, 2016) at the experimental room, Parot Racha Building, Chulalongkorn University.

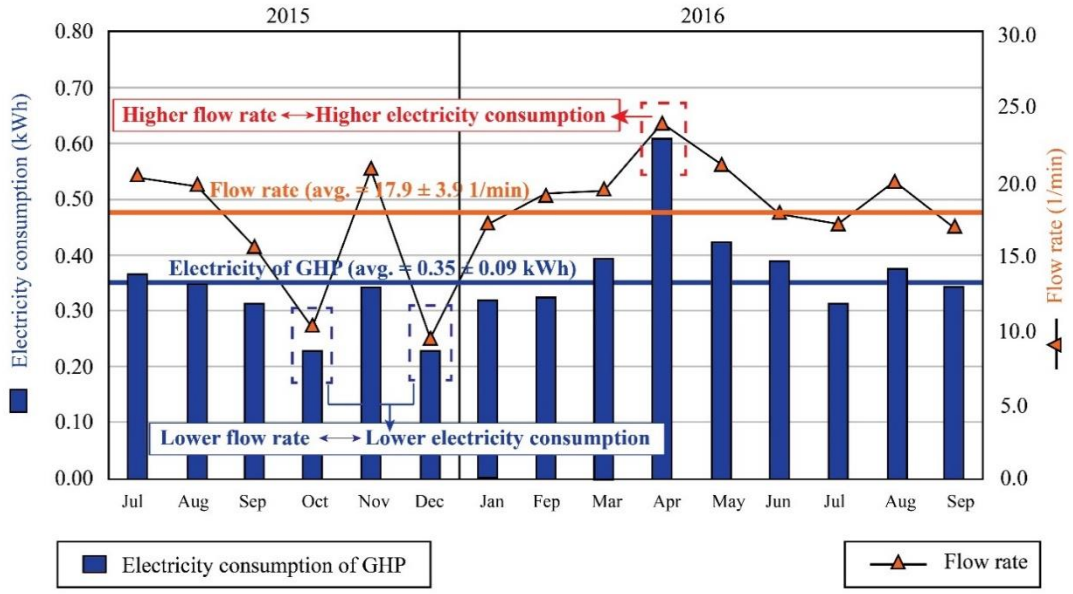

Figure 3.19 Comparison of electricity consumption and flow rate of GHP air-conditioner when operating at 25°C in long-term measurement (from July 2015 to September 2016) at the experimental room, Parot Racha Building, Chulalongkorn University.

Electricity consumption of Normal air-conditioner (AC) were recorded in each month for 1-hour operation at 25°C as shown in Table 3.15.

Table 3.15 Electricity consumption of AC when operated for1-hour at 25°C from June 2015 to September 2016.

Month	Electricity consumption of AC (kWh)
June 2015	0.55
July 2015	0.61
August 2015	0.60
September 2015	0.46
October 2015	0.69
December 2015	0.41
January 2016	0.37*[2]
March 2016	0.54
April 2016	0.76*[1]
May 2016	0.59
June 2016	0.42
July 2016	0.45
August 2016	0.49
September 2016	0.37*[2]
Average	**0.52**

*[1] highest electricity consumption

*[2] lowest electricity consumption

The highest electricity consumption of AC was 0.76 kWh in April, 2016 and the lowest electricity consumption was 0.37 kWh in January, 2015 and September, 2016 (Figure 3.20). Moreover, an average electricity consumption of AC was 0.52 kWh.

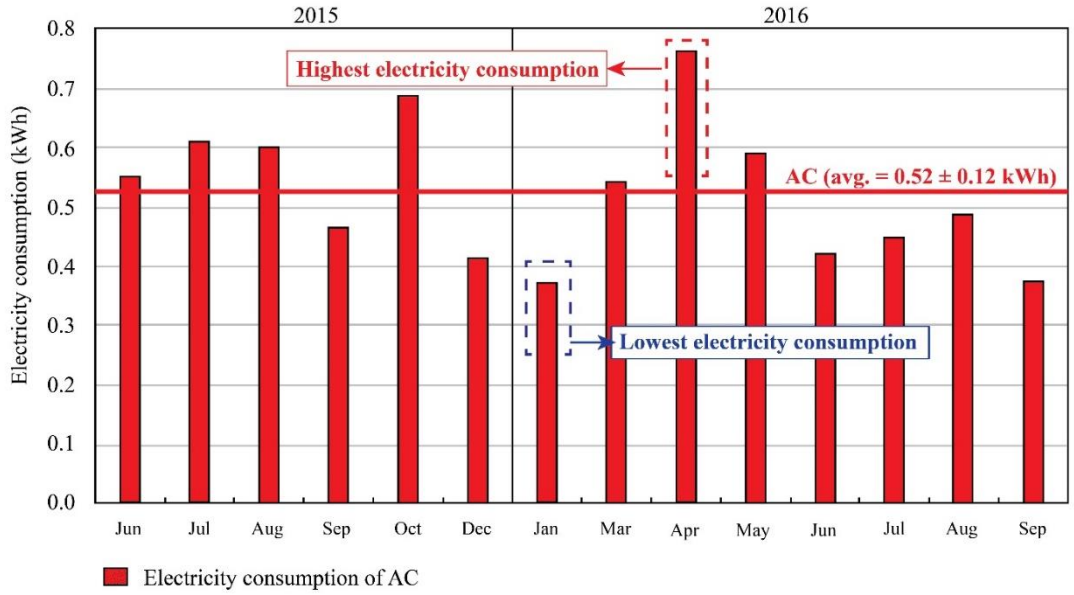

Figure 3.20 Electricity consumption of normal air-conditioner (AC) when operating at 25°C in a long-term measurement (June 2015 to September 2016) at the experimental room, Parot Racha Building, Chulalongkorn University.

3.5.3 Electricity reducing of GHP

A comparison was made for the GHP air-conditioner (GHP) and the normal air-conditioner (AC). The parameters in the formula below was applied at 25 ºC with 1-hour operation for both air-conditioners. The electricity consumption from both air-conditioners were recorded as shown in the Table 3.16.

Formula for electricity reducing of GHP can be calculated in (Eq.1)

$$100 - \left[\frac{\text{Electricity consumption of GHP x 100}}{\text{Electricity consumption of AC}} \right] \quad \text{..... (Eq.1)}$$

Table 3.16 Electricity reducing of GHP when operating at 25°C from July, 2015 to September, 2016.

Month/Year	Electricity reducing of GHP (%)
July, 2015	39.60
August, 2015	42.29
September, 2015	32.36
October, 2015	67.03*[1]
December, 2015	45.70
January, 2016	14.05
March, 2016	28.02
April, 2016	20.06
May, 2016	28.84
June, 2016	7.81*[2]
July, 2016	30.87
August, 2016	22.99
September, 2016	8.94
Average	**29.89**

*[1] highest electricity reducing

*[2] lowest electricity reducing

The highest electricity reducing of GHP is 67.03 % in October, 2015 while the lowest electricity reducing is 7.81 % in June, 2016 as shown in Figure 3.21.

The result indicated that in one-day (i.e. 1 hours) operation, the GHP and normal air-conditioners consumed average electricity at about 0.35 and 0.52 kilowatts, respectively, so that, on average, the electricity can be saved around 30 %.

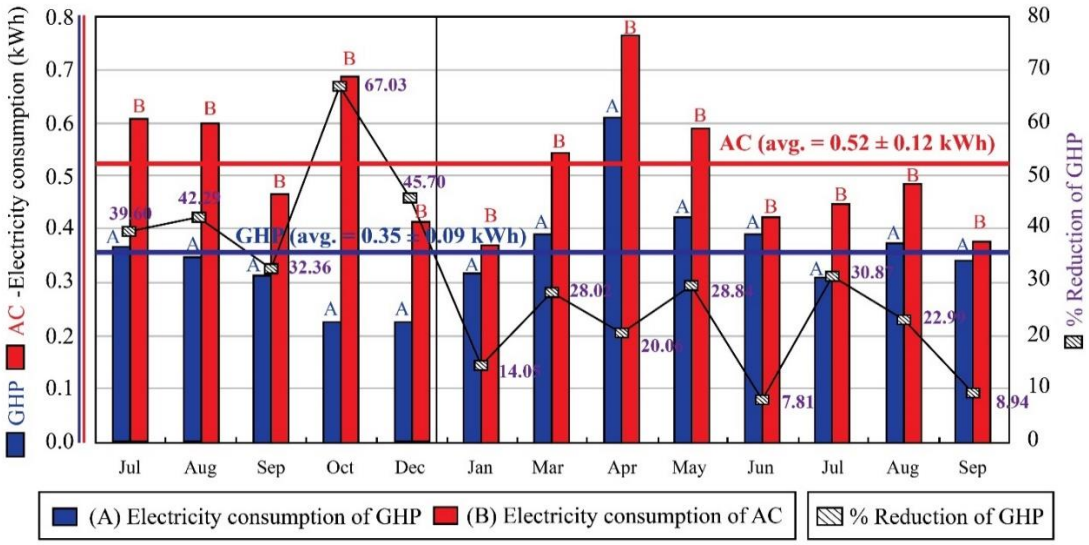

Figure 3.21 The comparison of electricity consumption of GHP- and normal air-conditioners (AC) when operating at 25°C in a long-term measurement (July 2015 to September 2016) at the experimental room, Parot Racha Building, Chulalongkorn University.

CHAPTER 4
DISCUSSION

This Chapter can primarily be divided into five parts as follows:

4.1 Comparisons between subsurface temperatures and outside-air temperatures

In this study, we have selected 6 locations of temperature observation wells around Bangkok (Lower Chao Phraya Plain) for comparing lithostratigraphy of Bangkok form Department of Groundwater Resources (DGR) (see the location in Figure 4.1). A total of six logs including the Central part of Bangkok (T-BKP and T-PW logs), the Eastern part of Bangkok (T-LLK and T-LKB logs), and the Western part of Bangkok (T-BKT and T-BY logs) were carried out.

Figure 4.1 Index map of Lower Chao Phraya Plain showing the locations of temperature observation wells around Bangkok (yellow triangle). The eastern part of Bangkok includes T-LLK and T-LKB. The central part of Bangkok includes T-BKP and T-PW. The western part of Bangkok includes T-BKT and T-BY.

Based on temperatures of six observation wells around the Lower Chao Phraya Plain, the obtained subsurface temperature can be fallen into three areas including the central part of Bangkok, the eastern part of Bangkok and the western part of Bangkok. As regards the data of the western Bangkok, at the depth of 54 to 80 m of T-BKT log, the subsurface temperature appeared to be in ranges of 29.7 to 30.7 °C which show the deeper the depth, the higher the temperature. At the depth of 30 to 80 m of T-BY log, the subsurface temperature was in the ranges of 29.6 to 31.0 °C which the temperature gently increased with the depth. In terms of the zone of the eastern Bangkok, T-LLK had the temperature in ranges of 29.8 to 30.7 °C at the depth of 56 to 80 m, and T-LKB had the temperature in the ranges of 28.9 to 30.3 °C at the depth of 14 to 80 m. They both showed the moderately increase in the temperature with the vertical depth. The Central Bangkok consists of T-BKP and T-PW logs. The first one, the subsurface temperature at the depth of 38 to 80 m, appeared to be in the ranges of 30.2 to 31.3 °C. The second displayed the subsurface temperature in the ranges of 29.2 to 30.8 °C at the depth of 42 to 76 m. The subsurface temperatures of both rose gradually.

Additionally, in this research, the subsurface temperature of log at the depth of 1.5 to 50 m was compared with those logs as mentioned above. It is founded that the all of the subsurface temperature are prone to be in the same direction, that is to say, when the depth increase, the subsurface temperatures the similarity of subsurface temperature which values are much closed or gradually different (not to exceed 1 °C). However, the eastern parts of Bangkok including this study, the subsurface temperature are sparsely higher around 1 °C. Inasmuch as, the possibility of the high temperature may likely be affected by the groundwater flow (Figure 4.2). In addition to, GHP use the groundwater flow to provide space heating and cooling for more energy efficient than use outside-air (Galgaro et al., 2014).

From the foregoing description, GHP system installing on the western and the eastern part of Bangkok is more presumably effective than the central part of Bangkok.

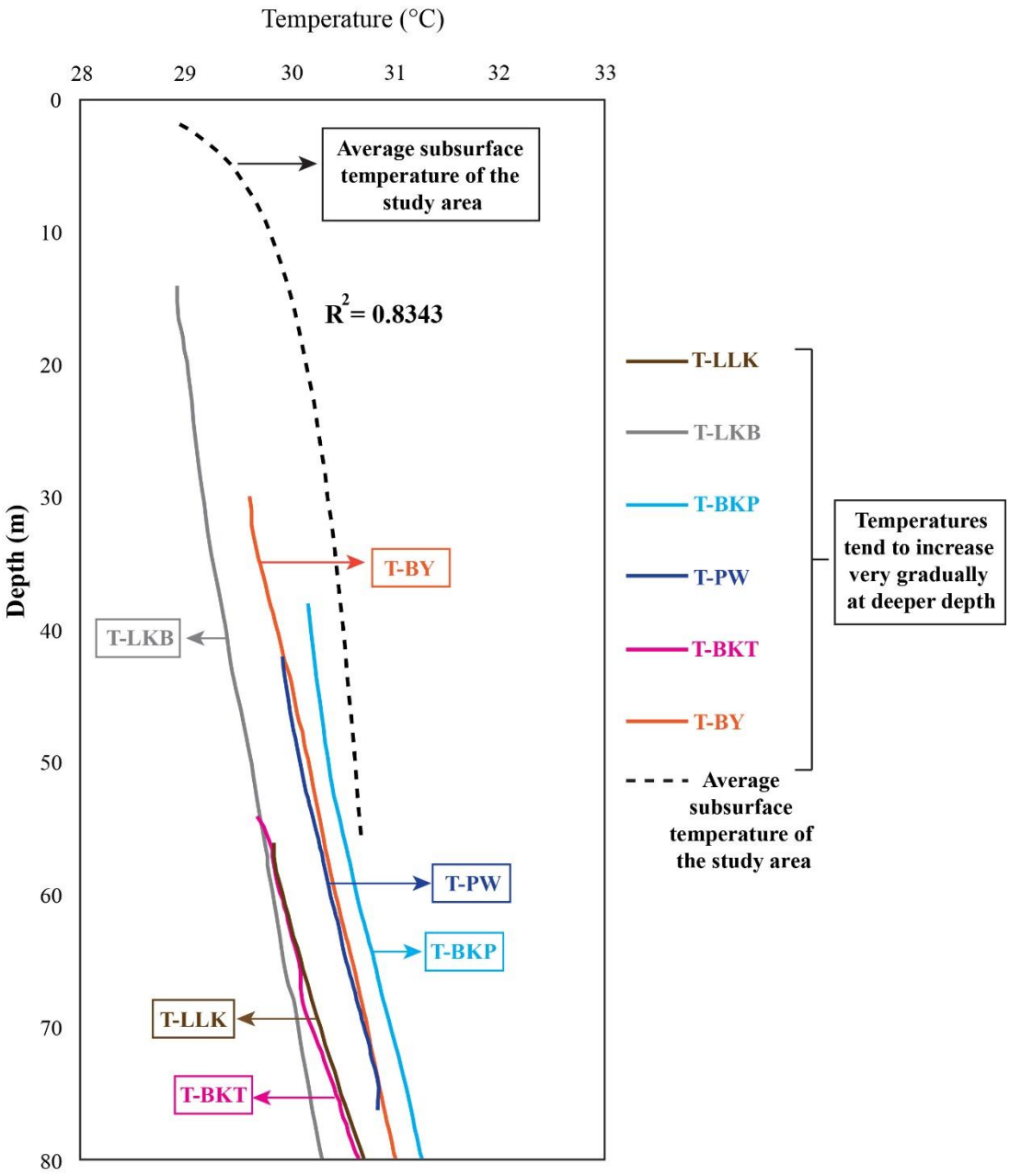

Figure 4.2 Comparison between well temperature profiles around Bangkok including the study area (data from Uchida et al. (2009)).

According to Figure 4.2, the comparison between the subsurface and the outside-air temperature of this study was showed. It is founded that the subsurface temperatures appear to be constant throughout the year of 2009 when comparing with the outside-air temperature. Some month in the year of 2009 (from February to September), nevertheless, is equal and/or lower than the outside-air temperature. This can make the GHP system work ineffectively. From the study of Yasukawa et al.

(2009b) regarding the subsurface temperature and the outside-air temperature at the depth of 20 to 50 m as well as this study, we can concluded that the subsurface temperature had a constant value which lower than the outside-air temperature throughout the year, yet the eastern zone of Bangkok is gradually lower. From these preliminary data, both of works are consistent on the basis of the subsurface temperature, i.e. the value has the proximity and stability throughout the year; nonetheless, the outside-air temperature is different. The outside-air temperature in this study is lower than the subsurface temperature in some month (October to January) because the temperature measurement in this study was performed during winter season as shown in Figure 4.3.

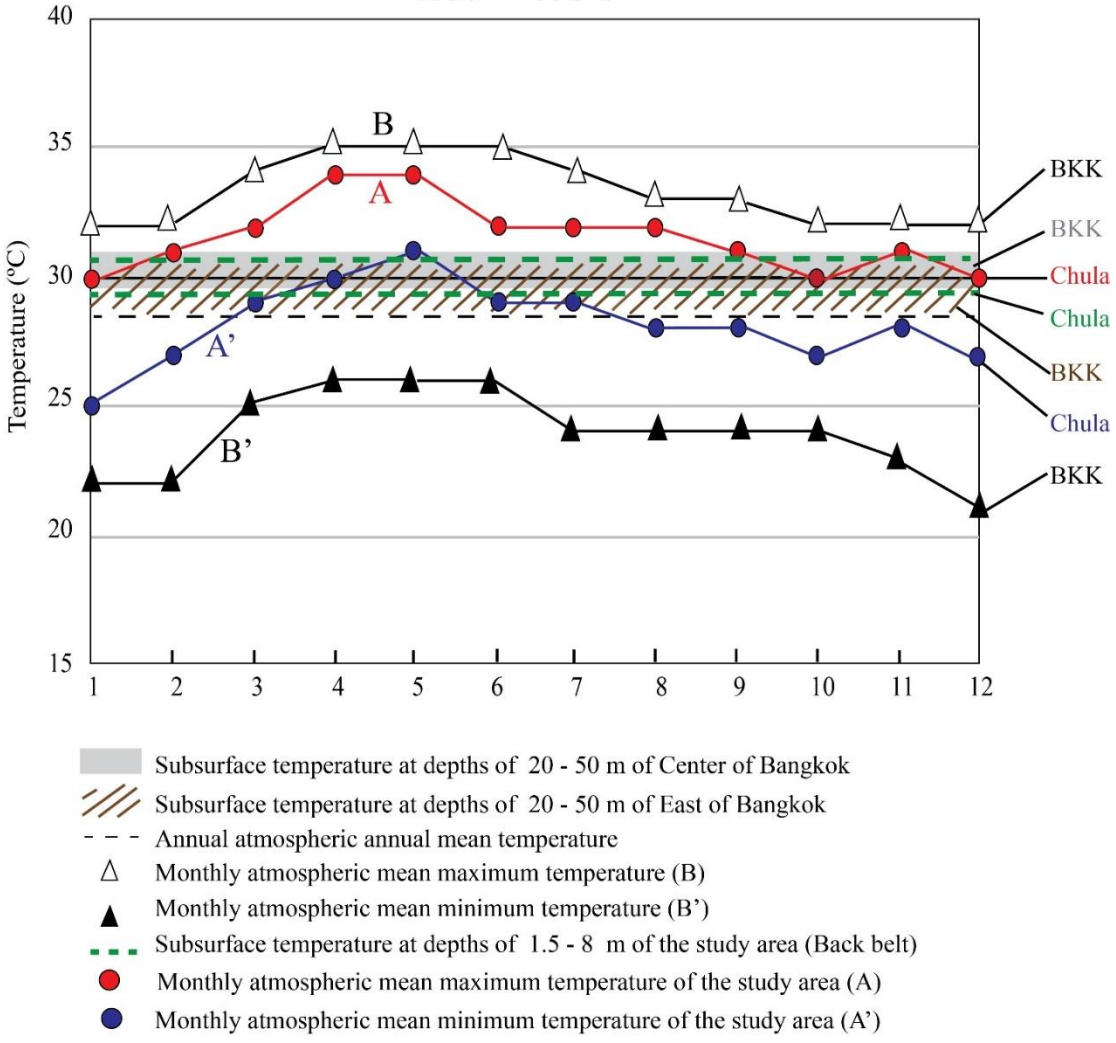

Figure 4.3 Comparison of atmospheric and subsurface temperatures of Bangkok area (data from Yasukawa et al., 2009b) and this study.

4.2 Holocene stratigraphic correlation

The correlation of lithologic logs between study area (well nos. 1&2) and groundwater well of Department of Groundwater Resources (DGR) located at Chulalongkorn University Dhamma Centre can be correlate into 4 layers as shown in Figure 4.4.

- The 1st layer: An average thickness is 20 meters and consists of clay that is highly plastic and homogeneous.

- The 2nd layer: An average thickness is 12 meters and consists of pale brown to yellowish brown sandy clay. It composed of 60% of clay that is moderate plastic, heterogeneous and 40 % of sand that is fine- to medium-grained, poorly sorted and sub-angular. Moreover, it mostly composes of quartz with subordinated feldspar and rock fragments.

- The 3rd layer: An average thickness is 16 meters-thickness and consists of pale brown sand that is fine- to medium-grained, good sorted, sub-angular. It is mostly composed of quartz with subordinated feldspar, rock fragments and clay minerals.

- The 4th layer: An average thickness is 9 meters-thickness and comprises yellowish brown clay that is moderate plastic, heterogeneous and some parts of medium sand and silt.

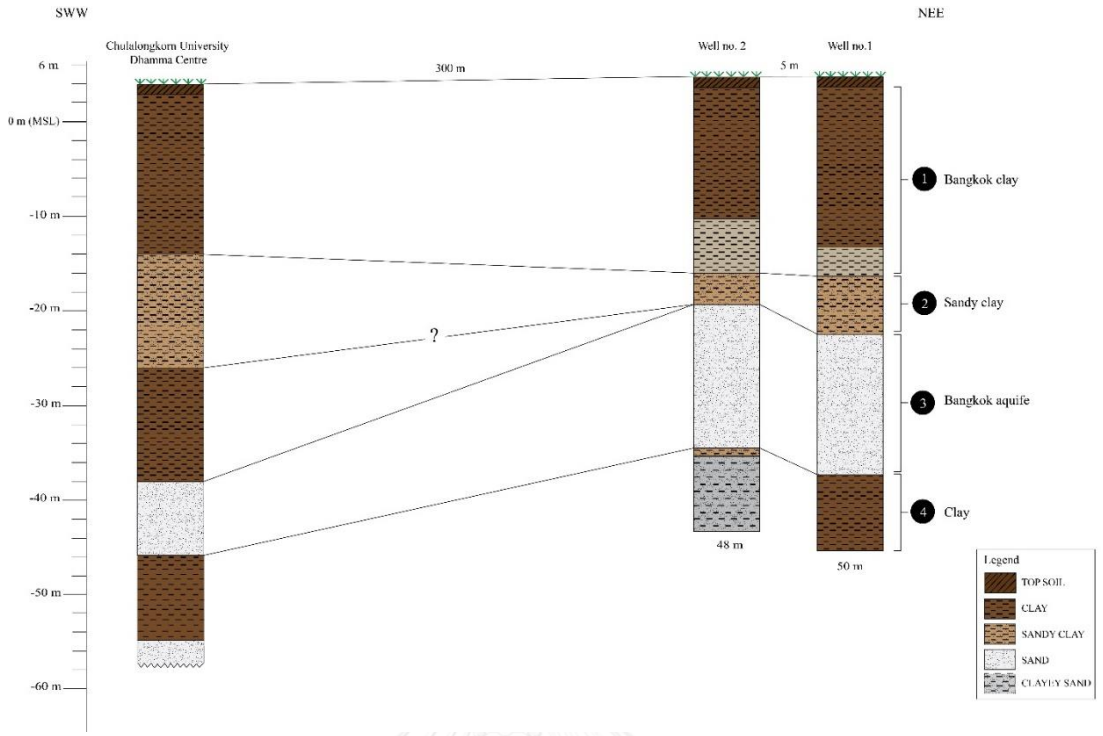

Figure 4.4 Correlation of lithologic logs of well nos. 1, 2 and Chulalongkorn University Dhamma Centre log (elevation above MSL based on GPS measurement from this study) (see locations in Figures 2.1 and 2.2).

Based on Figure 4.4, it is founded that the comparison of lithostratigraphy in this study and the vicinity of previous work (Chulalongkorn University Dhamma Center) shows both similarities and differences as follows:

The correlation of lithology of the first layer is Bangkok clay at the depth of 0 to 20 m from the ground surface. The second layer comprises of sandy clay at the depth of 19 to 30 m. from the ground surface, while sandy clay is located between 20 to 29 m deep. Furthermore, clay at the depth of 30 to 41 m of the vicinity was observed, whereas it is absent in this study. This possible explanation is that the cause the elevation during the sedimentation in the past resembles a convex or concave lens. The correlation of lithology at the third layer is a sand layer. In this study, the sand layer is located at the depth of 23 to 41 m, whereas the vicinity the sedimentation is at around 41 to 49 m. It is possible that it is the effect of the convex or concave lens which overly on the top. Also, it can cause the negative effect on GHP system because this system needs to exploit the groundwater to cool the heat flowing through sand layer. Hence, if sand

layer is in the deeper part, the drilling must be operated deeper as well. Groundwater utilized in this study is located in the 1st aquifer at the depth around 25 to 50 m (Figure 4.5). Finally, the correlation of the forth layer is the clay deposits. In the second wells, the thickness of clay is only 1 m. It might be the error during data collection.

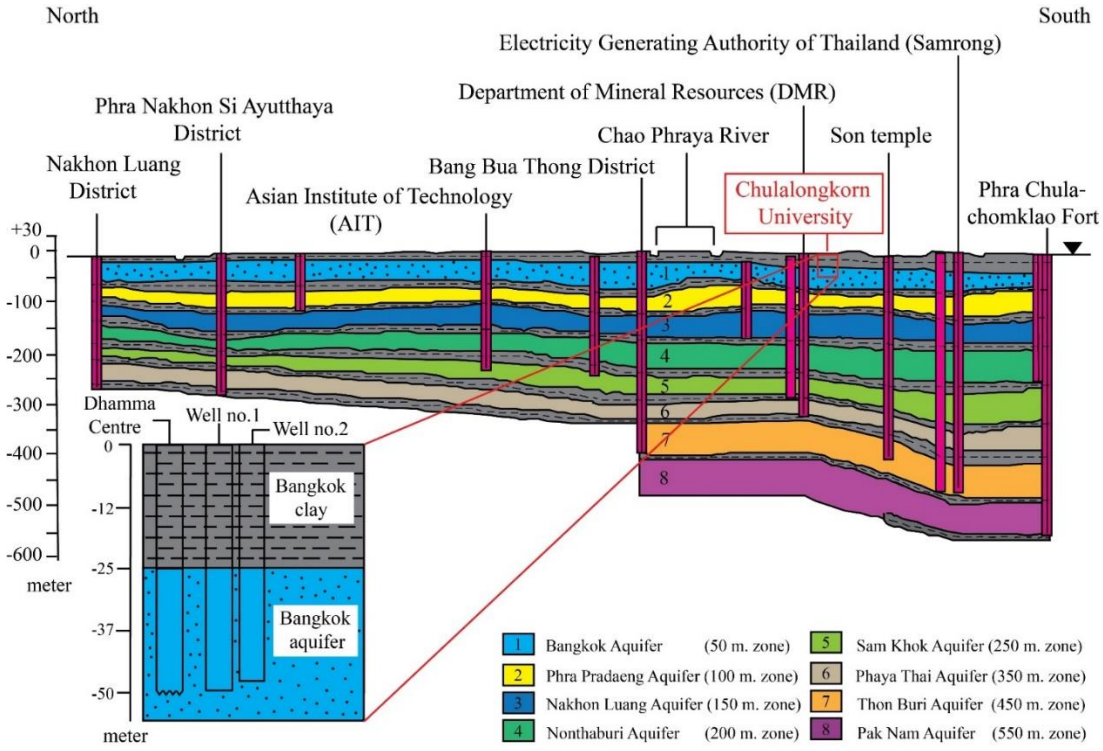

Figure 4.5 Subsurface stratigraphy and aquifer of the Lower Chao Phraya Plain (modified after Department of Mineral Resources (DMR) (2011)).

4.3 Depth of drilling

From the section 4.1, Bangkok area is divided into three parts including the central part of Bangkok, the eastern part of Bangkok and the western part of Bangkok. According to the subsurface temperature data, this section discuss about groundwater flowing through the 1st sand layer (or Bangkok aquifer) for installing the GHP system. The referenced wells based on the data of DGR. In order to establishing southwest to northeast cross section of Bangkok, we used stratigraphic data from six wells in this study including TLC-1, TLC-2 (the western part of Bangkok), LKB-1, LKB-2 (the eastern part of Bangkok), HK, PKN, BKP and study area (the central part of Bangkok) (Figure 4.6).

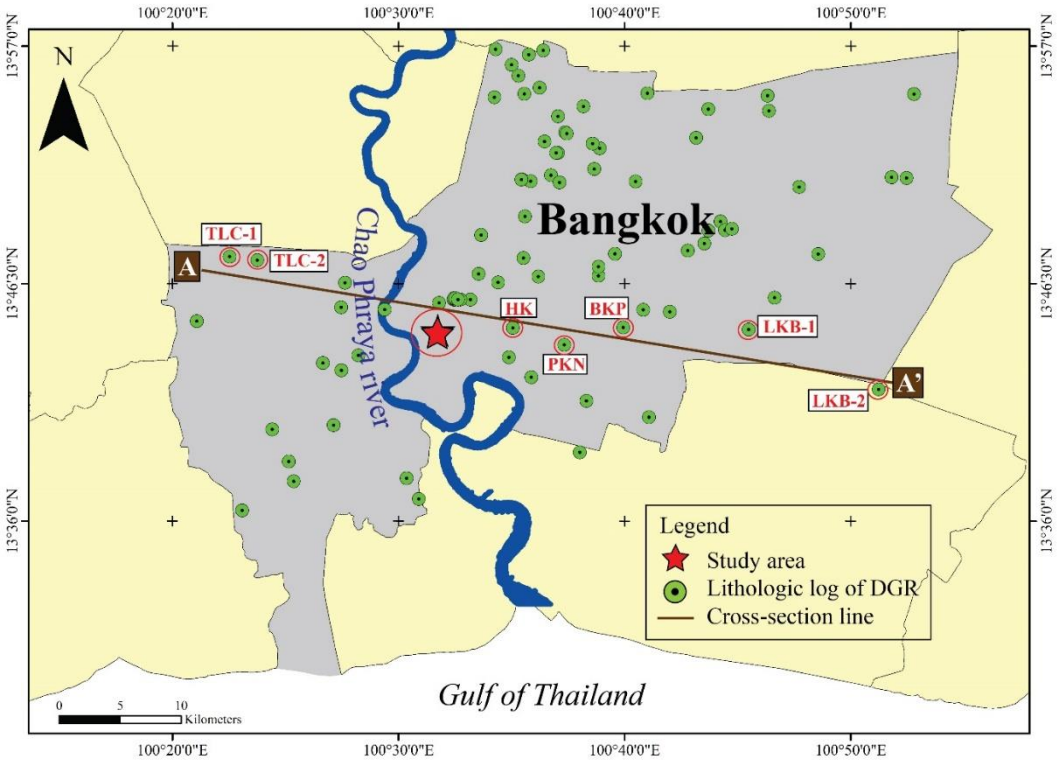

Figure 4.6 Index map of the Lower Chao Phraya Plain showing the locations of the study area (★) and nearest temperature observation wells (circle) with A-A' cross section line (data from Department of Groundwater Resources (DGR) , digital files).

Southwest to northeast cross section line (A to A') was created by using a total of eight groundwater wells, including TLC-1, TLC-2, HK, PKN, BKP, LKB-1, LKB-2 and log well in study area. The correlation of all log wells use sand layer, being in Bangkok aquifer as a diagnostic key. TLC-1 and TLC-2 is located in the western Bangkok have sandy gravel at depth of 28 to 60 m and 17 to 67 m, while sand layer of this study (well nos. 1 and 2) was observed at the depth of 23 to 41 m. In addition, sand layer of HK, PKN and BKP in the central Bangkok is the depth of 27 to 36 m, 20 to 30 m and 18 to 31 m respectively. Also, sand layers of logs at the eastern Bangkok (LKB-1 and LKB-2) appear to be in the depth 22 to 30 m and 21 to 50 m. Thus, according to the log results of cross section, it can be summarized that the GHP system is recommended to install in the Bangkok aquifer so as to heat-transferring with the groundwater flowing t through the sand layer. It is implied that the GHP system should be installed at the depth of 25 to 50 m. and of 30 to 50 m. in the eastern part and western part of Bangkok, respectively. Moreover, the central part of Bangkok should be drilled at the depth of 25 to 30 m, but the deep of this part may drastically vary, depending on the convex or concave lens of clay.

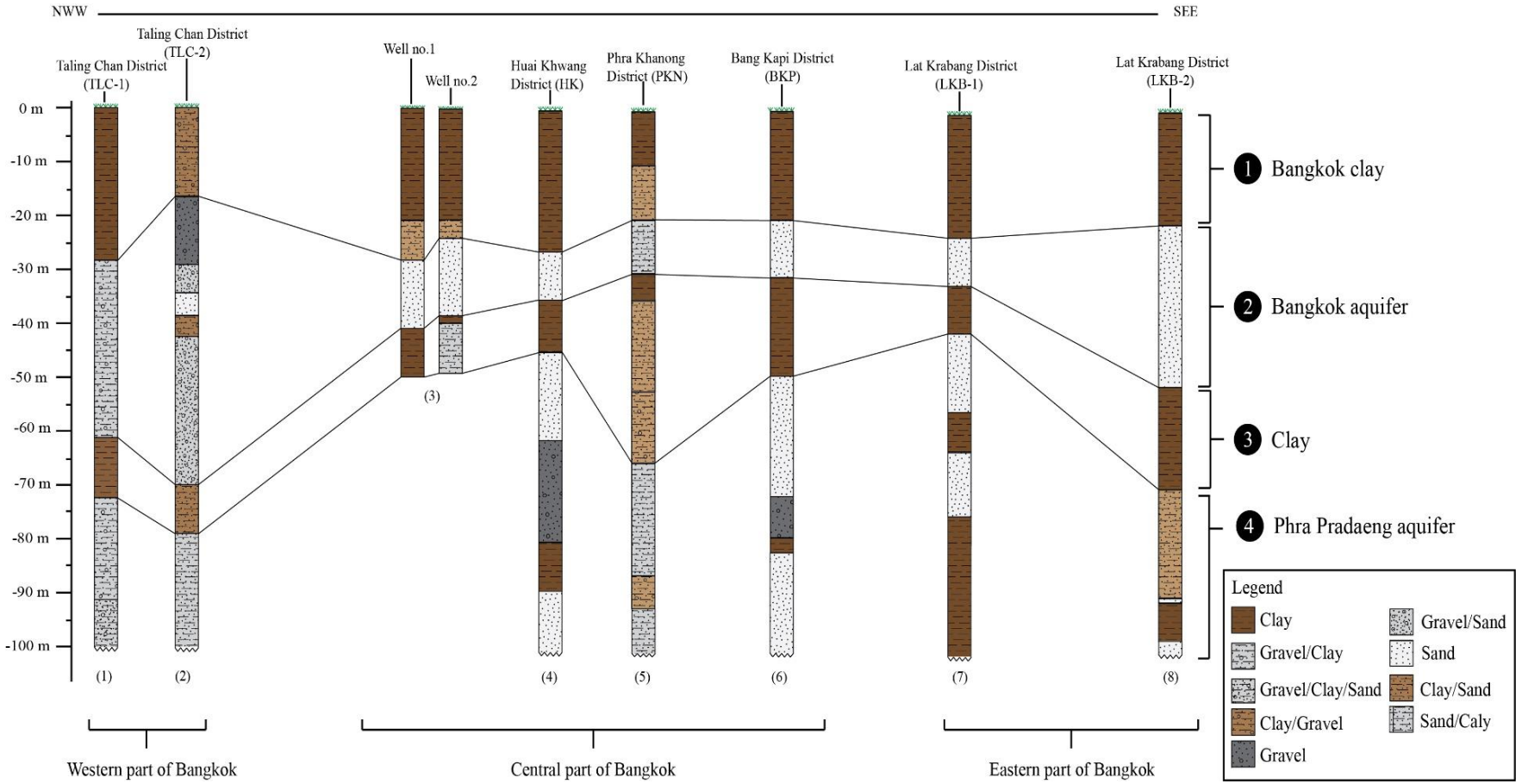

Figure 4.7 Correlation of lithologic logs of well nos. 1, 2 and lithologic logs of Department of Groundwater Resources (DGR): LH-BKT, LH-BKP and LH-LLK (elevation above MSL based on GPS measurement from DGR).

4.4 Factors of energy saving

In this section, we described about the factors affecting on energy saving of GHP. It can be divided into two sub-sections as follows:

4.4.1 Outside-air temperatures

The Figure 4.8A shows the comparison of electricity consumption and outside-air temperatures (ATM) when operating at 25°C in the long-term measurement (July 2015 to September 2016) at the experimental room, Parot Racha Building, Chulalongkorn University. It is discovered that the higher outside-air temperatures can influence the higher electricity consumption. Notably, the consumption of normal air-conditioner and GHP was compared and this study can be concluded that the consumption of GHP has lower quantity of electric consumption because the GHP system exchanges the heat of flowing water with the lower and stable subsurface temperature, while the normal air-conditioner apply the outside-air temperatures for ventilating the heat, which experienced with the daily tentative fluctuation of the weather. Consequently, the main affected factor of both systems is the outside-air temperatures; that is to say, the warmer the temperature, the higher the consumption (Figure 4.8).

Even so, some days although the outside-air temperature is low, the electric consumption of both systems become higher because there are other factors that have an effect on the saving energy. For example, in October, 2015, it is founded that in spite of the low outside-air temperatures, the electric consumption is higher than that the day of higher outside-air temperatures. It is likely that the humidity plays a major role of high electric consumption.

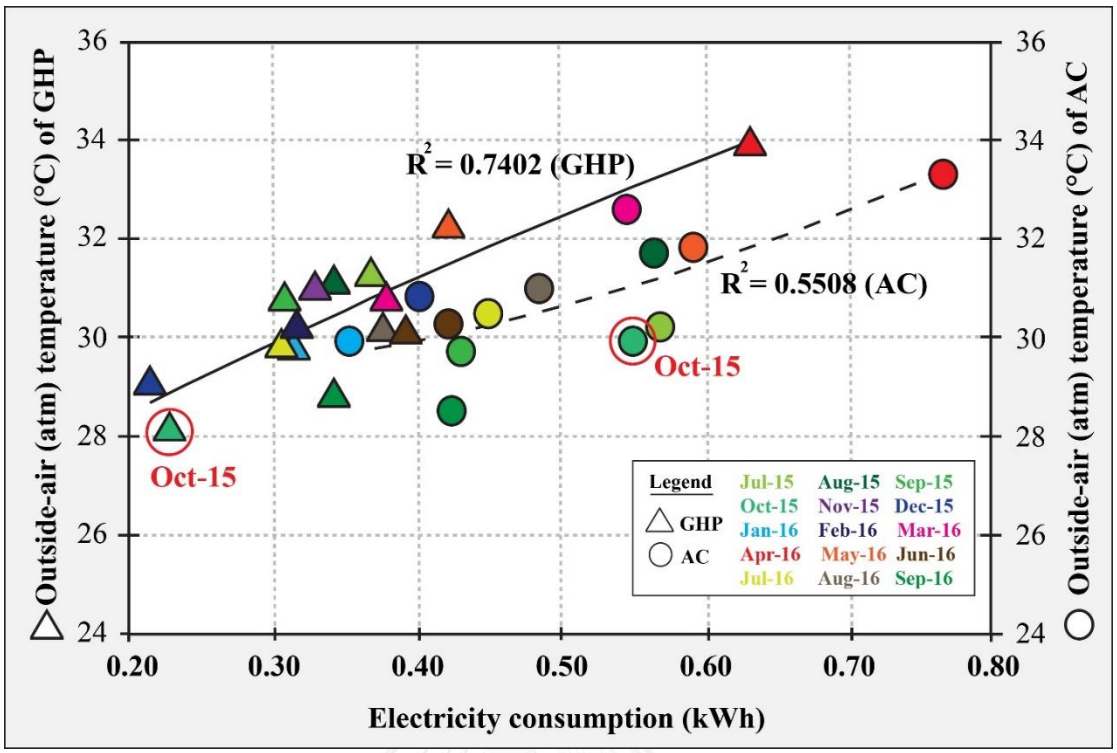

Figure 4.8 Comparison of electricity consumption and outside-air temperatures (ATM) when operating at 25°C in long-term measurement (July 2015 to September 2016) at the experimental room, Parot Racha Building, Chulalongkorn University.

4.4.2 Humidity

As mentioned in the previous section, it is pointed out that the outside-air temperature is one of the important factor, which influences on the energy- saving performance of both GHP and normal air-conditioner system. However, in some months the results seem to be peculiar, for example, data collected in October, 2015 (Figure 4.9), even if the outside-air temperature is low, the electric consumption become relatively high. Thus, the high humidity results in the electrical consumption. It can be concluded that besides the high outside-air temperatures, humidity plays a major part, directly affecting the electric consumption.

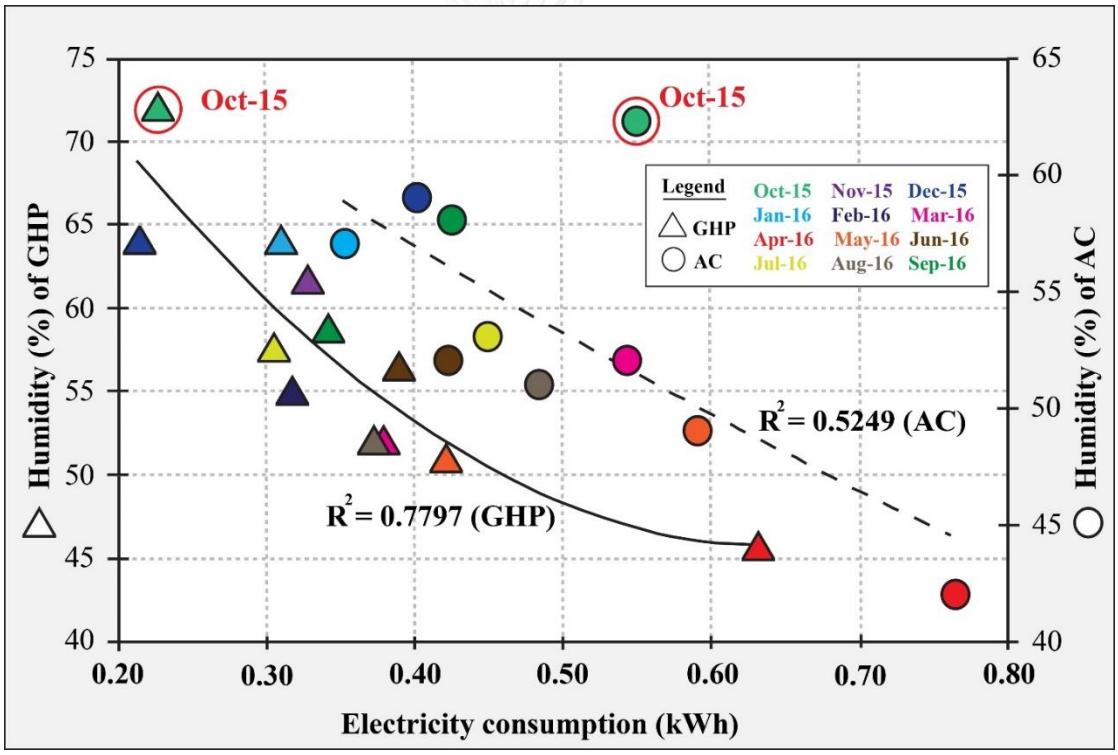

Figure 4.9 Comparison of electricity consumption and humidity when operating at 25°C in long-term measurement (October 2015 to September 2016) at the experimental room, Parot Racha Building, Chulalongkorn University.

4.5 Coefficient of Performance (CoP)

As mentioned in Chapter 1 (section 1.2.7), Coefficient of Performance **(**CoP) of air-conditioner can be determined according to the definition belows:

The coefficient of performance (CoP) is the performance of data, measured as the heat output (kWh) and divided by the electrical input (kWh)

This section shows the comparison between CoP of GHP and CoP of normal air-conditioner (AC). Additionally, factors of energy saving e.g., outside-air (atm) temperature and humidity were compared as mentioned in the section 4.4

As mentioned before, CoP of the GHP can be computed as follows:

$$\text{CoP} = \frac{Cooling\ capacity}{power\ input}$$

$$= \frac{Q_H - W}{W} \quad \text{..... (Eq.2)}$$

Where:

Q_H = Heat transferred to the ground (kW)

V = circulating fluid flowrate (m^3/s)

ρ = circulation fluid volume mass density (kg/m^3)

c = specific heat of circulating fluid (J/(kgK)

$\Delta T = T_O - T_I$ = temperature different of circulating fluid between outlet and outlet

W = the heat output or Total electricity consumption = E_E (kWh)

In contrast, this study the electricity consumption is total daily utilization; so it cannot calculate CoP of GHP in the real time. For this reason, the formula in (Eq.2) need to be calculated which based on the average total daily energy as follows the formula of National Rural Electric Cooperative and Oklahoma State University. Division of Engineering (1988); Widiatmojo (2017)..

$$\text{The daily average CoP} = \frac{E_H - E_E}{E_E} \quad \text{..... (Eq.3)}$$

Where:

$E_H = Q_H \, x \, \Delta t$ …… (Eq.4)

Δt = Measurement interval

For instance, the data of 15 July 2015 was recorded by data logger as shown in Table 4.1

Table 4.1 The data of 15 July 2015 based on Data logger on GHP's operation day at 25°C temperature control from 9.00 AM to 4.00 PM.

No.	Ch-1	Ch-2	Ch-3	Ch-4	Ch-5	Ch-6	Ch-7	Ch-8
	Date & Time	Room temp. (°C)	Outside-air temp (°C)	Inlet temp. (°C)	Outlet temp. (°C)	Flow Rate (l/min)	Flow Rate (m^3/s)	E_H (KW)
1	7/15/2015 9:06	25.7	29.8	30.8	32.3	25.11	0.000418542	0.8236
2	7/15/2015 9:26	25.7	30.0	31.1	32.4	0.08	0.00000125	0.0021
3	7/15/2015 9:46	25.1	30.4	31.4	32.8	25.48	0.000424583	0.7798
4	7/15/2015 10:06	25.2	30.3	31.3	32.7	25.40	0.000423333	0.7775
5	7/15/2015 10:26	25.4	30.7	31.3	32.7	25.46	0.000424375	0.7794
6	7/15/2015 10:46	25.4	30.5	31.3	32.7	25.23	0.000420417	0.7721
7	7/15/2015 11:06	25.6	30.4	31.5	32.8	25.46	0.000424375	0.7237
8	7/15/2015 11:26	26.2	30.5	31.2	32.4	25.46	0.000424375	0.6681
9	7/15/2015 11:46	26.1	31.0	31.8	32.8	0.08	0.00000125	0.0016
10	7/15/2015 12:06	25.1	30.9	32.1	33.5	25.63	0.000427083	0.7844
11	7/15/2015 12:26	25.6	30.9	32	33.2	25.64	0.000427292	0.6727
12	7/15/2015 12:46	26.2	31.0	31.8	33.0	25.53	0.000425417	0.6697
13	7/15/2015 13:06	25.3	31.5	32.5	33.8	25.29	0.000421458	0.7188
14	7/15/2015 13:26	25.9	31.3	32.1	33.3	25.59	0.000426458	0.6713
15	7/15/2015 13:46	25.3	31.2	32.5	33.8	25.61	0.000426875	0.7280
16	7/15/2015 14:06	26.2	31.4	32.6	33.7	0.06	1.04167E-06	0.0015

No.	Ch-1	Ch-2	Ch-3	Ch-4	Ch-5	Ch-6	Ch-7	Ch-8
	Date & Time	Room temp. (°C)	Outside-air temp (°C)	Inlet temp. (°C)	Outlet temp. (°C)	Flow Rate (l/min)	Flow Rate (m^3/s)	E_H (KW)
17	7/15/2015 14:26	25.3	31.5	32.8	34.2	25.60	0.000426667	0.7836
18	7/15/2015 14:46	25.1	31.6	32.9	34.2	25.69	0.000428125	0.73014
19	7/15/2015 15:06	25.5	31.9	32.8	34.2	25.50	0.000425	0.7806
20	7/15/2015 15:26	25.2	31.9	33.1	34.4	25.43	0.00042375	0.7227
21	7/15/2015 15:46	25.5	31.7	33.2	34.5	25.48	0.000424583	0.7241
Sum								**13.3155**

Note: Ch-1 to Ch-6 is the recorded data
Ch7 to Ch-8 is the calculated data

Ch-6 in Table 4.1is flow rate in l/min unit that can change to m^3/s as follows:

Flow rate (m^3/s) = Flow rate (l/min) x $\frac{10^{-3}}{60}$ … (Eq.5)

For instance, flow rate (l/min) at 9.06 AM = 25.11 (No.1, Ch-6)

Then, substitute 25.11 in (Eq.5) = 25.11 x $\frac{10^{-3}}{60}$

Therefore, flow rate (V) = 25.11 l/min = 0.000418542 m^3/s (No.1, Ch-7)

Ch-8 in Table 4.1 is E_H (KW) that can calculate as follows:

From (Eq.4) shown that E_H = $Q_H \, x \, \Delta t$

= $\left[\frac{V \rho c \Delta T}{1000}\right] x \, \Delta t$

Where:

V = 0.000418542 m^3/s

$\Delta T = T_O - T_I$ = Outlet temperature (No.1, Ch-5) – Inlet temperature (Ch-4)

= 32.3 °C -30.8 °C

= 1.5 °C

Δt = 20 min = 0.333 hrs.

Constant values:

c = 3810 J kg^{-1} C^{-1}

ρ = 1034 kg m^{-3}

$$E_H = \left[\frac{0.000418542 \text{ x } 1034 \text{ x } 3810 \text{ x } 1.5}{1000}\right] x\ 0.333$$

$$= 0.8236 \text{ KWh}$$

Form (Eq.3): The daily average CoP $= \frac{E_H - E_E}{E_E}$

Where:

$E_H = E_{H\ \textbf{Sum (No.1-21)}} = 13.3155$ (Table 4.1)

W = E_E = 2.45 KWh (total electricity consumption)

$$\text{CoP of GHP} = \frac{13.3155 - 2.45}{2.45}$$

$$= 4.43$$

For CoP of normal air-conditioner (AC) is shown in EER (the energy efficiency ratio) value that indicate in the manual book.

EER of AC = 11.78 BTU/hr./watt

Where

1 Watt = 3.412 BTU/hr.

$$\text{COP of AC} = \frac{EER}{3.412} \quad \text{……. (Eq.6)}$$

$$= \frac{11.78}{3.412}$$

$$= 3.45$$

In conclusion, the CoP value of GHP is higher than the CoP value of AC.

4.5.1 Outside-air temperatures

This section is the comparison between CoP value of GHP, AC and outside air temperature (ATM) when operating at 25°C in long-term measurement (July 2015 to October 2016) at Parot Racha Building, Chulalongkorn University.

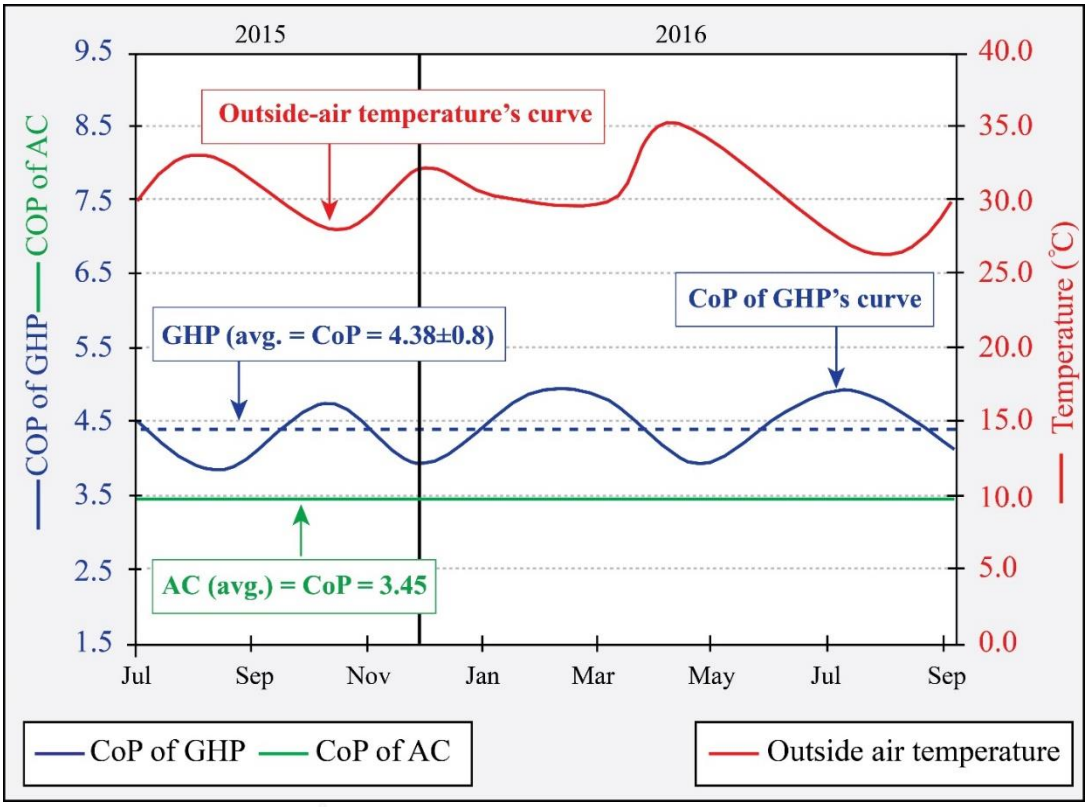

Figure 4.10 The comparison between CoP value of GHP, AC and outside air temperature (ATM) when operating at 25°C in long-term measurement (July 2015 to October 2016) at Parot Racha Building, Chulalongkorn University.

In Figure 4.10, the average of CoP of GHP and AC are 4.38 and 3.45 respectively. For this results, efficiency of GHP is higher than AC. Furthermore, outside-air temperature's curve is the highest in the summer season (April to May 2016). As a result of hot temperature, this affects CoP's curve of GHP and make the value become low. In other words, CoP's curve is high when outside-air temperature is low.

4.5.2 Humidity

This section is the comparison between value of CoP of GHP, AC and humidity when operating at 25°C in long-term measurement (July 2015 to October 2016) at Parot Racha Building, Chulalongkorn University.

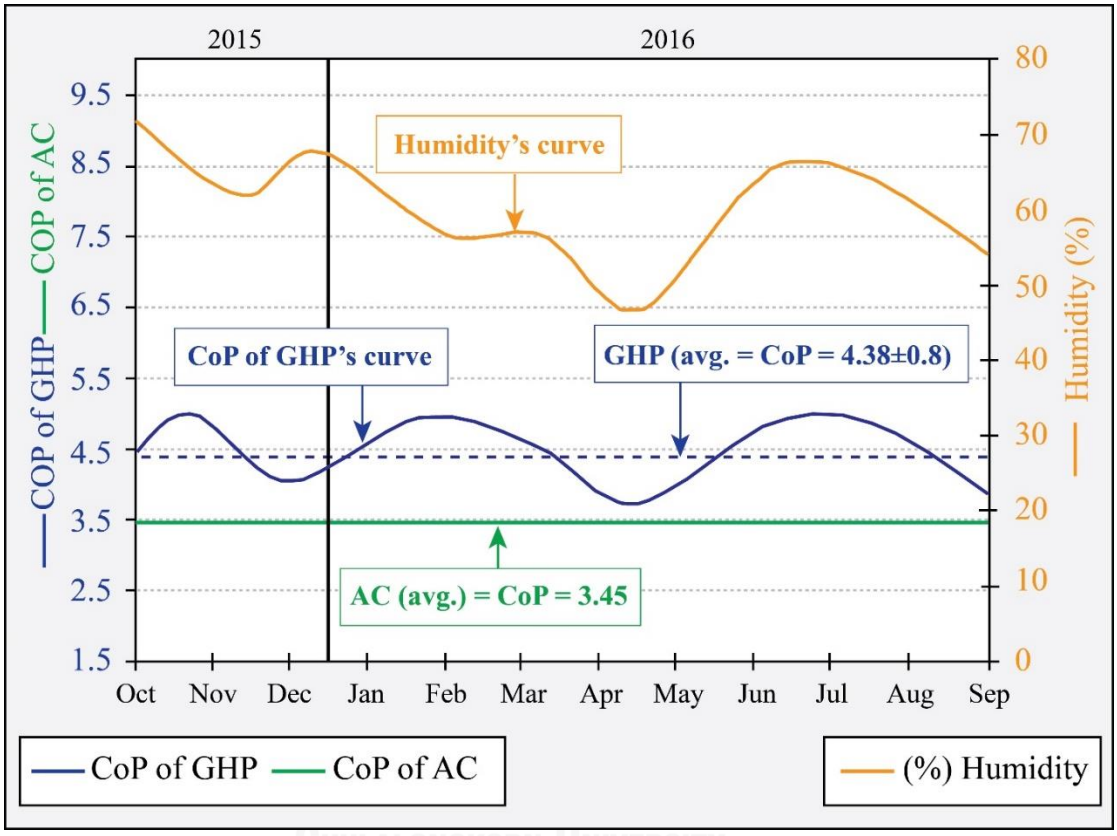

Figure 4.11 The comparison between value of CoP of GHP and humidity when operating at 25°C in long-term measurement (October 2015 to September 2016) at Parot Racha Building, Chulalongkorn University.

From the section 4.4.2, it is shown that humidity is one of the important factor influencing the energy-saving performance of both GHP and normal air-conditioner system. Thus, when the comparison between CoP of GHP and humidity was conducted, the results are significantly clear in Figure 4.11. It is founded that the high humidity curve can affect the high CoP curve. In some range of curve (December 2015 to January 2016), on the other hand, the curve seems to be peculiar since those months have high outside-air temperature.

CHAPTER 5
CONCLUSIONS AND RECOMMENDATIONS

5.1 Conclusions

The vertical loop geothermal heat pump system (GHP) was installed at Chulalongkorn University and equipped along with two drilled holes (totally about 170 m-long) for electricity reduction. The long-term measurement of underground temperatures shows that the temperatures have been quite consistent and lower than the average outside-air temperatures for almost the whole 2 years. However, the underground water utilized in this study is in the first groundwater aquifer (Bangkok aquifer) at the depth around 25 to 50 m for heat exchange. Thus, this can be summarized that drilling for circulation by using Bangkok aquifer so as to heat-transferring with groundwater flowing through the aquifer. The findings from this study suggested the GHP should be installed at the depths of 25 to 50 m. and of 30 to 50 m. in the eastern and western parts of Bangkok. For the central part of Bangkok, it should be drilled at the depths of 25 to 30 m, but the depth of drilling is in the wide range, depending on the convex or concave lens of clay. Additionally, the main affected factor of air-conditioner (GHP and AC) on an energy-saving performance are the outside-air temperatures and humidity. The higher outside-air temperature can influence the higher electricity consumption. In the same way, when humidity becomes higher, the uses of electricity become slightly higher. To sum up, in Bangkok area, the vertical installation of GHP system should equip groundwater circulatory system in the Bangkok aquifer in order to utilize Bangkok groundwater in heat transfer efficiently.

A comparison was made between the geothermal heat pump (GHP) and the normal air conditioner (AC) in the same room and the similar specification, it is found that the electricity consumption has been saved about 30%. Data on underground temperature measurement in Bangkok allow the high possibility of using GHP in this Bangkok and nearby areas where subsurface geology is similar.

5.2 Recommendations

5.2.1 Unworkable case

As a results, efficiency of GHP system is higher than normal air-conditioner (AC), but there is some unworkable place where cannot install GHP. As mentioned before, GHP system has high efficiency when underground temperature is constant and lower than outside-air (atm) temperature. For instance, the underground temperature at depths of 20-50 m of Sukhothai area is higher than outside-air temperature almost whole year (Figure 5.1). Thus, GHP cannot use in this area.

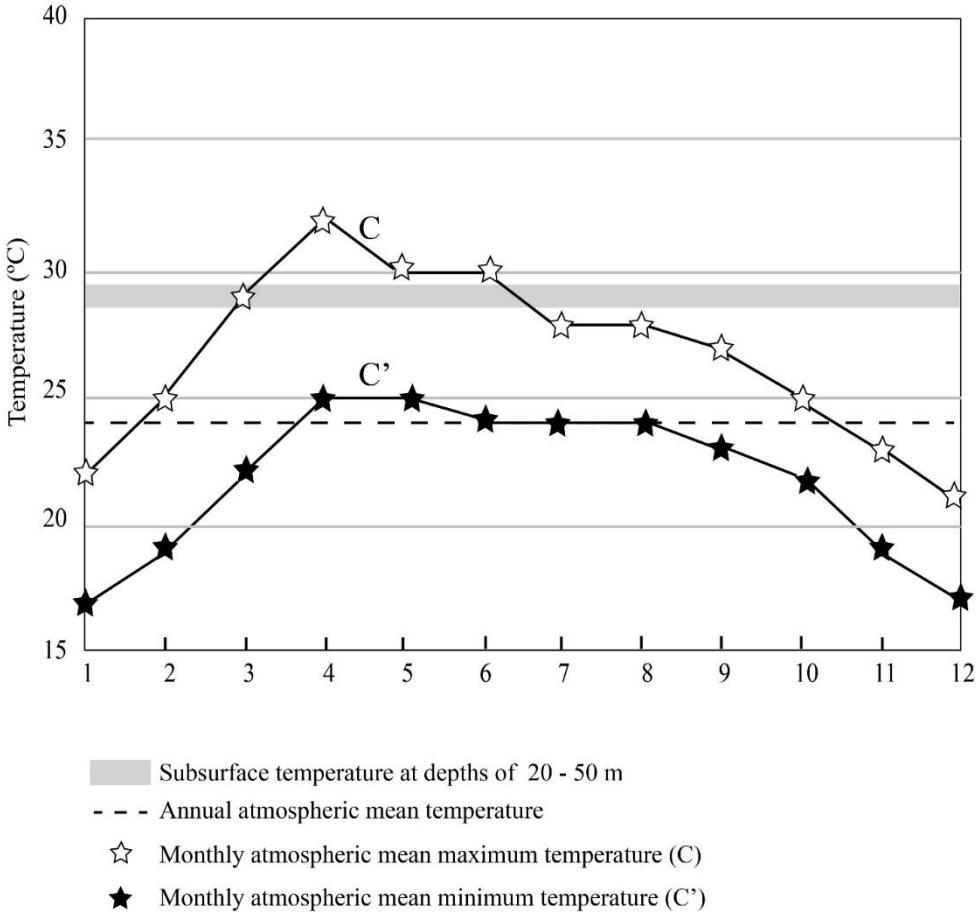

Figure 5.1 Comparison of atmospheric and subsurface temperatures of Sukhothai area (modified after Yasukawa et al. (2009b)).

5.2.2 Installation cost

GHP in this study was installed in vertical loop, leading the cost of drilling is expensive. For this reason, if GHP system is installed by other ways such as horizontal loop or pond loop, the cost will be reduced substantially.

REFERENCES

Balasubramaniam, A., Oh, E., and Phienwej, N. 2009. Bored and driven pile testing in Bangkok sub-soils. Journal of Lowland Technology International 11: 29-36.

Blum, P., Campillo, G., Münch, W., and Kölbel, T. 2010. CO 2 savings of ground source heat pump systems–a regional analysis. Renewable Energy 35: 122-127.

Build-It-Solar. Ground Temperatures as a Function of Location, Season, and Depth [online]. [Online]. Available from: http://www.builditsolar.com/Projects/Cooling/EarthTemperatures.htm

Corona. 2012. 業界初の再生可能エネルギー“地中熱”を利用した住宅用ヒートポンプエアコン [Online]. [Online]. Available from: https://www.corona.co.jp/news/news_120409.pdf

Curtis, R., Lund, J., Sanner, B., Rybach, L., and Hellström, G. 2005. Ground source heat pumps–geothermal energy for anyone, anywhere: current worldwide activity. in Proceedings World Geothermal Congress, Antalya, Turkey. pp. 24-29.

Department of Groundwater Resources (DGR). Litho-Bangkok [Digital file] Trans.). In (Ed.),^(Eds.), (ed., Vol. pp.). Thailand, [2016, February 23]. (Reprinted from.

Department of Groundwater Resources (DGR). 2011. Observation wells reports edit [Digital file] Trans.). In (Ed.),^(Eds.), (ed., Vol. pp.). Thailand, [2016, February 23]. (Reprinted from.

Department of Mineral Resources (DMR). 2011. Geology of Thailand: The Royal Crest Commemorating the 6th Cycle Birthday Anniversary 5th December 2009. Bangkok: DMR (in Thai).

Energy Saving Trust. 2007. Domestic Ground Source Heat Pumps: Design and installation of closed-loop systems (2007 edition) [online]. [Online]. Available

from:
http://www.icax.co.uk/pdf/Domestic_Ground_Source_Heat_Pumps_Design_Installation.pdf

Fridleifsson, I.B. 2001. Geothermal energy for the benefit of the people. Renewable and sustainable energy reviews 5: 299-312.

Galgaro, A., Emmi, G., Zarrella, A., and De Carli, M. 2014. Possible applications of ground coupled heat pumps in high geothermal gradient zones. Energy and Buildings 79: 12-22.

Hatyaiair. Panasonic: CS-PN12SKT [online]. [Online]. Available from: http://www.hatyaiair.co.th/a16.air

Hepbasli, A., and Akdemir, O. 2004. Energy and exergy analysis of a ground source (geothermal) heat pump system. Energy conversion and management 45: 737-753.

Hepbasli, A., Akdemir, O., and Hancioglu, E. 2003. Experimental study of a closed loop vertical ground source heat pump system. Energy Conversion and Management 44: 527-548.

İnallı, M., and Esen, H. 2004. Experimental thermal performance evaluation of a horizontal ground-source heat pump system. Applied thermal engineering 24: 2219-2232.

Lund, J., Sanner, B., Rybach, L., Curtis, R., and Hellstrom, G. 2004. Geothermal (ground-source) heat pumps-a world overview.

National Rural Electric Cooperative, A., and Oklahoma State University. Division of Engineering, T. 1988. Closed-loop/ground-source heat pump systems : installation guide. Stillwater, Okla. :: Distributed by International Ground Source Heat Pump Association.

Omer, A.M. 2008. Ground-source heat pumps systems and applications. Renewable and sustainable energy reviews 12: 344-371.

Orbis Geothermal. How Geothermal works [Online]. [Online]. Available from: http://www.orbisgeothermal.com/how-it-works

Rybach, L., Brunner, M., and Gorhan, H. 2000. Swiss geothermal update 1995–2000. in Proceedings World Geothermal Congress. pp.

Sanner, B., Karytsas, C., Mendrinos, D., and Rybach, L. 2003. Current status of ground source heat pumps and underground thermal energy storage in Europe. Geothermics 32: 579-588.

Spitler, J. 2005. Editorial: ground-source heat pump system research—past, present, and future Trans.). In (Ed.),^(Eds.), (ed., Vol. pp.). Taylor & Francis. (Reprinted from.

Takashima, I., Yasukawa, K., Uchida, Y., Yoshioka, M., and Won-In, K,. 2011. A Geothermal Heat Pump System in Bangkok, Thailand. Proceedings of the 9th Asian Geothermal Symposium Japan: Institute for Geo-Resources and Environment (GREEN), National Institute of Advanced Industrial Science and Technology (AIST), Japan Korea Institute

Tenma, N., Yasukawa, K., Takashima, I., Uchida, Y., Lorphensri, O., and Zyvoloski, G. 2009. Subsurface thermal influence of experimental geothermal heat pump system operation for space cooling in Kamphaengphet, Thailand. Bulletin of the Geological Survey of Japan 60: 503-509.

Uchida, Y., Yasukawa, K., Tenma, N., Taguchi, Y., Suwanlert, J., and Buapeng, S. 2009. Subsurface Thermal Regime in the Chao-Phraya Plain, Thailand. Bulletin of the Geological Survey of Japan 60: 469-489.

Wanichbuncha, K. 2009. Analysis of statistical data by Excel. Bangkok: Department of Statistics, Faculty of Commerce and Accountancy, Chulalongkorn University, (in Thai).

Widiatmojo, A. 2017. Workshop on Practical Analysis of GSHP Logging Data Trans.). In Chokchai, S. (Ed.),^(Eds.), (ed., Vol. pp.). (Reprinted from.

Yamtraipat, N., Khedari, J., Hirunlabh, J., and Kunchornrat, J. 2006. Assessment of Thailand indoor set-point impact on energy consumption and environment. Energy Policy 34: 765-770.

Yasukawa, K., Takashima, I., Uchida, Y., Tenma, N., and Lorphensri, O. 2009a. Geothermal heat pump application for space cooling in Kamphaengphet, Thailand. Bulletin of the Geological Survey of Japan 60: 491-501.

Yasukawa, K., et al. 2009b. Groundwater temperature survey for geothermal heat pump application in tropical Asia. Bulletin of the Geological Survey of Japan 60: 459-467.

APPENDIX

VITA

Miss Sasimook Chokchai was born on December 14, 1990 in Rayong Province, eastern part of Thailand. After she finished high school from Rayongwittayakom School at Rayong, in 2008, she studied on Geology at the Department of Geology, Faculty of Science, Chulalongkorn University, Thailand and graduated a Bachelor degree in 2013. In the same year, she was interested in Geothermal (Ground Source) Heat Pump project in Thailand, so she determined to study on master degree on the subject of GHP/GSHP in Thailand at Department of Geology, Faculty of Science, Chulalongkorn University and she graduated a master degree in 2017.